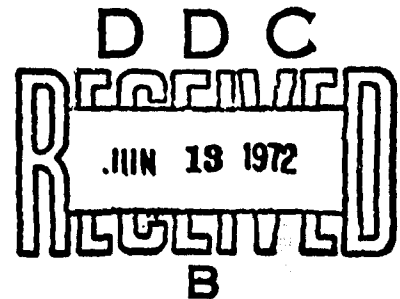


AD743064

# Operating Characteristics for Continuous Square-Law Detection in Gaussian Noise

ALBERT H. NUTTALL  
DAVID W. HYDE  
*Office of the Director of Science  
and Technology*



3 April 1972

## NAVAL UNDERWATER SYSTEMS CENTER

Reproduced by  
**NATIONAL TECHNICAL  
INFORMATION SERVICE**  
Springfield, Va. 22151

Approved for public release; distribution unlimited.

112

R

### ADMINISTRATIVE INFORMATION

This report was prepared under NUSC Project No. A-752-05, "Statistical Communication with Application to Sonar Signal Processing" (U), Principal Investigator, Dr. A. H. Nuttali (Code TC), Navy Subproject and Task No. ZF XX 112 001, Program Manager, Dr. J. H. Huth (DLP/MAT 03L4).

The Technical Reviewer for this report was Dr. P. G. Cable (Code TC).

REVIEWED AND APPROVED: 3 April 1972

1	WHITE SECTION	<input checked="" type="checkbox"/>
2	BUFF SECTION	<input type="checkbox"/>
3	UNCEDED	<input type="checkbox"/>
4	CLASSIFICATION	
BY		
DISTRIBUTION/COMMUNITY CODES		
DISC.	ANAL.	and/or SYSTEM
A		

*W A Von Winkle*

W. A. Von Winkle  
Director of Science and Technology

Inquiries concerning this report may be addressed to the authors,  
New London Laboratory, Naval Underwater Systems Center, New  
London, Connecticut 06320

UNCLASSIFIED  
Security Classification

DOCUMENT CONTROL DATA - R & D

(Security classification of title, body of abstract and indexing annotation must be entered when the overall report is classified)

1. ORIGINATING ACTIVITY (Corporate author) Naval Underwater Systems Center Newport, Rhode Island 02840		2a. REPORT SECURITY CLASSIFICATION UNCLASSIFIED	
		2b. GROUP	
3. REPORT TITLE OPERATING CHARACTERISTICS FOR CONTINUOUS SQUARE-LAW DETECTION IN GAUSSIAN NOISE			
4. DESCRIPTIVE NOTES (Type of report and inclusive dates) Research Report			
5. AUTHOR(S) (First name, middle initial, last name) Albert H. Nuttall David W. Hyde			
6. REPORT DATE 3 April 1972		7a. TOTAL NO. OF PAGES 114	7b. NO. OF REFS 21
8a. CONTRACT OR GRANT NO.		9a. ORIGINATOR'S REPORT NUMBER(S) TR 4233	
b. PROJECT NO. A-752-05		9b. OTHER REPORT NO(S) (Any other numbers that may be assigned this report)	
c. ZF XX 112 001			
d.			
10. DISTRIBUTION STATEMENT Approved for public release; distribution unlimited.			
11. SUPPLEMENTARY NOTES		12. SPONSORING MILITARY ACTIVITY Department of the Navy	
13. ABSTRACT <p>The exact detection probabilities and false-alarm probabilities for continuous square-law detection of a signal in Gaussian noise are calculated, with no restrictive assumptions about the size of the observation-time-bandwidth products. Two cases are considered; they are called the low-frequency (LF) and narrowband (NB) cases. In both cases, the signal has coherent and incoherent components.</p> <p>Results for the detection probability versus signal-to-noise ratio (S/N), with false-alarm probability as a parameter, are given for both the LF and NB cases for observation-time-bandwidth products equal to <math>2^m</math> (<math>m = 0(1)7</math>) and for the fraction of coherent signal power equal to 0, .2, 1. For a specified detection probability of .5 and false-alarm probabilities of <math>10^{-n}</math> (<math>n = 1(1)8</math>), the required S/N is also plotted for the same range of time-bandwidth products and fractions of coherent signal power as above.</p>			

UNCLASSIFIED

Security Classification

14. KEY WORDS	LINK A		LINK B		LINK C	
	ROLE	WT	ROLE	WT	ROLE	WT
Arbitrary Time-Bandwidth Product						
Characteristic Function						
Coherent and Incoherent Signals						
Continuous Square-Law Detection						
Detection and False-Alarm Probabilities						
Exponential Correlation						
Fredholm Determinant						
Gaussian Noise						

## ABSTRACT

The exact detection probabilities and false-alarm probabilities for square-law detection of a signal in Gaussian noise are calculated, with no restrictive assumptions about the size of the observation-time-bandwidth products. Two cases are considered: in the first, called the low-frequency (LF) case, the signal is a combination of a dc component and a Gaussian process component with exponential correlation. Here the noise is a Gaussian process with identical exponential correlation. In the second case, called the narrowband (NB) case, the signal is a combination of a sine wave component and a Gaussian process component with an exponentially damped cosinusoidal correlation at the same center frequency as the sine wave. Here the noise is a Gaussian process with identical exponentially damped cosinusoidal correlation. The two components of the signal are called the coherent and incoherent components, respectively, in both the LF and NB cases.

The output of the square-law detector is integrated continuously over the observation time and compared with a threshold for statements about signal presence. It is not assumed that the square-law detector output is sampled infrequently enough to yield independent samples.

Results for the detection probability versus signal-to-noise ratio ( $S/N$ ), with false-alarm probability as a parameter, are given for both the LF and NB cases for observation-time-bandwidth products equal to  $2^n$  ( $n = 0(1)7$ ) and  $\rho$  - the fraction of coherent signal power equal to 0, .2, 1. For a specified detection probability of .5 and false-alarm probabilities of  $10^{-n}$  ( $n = 1(1)8$ ), the required  $S/N$  is also plotted for the same range of time-bandwidth products and fractions of coherent signal power as above. Comparisons with a Gaussian approximation for large time-bandwidth products are made; it is shown that the Gaussian assumption is optimistic in predicting performance of the square-law detector, the exact amount depending on the time-bandwidth product.

## TABLE OF CONTENTS

	Page
ABSTRACT . . . . .	i
LIST OF TABLES . . . . .	v
LIST OF ILLUSTRATIONS . . . . .	v
LIST OF SYMBOLS . . . . .	vii
ABBREVIATIONS . . . . .	viii
Section	
1 INTRODUCTION . . . . .	1
2 PROBLEM DEFINITION . . . . .	5
2.1 Low-Frequency Case . . . . .	5
2.2 Narrowband Case . . . . .	6
2.3 Performance Comparison between Low-Frequency and Narrowband Cases . . . . .	7
3 RESULTS . . . . .	9
3.1 Low-Frequency Case . . . . .	9
3.2 Narrowband Case . . . . .	15
4 DISCUSSION . . . . .	17
APPENDIX A — COMPLEX ENVELOPE RELATIONS . . . . .	83
APPENDIX B — DERIVATION OF CHARACTERISTIC FUNCTION FOR LOW-FREQUENCY AND NARROWBAND CASES . . . . .	87
APPENDIX C — DETECTION PROBABILITIES FOR ONE SAMPLE . . . . .	97
APPENDIX D — ASYMPTOTIC BEHAVIOR OF CHARACTERISTIC FUNCTION AND ERROR BOUND . . . . .	101
APPENDIX E — DETECTION PROBABILITY UNDER GAUSSIAN ASSUMPTION . . . . .	103
LIST OF REFERENCES . . . . .	105

## LIST OF TABLES

Table		Page
1	Thresholds for LF Processor . . . . .	10
2	Thresholds for NB Processor . . . . .	15

## LIST OF ILLUSTRATIONS

Figure		Page
1	Low-Frequency Processor . . . . .	19
2	Narrowband Processor . . . . .	19
3	Detection Probability; LF, $\beta = 0$ . . . . .	20
4	Detection Probability; LF, $\beta = 1$ . . . . .	23
5	Detection Probability; LF, $\beta = 2$ . . . . .	26
6	Detection Probability; LF, $\beta = 4$ . . . . .	29
7	Detection Probability; LF, $\beta = 8$ . . . . .	32
8	Detection Probability; LF, $\beta = 16$ . . . . .	35
9	Detection Probability; LF, $\beta = 32$ . . . . .	38
10	Detection Probability; LF, $\beta = 64$ . . . . .	41
11	Detection Probability; LF, $\beta = 128$ . . . . .	44
12	Detection Probability; LF, $\beta = 128$ , Gaussian Assumption . . . . .	47
13	Required Signal-to-Noise Ratio; LF . . . . .	50
14	Detection Probability; NB, $\hat{\beta} = 0$ . . . . .	53
15	Detection Probability; NB, $\hat{\beta} = 1$ . . . . .	56
16	Detection Probability; NB, $\hat{\beta} = 2$ . . . . .	59
17	Detection Probability; NB, $\hat{\beta} = 4$ . . . . .	62
18	Detection Probability; NB, $\hat{\beta} = 8$ . . . . .	65
19	Detection Probability; NB, $\hat{\beta} = 16$ . . . . .	68
20	Detection Probability; NB, $\hat{\beta} = 32$ . . . . .	71
21	Detection Probability; NB, $\hat{\beta} = 64$ . . . . .	74
22	Detection Probability; NB, $\hat{\beta} = 128$ . . . . .	77
23	Required Signal-to-Noise Ratio; NB . . . . .	80

## Appendix A

A-1	Single-Sided Filter . . . . .	83
-----	-------------------------------	----

## LIST OF SYMBOLS\*

$t$	time
$y(t)$	waveform at time $t$
$l, l_k$	decision variable
$c(t)$	coherent component of received signal
$s(t)$	incoherent component of received signal
$n(t)$	received noise
$\tau$	delay variable
$R_{s,n}(\tau), R(\tau)$	correlation function
$\sigma_{s,n}^2, \sigma_x^2$	variance
$W_e, \hat{W}_e$	effective bandwidth
$f$	frequency; fraction of received coherent signal power
$G_{s,n}(f)$	spectrum
$T$	observation interval
$f_o$	center frequency
$W$	frequency band
$t_o$	time instant
$P$	cumulative distribution function
$f(\xi), f_l(\xi)$	characteristic function
$X, Th$	threshold
$\Lambda_n$	normalized threshold
$\beta, \hat{\beta}$	time-bandwidth product
$P_F$	false-alarm probability
$P_D$	detection probability
$P_c$	received coherent signal power
$R_c, R_s, R, d^2$	signal-to-noise ratio (power)
$\Phi$	Gaussian cumulative distribution function
$x, n$	auxiliary variable
$w_k$	weight
$N$	number of branches
$U$	unit step function
$i$	$(-1)^{1/2}$

\*In order of appearance.

## LIST OF SYMBOLS (Cont'd)

$x_+(t)$	positive frequency component of $x(t)$
$x_H(t)$	Hilbert transform of $x(t)$
$\underline{x}(t)$	complex envelope of $x(t)$
$x_c(t), x_s(t)$	in-phase and quadrature components of $x(t)$
$H(f)$	transfer function
Re, Im	real, imaginary
$r(t), x(t)$	normalized processes
$P, P_c, P_s$	auxiliary random variables
$\xi$	characteristic function argument
$\lambda_j$	eigenvalue
$\phi_j$	eigenfunction
$x_j, r_j$	expansion coefficients
$\delta_{jk}$	1 if $j=k$ , 0 if $j \neq k$
$\Gamma, \hat{\Gamma}$	resolvent kernel
$D, \hat{D}$	Fredholm determinant
$c_1(t)$	normalized waveform
$\phi(u)$	auxiliary function
$\gamma, \omega$	auxiliary variables
$E, \phi$	envelope and phase modulations
Prob(x)	probability of $x$
$\hat{x}$	narrowband analogue of $x$
Overbar	ensemble average
Underbar	complex envelope

## ABBREVIATIONS

CDF	cumulative distribution function
CF	characteristic function
FFT	fast Fourier transform
LF	low frequency
NB	narrowband
PDF	probability density function
ROC	receiver operating characteristics
RV	random variable
S/N	signal-to-noise ratio

## OPERATING CHARACTERISTICS FOR CONTINUOUS SQUARE-LAW DETECTION IN GAUSSIAN NOISE

### 1. INTRODUCTION

Often, signals in noise are detected by filtering a received process to the frequency band of interest, squaring the filtered output, continuously integrating over an observation interval where the signal is anticipated, and comparing this decision variable with a threshold or with the past history of this variable. In fact, under certain conditions, the optimum detector for stochastic signals takes this form (for example, Ref. 1, Chapter XI). This form of processor could be employed whether the received signal is deterministic (known or unknown), stochastic, or a combination of both, although it is not necessarily optimum in all these cases. This processor is, in fact, frequently adopted for passive detection of targets of unknown statistics.

Two important parameters that characterize the performance of this processor are the bandwidth of the stochastic process at the input to the squarer and the observation (or integration) time. Practical cases occur where this time-bandwidth product ranges from the order of unity to several thousand. In the latter case of very large time-bandwidth products, the decision variable can often be accurately approximated by a Gaussian random variable (RV). However, when the time-bandwidth product is of the order of unity, it can not be approximated as Gaussian, especially when very low false-alarm probabilities or high-detection probabilities are of interest. The question then arises as to the exact performance of the processor. Calculation of the performance is complicated by the difficulty in analyzing the continuous integration of a non-Gaussian process since a "sum" of dependent random variables is formed. Also, approximation of the performance by using a sum of independent variables is tenuous, because the exact value of the "effective" number of independent samples to use is not easily ascertained. Thus, there is a need for (1) the exact evaluation of the receiver operating characteristics (ROC) of the square-law detector followed by an integrator, both as a benchmark against which other processors and approximations can be compared, and (2) the determination of when the Gaussian assumption can be validly employed, especially for medium time-bandwidth products and very small false-alarm probabilities.

Two cases of signal and noise spectra at the input to the squarer are considered: In the low-frequency (LF) case, the signal is a combination of a dc component and a stationary, zero-mean, Gaussian process component with exponential correlation, and the noise is a Gaussian process (of different power level) with identical exponential correlation. In the narrowband (NB) case, the signal is a combination of a sine-wave component and a Gaussian process component with an exponentially damped cosinusoidal correlation, and the noise is a Gaussian process with identical correlation, except for power level. The two components of the signal are called the coherent and incoherent components, respectively, in both the LF and NB cases, for ease of discussion.

Actually, the general derivations of processor performance capability presented here are not restricted to the cases above. They actually allow for an arbitrary deterministic coherent signal component (which may be known or unknown) and an arbitrary (but identical) correlation function for the incoherent signal component and the noise. However, numerical evaluation of performance capability requires evaluating the resolvent (or reciprocal) kernel and the Fredholm determinant of the correlation function. Hence, numerical results have been confined here to the cases given in the paragraph above.

Several practical applications fall under the framework above. For example, if the incoherent component of the received signal in the NB case is absent, we have detection of a sine wave; this is encountered in active or passive detection of a target or in binary on-off communication with another party. Or, if the coherent component is absent in the LF or NB case, we have detection of a random-signal process in noise; this situation can hold true in long-range transmission through a fluctuating medium or in reflection of an acoustic signal off the time-varying ocean surface. It is often employed in passive detection of a noisy source. Finally, if both signal components are present, relevant examples in the NB case are reflections of an acoustic signal from a surface with low roughness, or communication via a medium supporting both a direct (nonfluctuating) path and fluctuating paths. Extensions to multitone applications are also possible and are discussed in Section 4.

A great deal of work on the statistics of the time-average power of a Gaussian process has been presented in the past. Rice<sup>2</sup> gave the first four semi-invariants (or moments) for an arbitrary correlation function of the Gaussian process, and approximated the probability density function (PDF) for very small and large observation times. Emerson<sup>3</sup> gave an infinite product for the characteristic function (CF) of a filtered squared-Gaussian process and, via the first three

semi-invariants, approximated the PDF through Gram-Charlier and Laguerre expansions. Siegert<sup>4</sup> gave the CF in terms of the solution of an integral equation obtained by Kac and Siegert.<sup>5</sup> In the former, the CF was in terms of an infinite product, although it was shown that the resolvent kernel offered an alternative approach. No examples were presented. Darling and Siegert<sup>6</sup> and Siegert<sup>7</sup> showed that the CF of a more general functional could be obtained from the solution of two integral equations, and they obtained the CF in closed form for a finite-time exponential averager, for a Gaussian process with an exponential correlation. Slepian<sup>8</sup> obtained a series expansion for the PDF and cumulative distribution function (CDF), where each term was given by an integral. No extreme probabilities were evaluated and the accuracy was about 1 percent. Jacobs<sup>9</sup> considered a communications problem with random signals and made a finite approximation to the CF by increasing the number of terms until the CDF essentially stabilized. Schwartz<sup>10</sup> obtained a closed form CF for correlation functions whose corresponding homogeneous Fredholm integral equation reduces to an equivalent linear differential equation. Four examples were given, and both LF and NB cases were considered. Steenson and Stirling<sup>11</sup> conducted a simulation and gave results on the PDF and false-alarm rate and showed that the gamma distribution accurately fitted the data. Some related results on the distribution of quadratic forms are given in References 12, 13, and 14.

None of the previous results are of sufficient accuracy to allow calculating the cumulative distributions very near zero or unity — the regions of interest for very small false-alarm and high-detection probabilities. The complicated results for the CF, even when in closed form, indicate the need for quick and accurate CDF calculations that do not require moment evaluations or series expansions. Here we make no attempt to find analytic expressions for the PDF or CDF, but proceed directly numerically from the CF of the decision variable to the CDF via a Fast Fourier Transform (FFT).<sup>15,16</sup> The assumption that the incoherent component of the received signal has the same correlation (and, hence, spectrum) as the noise in both the LF and NB cases, except for power levels, enables evaluating the CF in closed form.

If the integrator following the squarer were replaced by a sampler and summer, calculation of the CF in closed form can be accomplished fairly simply once the eigenvalues of the matrix of sampled correlations are evaluated. This technique allows very general and different signal and noise spectra and will be the subject of a future report. For now, however, we restrict ourselves to continuous integration without sampling the squarer output.

## 2. PROBLEM DEFINITION

Two different cases will be considered in this report, namely, the LF and NB processors. Block diagrams of each processor will be given and the pertinent characteristics of the signal and noise described. Then the expected performance of the two cases will be briefly compared for the case of large time-bandwidth products.

### 2.1 LOW-FREQUENCY CASE

A block diagram of the LF processor is given in Fig. 1, where  $y(t)$  is a LF waveform composed of three components:

$$y(t) = c(t) + s(t) + n(t) \quad (1)$$

In (1),

a.  $c(t)$  is a LF deterministic waveform (known or unknown) and is called the coherent component of the received signal.

b.  $s(t)$  is a stationary, zero-mean, LF Gaussian process with correlation

$$R_s(\tau) = \sigma_s^2 \exp(-2W_e |\tau|) \quad (2)$$

and is called the incoherent component of the received signal.

The noise  $n(t)$  has the same statistical description as  $s(t)$ , but the two processes are independent. Its correlation is

$$R_n(\tau) = \sigma_n^2 \exp(-2W_e |\tau|) \quad (3)$$

The (double-sided) spectra of  $s(t)$  and  $n(t)$  are given by

$$G_{s,n}(f) = \sigma_{s,n}^2 \frac{W_e/\pi^2}{f^2 + (W_e/\pi)^2} \quad (4)$$

where  $W_e$  can be interpreted as the effective (or statistical) bandwidth<sup>17</sup> of the positive-frequency components of the LF random processes:

$$W_e = \frac{\left[ \int_0^{\infty} df G_{s,n}(f) \right]^2}{\int_0^{\infty} df G_{s,n}^2(f)} = \frac{R_{s,n}^2(0)}{2 \int_{-\infty}^{\infty} d\tau R_{s,n}^2(\tau)} \quad (5)$$

The identical spectral shape of the incoherent component  $s(t)$  and the noise  $n(t)$  is realized in practice by filtering fairly broadband received signal and noise processes through a low-pass RC filter. It can be interpreted physically as overresolving the received signal with a very low-pass filter.

The decision variable  $\ell$  in Fig. 1 is given by

$$\ell = \frac{1}{T} \int_T dt [c(t) + s(t) + n(t)]^2 \quad (6)$$

and is to be compared with a threshold for detecting signal presence. (No assumption about the size of the time-bandwidth product  $TW_c$  is made.) This is broadband-energy detection and contains three subcases of importance:

- a.  $c(t) = 0$ . Signal presence indicated by an increased power level in the received random process.
- b.  $s(t) = 0$ . Signal presence indicated by a nonzero, time-varying mean in the received random process.
- c. Both  $c(t)$  and  $s(t)$  nonzero. Signal presence indicated by adding a nonzero, time-varying, mean-random process to the received random process.

## 2.2 NARROWBAND CASE

A block diagram of the NB processor is given in Fig. 2. In the figure,  $y(t)$  is an NB waveform composed of three components, as in (1). The signal  $c(t)$  is an NB waveform centered at frequency  $f_0$ , with a deterministic complex envelope (known or unknown), and is called the coherent component of the received signal. Both  $s(t)$  and  $n(t)$  are independent, stationary, zero-mean, NB Gaussian processes with correlations

$$R_{s,n}(\tau) = \sigma_{s,n}^2 \exp(-\hat{W}_c |\tau|) \cos(2\pi f_0 \tau), \quad f_0 \gg \hat{W}_c \quad (7)$$

(It is assumed that  $f_0 T \gg 1$ , where  $T$  is the integration time in Fig. 2.) By definition,  $s(t)$  is called the incoherent component of the received signal.

The (double-sided) spectra of  $s(t)$  and  $n(t)$  are given by

$$G_{s,n}(f) = \sigma_{s,n}^2 \frac{\hat{W}_c}{4\pi^2} \left[ \frac{1}{(f-f_0)^2 + \left(\frac{\hat{W}_c}{2\pi}\right)^2} + \frac{1}{(f+f_0)^2 + \left(\frac{\hat{W}_c}{2\pi}\right)^2} \right] \quad (8)$$

where  $\hat{W}_c$  can be interpreted as the effective bandwidth of the positive-frequency components of the NB random processes:

$$\hat{W}_c = \frac{\left[ \int_0^{\infty} df G_{s,n}(f) \right]^2}{\int_0^{\infty} df G_{s,n}^2(f)} = \frac{R_{s,n}^2(0)}{2 \int_{-\infty}^{\infty} d\tau R_{s,n}^2(\tau)} \quad (9)$$

The identical spectral shape of the incoherent component  $s(t)$  and the noise  $n(t)$  are realized in practice by filtering fairly broadband received signal and noise processes through an RLC filter that is NB. It can be interpreted physically as overresolving the received signal with a very NB filter.

The decision variable  $\ell$  is given by

$$\ell = \frac{1}{2T} \int_T dt |\underline{c}(t) + \underline{s}(t) + \underline{n}(t)|^2, \quad (10)$$

where  $\underline{x}(t)$  denotes the complex envelope of  $x(t)$  (see Appendix A). The decision variable  $\ell$  is compared with a threshold in order to detect signal presence. (No assumption about the size of the time-bandwidth product  $TW_c$  is made.) This is NB energy detection and contains three subcases:

- a.  $c(t) = 0$ . Signal presence indicated by an increased power level in the received random process.
- b.  $s(t) = 0$ . Signal presence indicated by an NB waveform in the received random process.
- c. Both  $c(t)$  and  $s(t)$  nonzero. Signal presence indicated by adding an NB waveform and random process to the received random process.

### 2.3 PERFORMANCE COMPARISON BETWEEN LOW-FREQUENCY AND NARROWBAND CASES

The effective bandwidths of the LF and NB processes, which have been defined in (5) and (9), respectively, are measures of the spectral width of the positive-frequency components of the respective processes. A bandlimited low-pass process confined to frequencies  $(-W, W)$  must be sampled at least every  $(2W)^{-1}$  seconds in order not to lose any information. Thus, in a long time interval  $T$ , there would be  $(2W)T$  samples upon which to base a decision as to signal presence or absence. On the other hand, a bandlimited NB process confined to frequencies  $(f_c - W/2, f_c + W/2)$  and the corresponding negative frequency band

must have its in-phase and quadrature components sampled at least every  $W^{-1}$  seconds in order not to lose any information. Then in a time  $T$ , there would be  $2(W)T$  samples upon which to base a decision as to signal presence. Therefore, both bandlimited processes, LF and NB, yield the same number of information samples when  $W$  is interpreted as the spectral width of the positive-frequency components. As a result, in our investigation of nonbandlimited processes, we expect that when the effective positive-frequency bandwidths are equal, that is,  $W_c = W_c$ , the performance of the LF and NB processors should be comparable for large  $TW_c$ . This will be borne out by the numerical examples in the next section.

For small time-bandwidth products, however, the performance of the LF and NB processors differ. For example, as  $T \rightarrow 0$  in (6) and (10),  $l_{LF} \rightarrow y_{LP}^2(t_0)$ ,  $l_{NB} \rightarrow 1/2 [y_c^2(t_0) + y_s^2(t_0)]$  (see Appendix A). Thus, in the limit of small time-bandwidth products, LF processing contains one degree of freedom, whereas NB processing contains two degrees of freedom. The performance of the NB processor will be better than that of the LF processor for small time-bandwidth products.

### 3. RESULTS

The CFs for the LF and NB cases are derived in Appendix B, the general results being (B-22) and (B-46). These results are specialized to the cases of interest here, resulting in (B-31) and (B-51), respectively. For the special case of  $T \rightarrow 0$ , (6) and (10) reduce to a single sample of the input processes, and derivation of the detection probabilities and false-alarm probabilities is possible in closed form; these derivations are presented in Appendix C.

The CDF  $P$  of a nonnegative RV from its CF  $f$  can be evaluated numerically via use of any of the equivalent forms<sup>16</sup> :

$$\begin{aligned}
 F(X) &= \frac{1}{2} - \frac{1}{\pi} \int_0^{\infty} \frac{d\xi}{\xi} \operatorname{Im} \{ f(\xi) \exp(-i\xi X) \} \\
 &= \frac{2}{\pi} \int_0^{\infty} \frac{d\xi}{\xi} f_r(\xi) \sin(\xi X) \\
 &= 1 - \frac{2}{\pi} \int_0^{\infty} \frac{d\xi}{\xi} f_i(\xi) \cos(\xi X), \quad X > 0
 \end{aligned} \tag{11}$$

In (11),  $f_r$  and  $f_i$  are the real and imaginary parts, respectively, of CF  $f$ . The error in terminating the integrals in (11) at finite limits for computer evaluation is considered in Appendix D.

#### 3.1 LOW-FREQUENCY CASE

Suppose  $l$  in (6) is compared with a threshold  $X$  for purposes of signal detection. We now define a normalized threshold,

$$\Lambda_n = \frac{X}{\sigma_n^2}, \tag{12}$$

and the time-bandwidth product,

$$\beta = TW_c. \tag{13}$$

Values of the required normalized threshold  $\Lambda_n$  for different values of  $\beta$  and specified false-alarm probability  $P_F$  are given in Table 1.

Before presenting results for the detection probability, it is convenient to define several power signal-to-noise ratios ( $S/N_s$ ). We define the received coherent signal power

$$P_c = \frac{1}{T} \int_T c^2(t) dt. \tag{14}$$

Table 1  
THRESHOLDS FOR LF PROCESSOR

$\beta$ $P_F$	0	1	2	4	8	16	32	64	128
$10^{-1}$	2.706	2.065	1.841	1.634	1.461	1.329	1.233	1.164	1.115
$10^{-2}$	6.635	4.302	3.362	2.600	2.065	1.710	1.478	1.324	1.223
$10^{-3}$	10.828	6.706	4.971	3.564	2.630	2.047	1.684	1.455	1.307
$10^{-4}$	15.137	9.180	6.631	4.540	3.182	2.364	1.872	1.571	1.381
$10^{-5}$	19.511	11.693	8.322	5.526	3.728	2.670	2.050	1.678	1.448
$10^{-6}$	23.928	14.250	10.031	6.523	4.272	2.970	2.221	1.779	1.511
$10^{-7}$	28.374	16.785	11.753	7.527	4.815	3.265	2.387	1.877	1.570
$10^{-8}$	32.841	19.352	13.483	8.537	5.389	3.558	2.549	1.970	1.627

The coherent and incoherent S/Ns are defined, respectively, as

$$R_c = \frac{P_c}{\sigma_n^2} \quad (15)$$

and

$$R_s = \frac{\sigma_s^2}{\sigma_n^2} \quad (16)$$

The total received S/N is defined as

$$R = \frac{P_c + \sigma_s^2}{\sigma_n^2} = R_c + R_s \quad (17)$$

We also define the fraction  $f$  of total received signal power that is coherent as

$$f = \frac{P_c}{P_c + \sigma_s^2} = \frac{R_c}{R} \quad (18)$$

using (15), (16), and (17). Then we can express

$$\begin{aligned} R_c &= fR, \\ R_s &= (1-f)R, \end{aligned} \quad (19)$$

and, thereby, utilize the total received S/N  $R$  and the fraction  $f$  of coherent signal power as the fundamental parameters characterizing the performance of the processor.

In the series of Figs. 3 through 11, to follow, plots of the detection probability  $P_D$  versus  $R^{1/2}$  are given, with  $P_F$  as a parameter. Each figure corresponds to a different value of  $\beta$ , specifically  $\beta = 0, 1, 2, 4, 8, 16, 32, 64,$  and  $128$ . Each figure is composed of three parts: Part A is for  $f = 1$ , part B is for  $f = .2$ , and part C is for  $f = 0$ .

The equation

$$dB = 10 \log_{10} R = 20 \log_{10} R^{1/2} \quad (20)$$

can be employed to convert the abscissa to decibels in Figs. 3 through 11. ( $R$  is a power S/N, whereas  $R^{1/2}$  is a measure of a voltage S/N.) Equation (20) is the total input S/N expressed in decibels.

The difference in performance for different fractions  $f$  of coherent signal power is very marked for small  $\beta$ . Thus, Fig. 3, for  $\beta = 0$ , illustrates a significant drop in  $P_D$  for large values of  $R^{1/2}$  when  $f$  is decreased from unity. In fact, this degradation in performance occurs even when  $f$  is decreased from 1 to .9 (this curve is not shown). As  $\beta$  increases, the difference in performance is lessened until, for large  $\beta$ , the opposite behavior occurs for large  $R^{1/2}$  (for example,  $P_D \approx .9999$ ). That is, the required value of  $R^{1/2}$  for a specified  $P_D$  near unity is less for  $f = 0$  than for  $f = 1$  for very large  $\beta$ ; see, for example, Fig. 11.

On the other hand, for small values of  $P_D$ , the smaller values of  $f$  yield the better performance for small  $\beta$ , whereas the larger values of  $f$  give better performance for large  $\beta$ . There is, however, rather slight differences in performance, that is, required S/N  $R$ , in the case of small  $P_D$ .

The reason for this cross-over of the curves is explained by the fact that we are considering a fixed receiver and varying the transmitted signal composition. The fixed receiver is more nearly optimum for some transmitted signals than others, and it is impossible to order the performance of the various combinations of coherent and incoherent signal power.

The situation is made more striking when the performance of the optimum receiver for completely coherent reception,  $f = 1$ , is considered. For a dc signal waveform, LF processing, and exponential noise correlation, we can use the first equation on p. 114 of Reference 1 to evaluate Helstrom's power  $S/N$   $d^2$  for the optimum receiver as

$$d^2 = R_c(1 + TW_c) = R(1 + TW_c) = R(1 + \beta) \quad (21)$$

The false-alarm and detection probabilities for this case are given by [Ref. 1, p. 106, Eq. (3.32)]

$$\begin{aligned} P_F &= \Phi(-x), \\ P_D &= \Phi(d-x) = \Phi(\sqrt{1+\beta}\sqrt{R}-x), \end{aligned} \quad (22)$$

where\*  $x$  is selected for prescribed  $P_F$ . (For a specified performance ( $P_F$ ,  $P_D$ ) of this optimum processor for  $f = 1$ , required values of  $d$  can be read from Ref. 1, p. 88, Fig. IV.1.) When (22) is superposed on part A of Figs. 3 through 11, it lies everywhere above the square-law detection curves, as is expected. Furthermore, the slope of the straight lines ((22)), is greater than the slopes of the square-law detection curves. However, when (22) is superposed on parts B and C of Figs. 3 through 11, the equation lies below the square-law detection curves for small  $R$  and above it for the larger values of  $R$ . The square-law detector can give better performance in some regions of  $R$  (for  $f < 1$ ) than the optimum coherent receiver (for  $f = 1$ ) for the flat transmitted signal, because the transmitted signal (the flat waveform) is not the optimum one to transmit in this noise spectrum. Rather, a deterministic signal that oscillates arbitrarily fast in the interval  $T$  and, thereby, occupies a region of low-noise-density does arbitrarily good; there is no optimum signal unless we impose some bandwidth constraint. This case has not been considered here.

Two analytical results along a related line are possible for  $\beta = 0$ . From (C-7), it is found that the detection probability for fixed  $P_F$  and fixed  $R (> 0)$  always decreases as  $f$  increases from zero (for  $\Lambda_n > 0$ ) regardless of the values of the false-alarm probability and  $S/N$ . ( $\Lambda_n \leq 0$  and  $R \leq 0$  are uninteresting situations.) Of course, for large  $\Lambda_n$ , that is, low  $P_F$ , the rate of decrease is not very large and may not be noticeable from the plots. However, for large  $\Lambda_n$  and  $R$ , for example,  $R = \Lambda_n - 1$ , (C-7) gives

\* $\Phi$  is the CDF for a zero-mean unit variance Gaussian RV; see (C-3).

$$\left. \frac{\partial P_D}{\partial f} \right|_{f=0} = -(2\pi)^{-1/2} \exp(-1/2) \left( 1 - \frac{1}{\Lambda_n} \right), \quad (23)$$

which is significant.

For  $f = 1$ , we find the same result for  $\beta = 0$ ; see (C-8). The slope can become very negative for large  $\Lambda_n$ ; in fact,

$$\left. \frac{\partial P_D}{\partial f} \right|_{f=1} \sim - \frac{\Lambda_n}{2(2\pi e)^{1/2}} \text{ as } \Lambda_n \rightarrow \infty \quad (24)$$

$$R^{1/2} = \Lambda_n^{1/2} - 1$$

Thus, for  $\beta = 0$ , performance of the square-law detector is degraded as  $f$  increases toward 1 for certain S/N  $R$  and normalized thresholds  $\Lambda_n$ .

For large time-bandwidth products  $\beta$ , it is anticipated that the decision variable  $l$  in (6) could be approximated by a Gaussian RV. In Appendix E are presented the equations for the detection and false-alarm probabilities under this Gaussian assumption; see (E-3) and (E-4). In Fig. 12, these equations are plotted for  $\beta = 128$ , where  $f = 1, .2$ , and  $0$ , respectively. These approximate curves are generally above the exact curves given in Fig. 11 for the same conditions; that is, the Gaussian assumption gives optimistic performance predictions compared to the true value. However, the deviation is not great at  $\beta = 128$ .

For a specified performance ( $P_F, P_D$ ), the required input S/N  $R$  decreases to zero as  $T \rightarrow \infty$ . In fact, from (E-4), we find

$$P_F \sim \Phi(\sqrt{\beta}(1 - \Lambda_n)) \text{ as } \beta \rightarrow \infty, \quad (25)$$

where normalized threshold  $\Lambda_n$  is selected to keep the argument fixed; that is,

$$\sqrt{\beta}(\Lambda_n - 1) = \text{Th}(P_F) \quad (26)$$

is kept fixed at a threshold value that depends on the prescribed  $P_F$ . Then (E-3) yields

$$P_D \sim \Phi(\sqrt{\beta}R - \text{Th}(P_F)) \text{ as } \beta \rightarrow \infty. \quad (27)$$

Thus, the required S/N  $R$  decays as  $T^{-1/2}$  as  $T \rightarrow \infty$ , rather than according to  $T^{-1}$ ; this is attributable to the square-law detector characteristic. Notice that this rate of decay of required  $R$  holds regardless of the value of  $f$ ; that

is, it is independent of the fraction of each type of signal component. Although this rule was deduced from the Gaussian assumption, it holds in the general case because the decision variable  $l$  approaches Gaussian as  $\beta \rightarrow \infty$ .

Figures 4 through 11 may be used to obtain the exact values of the input S/N  $R$  that are required to attain a specified performance. In particular, for  $P_F = 10^{-n}$ ,  $n = 1(1)8$ , and  $P_D = .5$ , the required value of  $R$  (in decibels) is plotted versus  $\beta$  in Fig. 13. The three parts of the figure correspond to  $f = 1, .2, \text{ and } 0$ , respectively. The rate of decay of  $R$  with increasing  $\beta$  is approximately  $\beta^{-1/2}$ , as discussed above. In decibels, the decay is  $-5 \log_{10} \beta$ .

The Gaussian assumption, Fig. 12, gives values of S/N  $R$  that are optimistic by amounts that depend on the quality of performance desired. For example, the Gaussian approximation for  $\beta = 128$ ,  $P_F = 10^{-8}$ , and  $P_D = .5$  indicates a required S/N of  $-3.05$  dB for all  $f$ ,\* whereas the actual required S/N is  $-1.98$  dB, a difference of  $1.07$  dB. In fact, the  $-3.05$ -dB S/N would yield a  $P_F$  greater than  $10^{-6}$  at  $\beta = 128$ . (For  $\beta = 64$ , the difference in decibels increases to almost  $1.5$  dB.) However, for  $P_F = .1$ , instead of  $10^{-8}$ , the decibel difference between the exact answer and the Gaussian approximation is only  $.28$  dB at  $\beta = 128$ . These comparisons have been made here only at the  $P_D = .5$  level, and conclusions at other levels can be very different. Figures 3 through 11 furnish information for required S/N at other performance levels of interest.

A note of caution is in order at this point: From (C-1), (C-5), and (C-6), for  $\beta = 0$ , if  $f = 1$ , the decision variable  $l$  is given by

$$l = (p_c^{1/2} + n)^2 \quad (28)$$

and

$$\begin{aligned} P_D &= \Phi(R^{1/2} - \Lambda_n^{1/2}) + \Phi(-R^{1/2} - \Lambda_n^{1/2}) \quad , \\ P_F &= 2\Phi(-\Lambda_n^{1/2}) \quad . \end{aligned} \quad (29)$$

\*This independence of  $f$  for required S/N is true only for  $P_D = .5$ ; see (E-3).

Now for a fixed  $P_F$ ,  $\Lambda_n$  is fixed, and  $P_D$  versus  $R^{1/2}$  plots as a straight line on normal-probability paper (for example, see Figs. 3 through 11) for all values of  $\Lambda_n$ . However, the RV  $l$  in (28) is definitely not Gaussian. Thus, a straight-line plot on normal-probability paper can not be interpreted as corresponding to a Gaussian RV.

### 3.2 NARROWBAND CASE

Most of the comments in the previous subsection are applicable here and will not be repeated, for the sake of brevity. Also the notation is similar, except that

$$\hat{\beta} = \hat{W}_c T \quad (30)$$

Values of the required normalized threshold  $\Lambda_n$  for different values of  $\hat{\beta}$  and specified  $P_F$  are given in Table 2. As anticipated in Section 2.3, the thresholds for large time-bandwidth product  $\hat{\beta}$  are virtually identical to those for the LF case (Table 1). However, the thresholds for small  $\hat{\beta}$  are quite different.

Table 2  
THRESHOLDS FOR NB PROCESSOR

$P_F \backslash \hat{\beta}$	0	1	2	4	8	16	32	64	128
$10^{-1}$	2.303	1.979	1.799	1.615	1.454	1.326	1.232	1.163	1.115
$10^{-2}$	4.605	3.680	3.123	2.528	2.044	1.703	1.475	1.324	1.222
$10^{-3}$	6.908	5.381	4.447	3.423	2.593	2.036	1.681	1.454	1.307
$10^{-4}$	9.210	7.083	5.770	4.316	3.129	2.349	1.868	1.569	1.381
$10^{-5}$	11.513	8.784	7.093	5.209	3.658	2.652	2.045	1.676	1.448
$10^{-6}$	13.816	10.485	8.416	6.101	4.184	2.948	2.215	1.778	1.510
$10^{-7}$	16.118	12.186	9.739	6.994	4.709	3.240	2.380	1.874	1.569
$10^{-8}$	18.421	13.687	11.063	7.886	5.233	3.528	2.541	1.968	1.626

In Figs. 14 through 22, plots of  $P_D$  versus  $R^{1/2}$  are presented for the NB processor, with  $P_F$  as a parameter. For  $\hat{\beta} = 128$ , the curves are virtually identical to those for the LF case; thus, the Gaussian approximation could be applied here with equal validity as for the LF case. Also, this corroborates the anticipated equality of performance for the definitions of effective bandwidth adopted earlier. The curves exhibit behavior similar to that for the LF case, particularly the cross-over for different values of  $f$ .

The required input S/N  $R$  to attain  $P_F = 10^{-n}$ ,  $n = 1(1)8$ , and  $P_D = .5$  is plotted in Fig. 23 for the NB case. The required S/N is less than the one in the LF case for small  $\hat{\beta}$ , but is virtually identical to the LF case for large  $\hat{\beta}$ . Required values of  $R$  for other detection probabilities are available from Figs. 14 through 22.

## 4. DISCUSSION

In the problem considered here, no assumptions about the size of the time-bandwidth product are necessary, and the decision variable need not be approximately Gaussian. Small false-alarm probabilities can be easily and very accurately investigated numerically. The complexity of the closed form CF, even for the relatively simple case considered here, precludes any analytic solution for the CDF; nevertheless, very accurate answers for the CDF can be obtained. This numerical approach is recommended for other problems of this type.

For each doubling of the time-bandwidth product, it has been shown that the required input S/N R decreases by 1.5 dB (for large products) in order to maintain a prescribed performance ( $P_F$ ,  $P_D$ ). This result is similar to that cited for an envelope detector [Ref. 18, p. 262, and Exercises 8.8 and 8.9] and is a result of the squaring operation in the receiver. The improved performance for  $f = 0$  versus  $f = 1$  at low S/N has also been observed for other processors operating in fading media [Ref. 18, pp. 208-9 and pp. 214-5].

Use of a Gaussian approximation on the decision variable for large time-bandwidth products is in error by approximately 1 dB when the time-bandwidth product is 100. For larger products, the Gaussian approximation yields progressively better estimates, at least for detection probabilities that are not extreme and for false-alarm probabilities that exceed  $10^{-8}$ . This applies to both the LF and NB processors under the conditions investigated here.

Some extensions of the problem studied here are possible. They center around the ability to obtain the CF of the decision variable either in a closed form or in a reasonable amount of computer time. For example, suppose the decision variable  $l$  is given as a weighted sum,

$$l = \sum_{k=1}^N w_k l_k, \quad (31)$$

where the  $k$ th branch output,  $l_k$ , has signal  $s_k(t)$  and noise  $n_k(t)$  independent of all other branches. (This occurs, for example, if a bank of filters is excited by broadband processes, and the filter in the  $k$ th branch is disjoint with that in the  $j$ th branch for  $j \neq k$ .) The statistical situation obtaining in the  $k$ th branch can be any one of the six cases listed under (6) and (10) and can be dissimilar in different branches. Furthermore, the time of observation, the effective bandwidth, center frequency, and S/N can be different in each branch. The CF corresponding to the RV  $l$  in (31) is given by

$$f_{\ell}(\xi) = \prod_{k=1}^N f_k(w_k \xi) , \quad (32)$$

where  $f_k(\xi)$  is the CF of the RV  $\ell_k$  in the  $k$ th branch.

Examples that fit into the framework of (31) include the following:

- a. Multitone active detection or communication in a time-varying random medium that gives rise to the scatter component of the received signal. (The multiple tones could be transmitted to combat fading or jamming or both.)
- b. Multitone passive detection, where the scatter component of the received signal may be due to either medium perturbations or source instabilities.
- c. Single-tone passive detection by comparison with a threshold established from neighboring filter outputs.

A compilation of performance-capability characteristics has been presented for continuous processing of both LF and NB processes. However, they are limited to an identical exponential correlation of the random received signal and noise processes; nonidentical spectra, for example, of the signal and noise processes are disallowed. The only other continuous processor that yields closed-form expressions for the CF of the decision variable is an exponential integrator [Ref. 7, p. 41], rather than the finite-time average considered here. However, it, too, requires an exponential correlation function. The only reasonable way to generalize to arbitrary (unequal) signal and noise spectra is to consider sampled processors. Often this is the practical situation anyway. The decision variable for the square-law detector can then be transformed into a sum of squares of independent Gaussian variables, and the CF evaluated as a finite product. If the size of this product is not excessive, direct numerical calculation of the CF and, hence, the CDF by the methods in Refs. 15 and 16 is possible. This approach will be the subject of future investigation on more general processors and spectra.

In passing, it is noticed that the detection problem posed here is theoretically a singular one for the purely incoherent signal; that is, detection can be accomplished with zero probability of error (see, for example, Ref. 1, pp. 304-306). However, the optimum method of processing is impractical — it would require precise knowledge and use of all the eigenvalues of the correlation kernel; equivalently, second-derivatives of the observed process are required. The physical impossibility of accomplishing this in a practical case forces us to adopt a suboptimum procedure similar to that considered here.

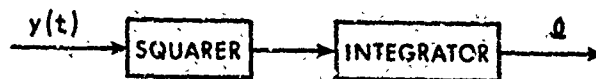


Fig. 1. Low-Frequency Processor

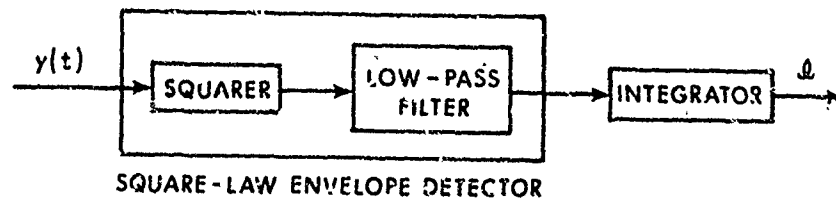


Fig. 2. Narrowband Processor

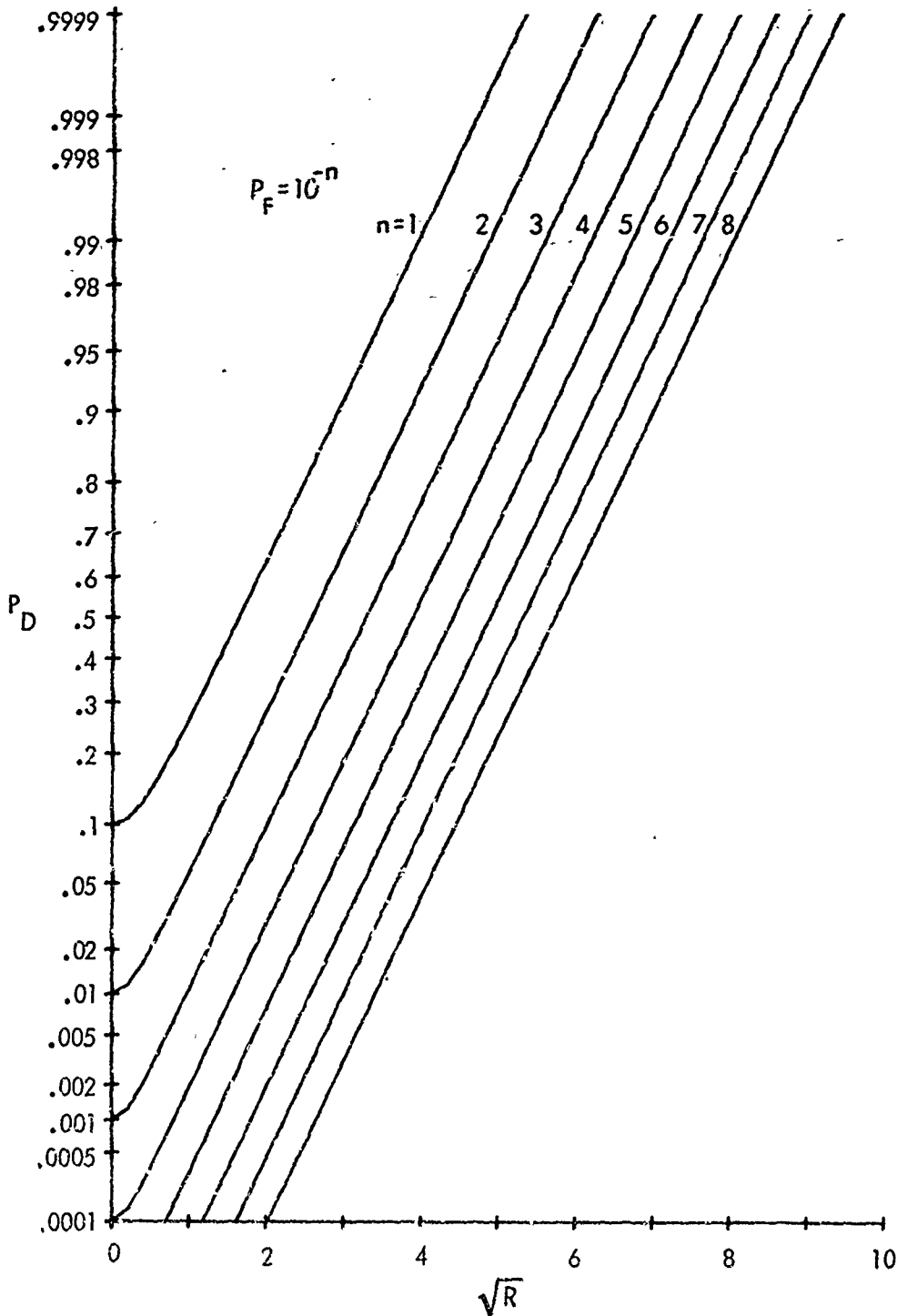


Fig. 3A.  $f = 1$   
 Fig. 3. Detection Probability; LF,  $\beta = 0$

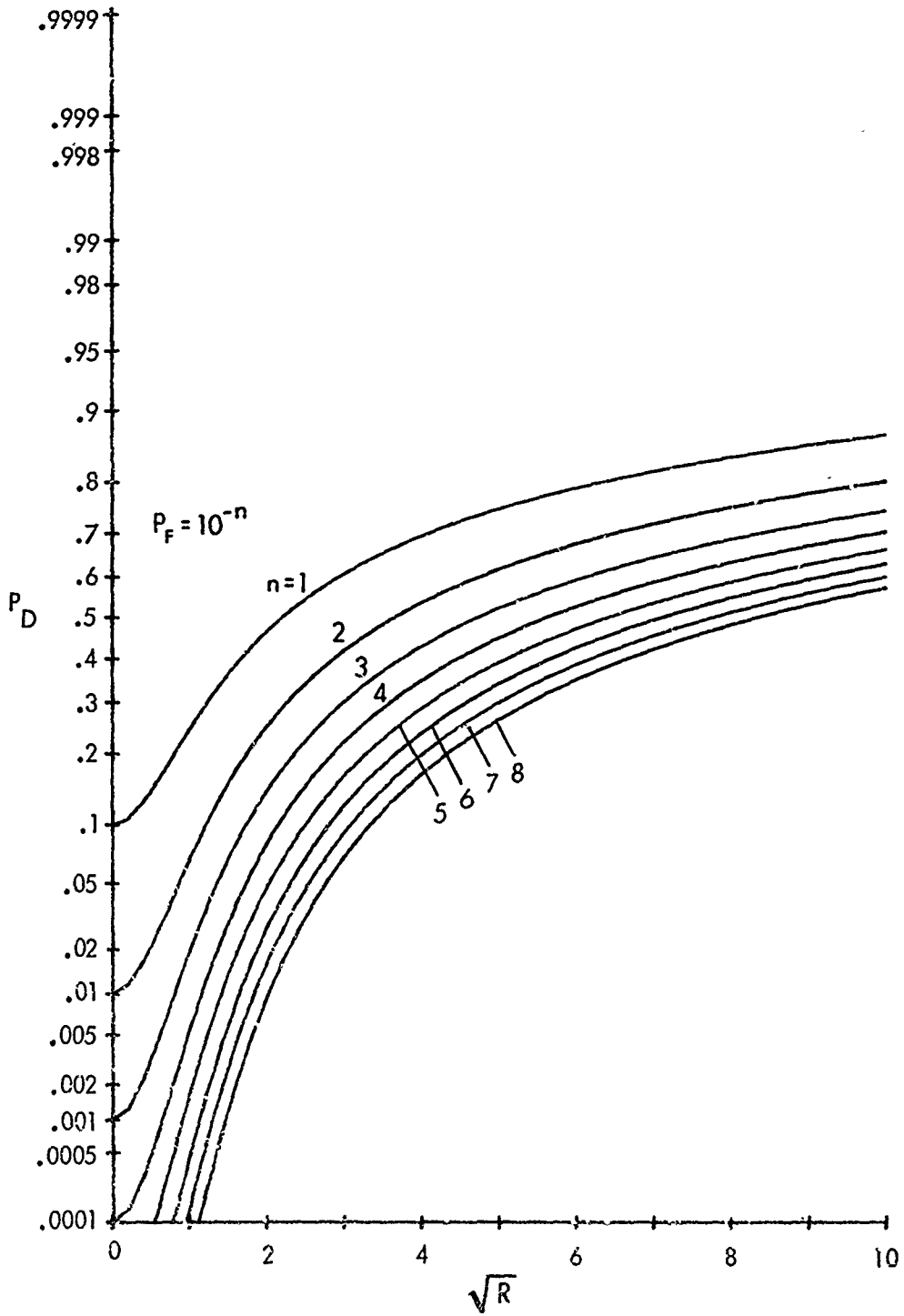


Fig. 3B.  $f = .2$   
 Fig. 3. Detection Probability; LF,  $\beta = 0$

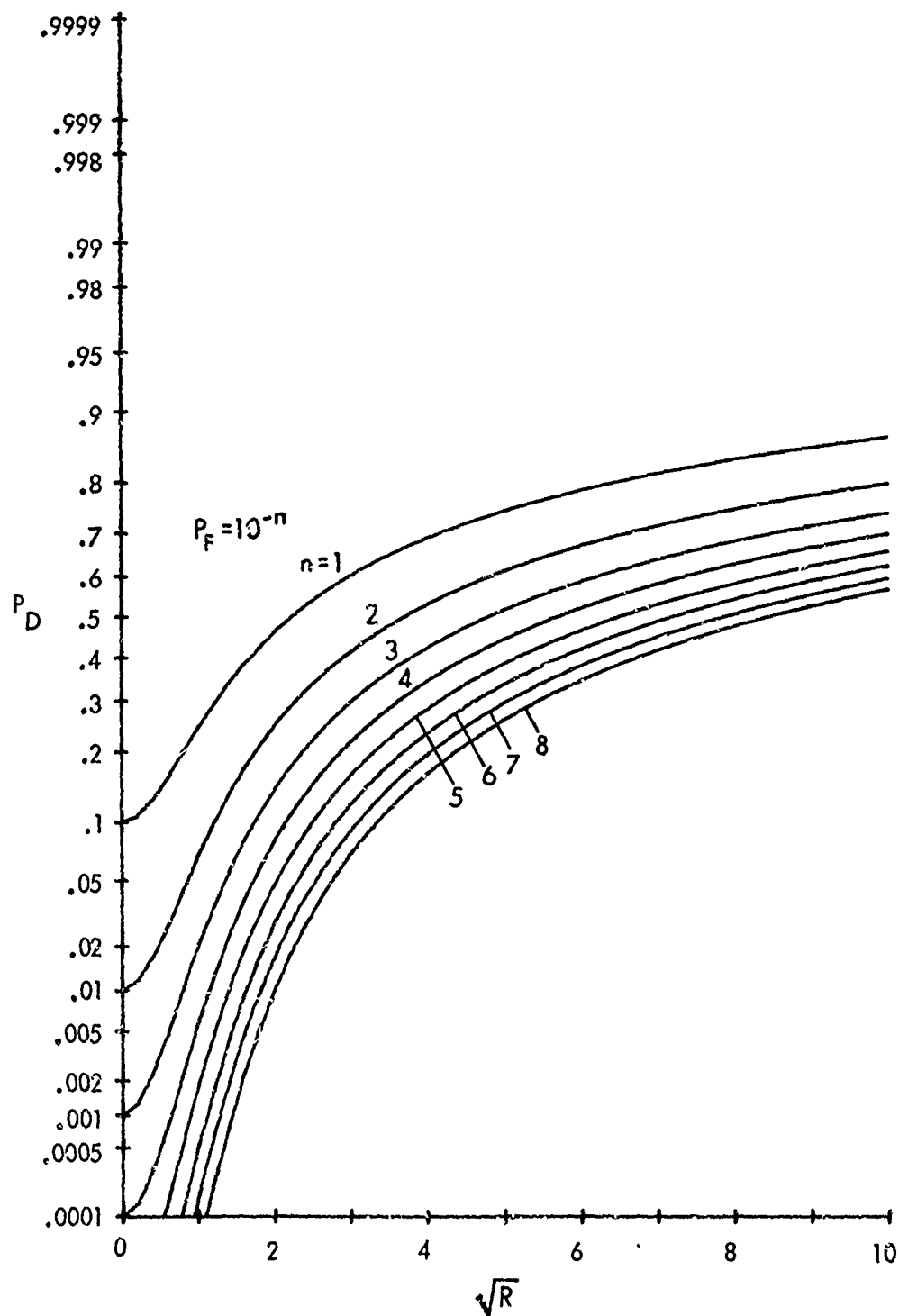


Fig. 3C.  $f = 0$   
 Fig. 3. Detection Probability; LF,  $\beta = 0$

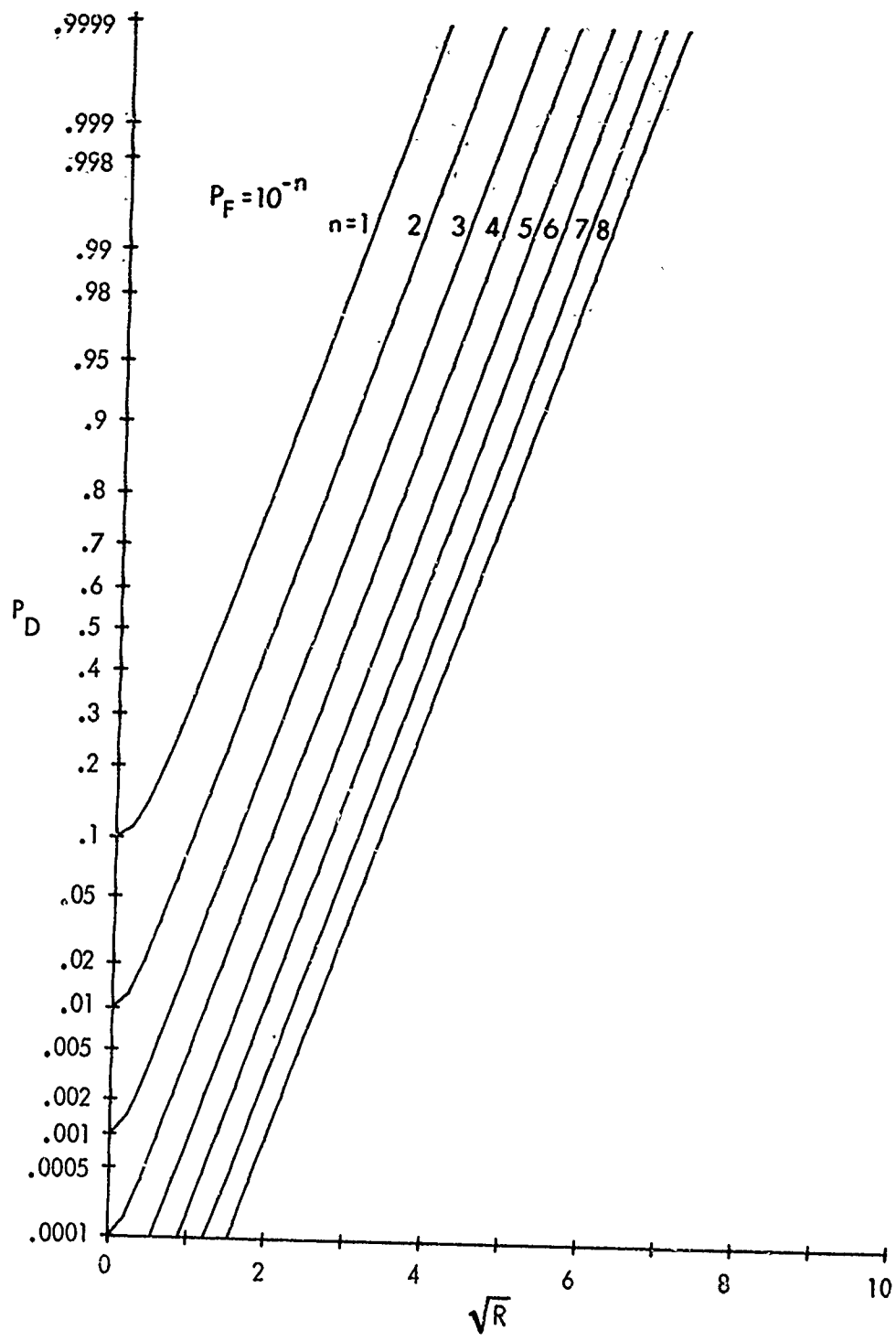


Fig. 4A.  $f = 1$   
Fig. 4. Detection Probability; LF,  $\beta = 1$

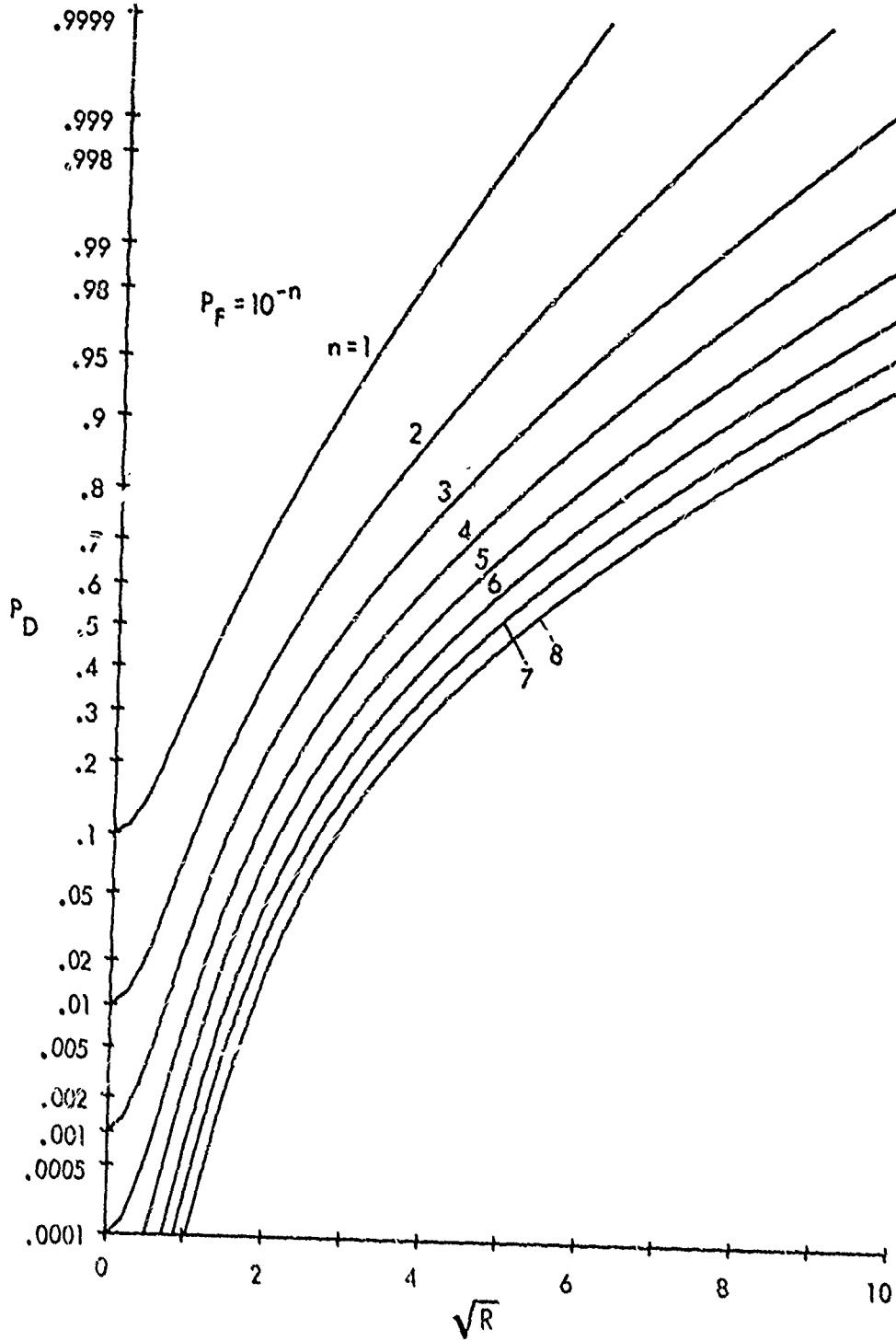


Fig. 4B.  $f = .2$   
Fig. 4. Detection Probability; LF,  $\beta = 1$

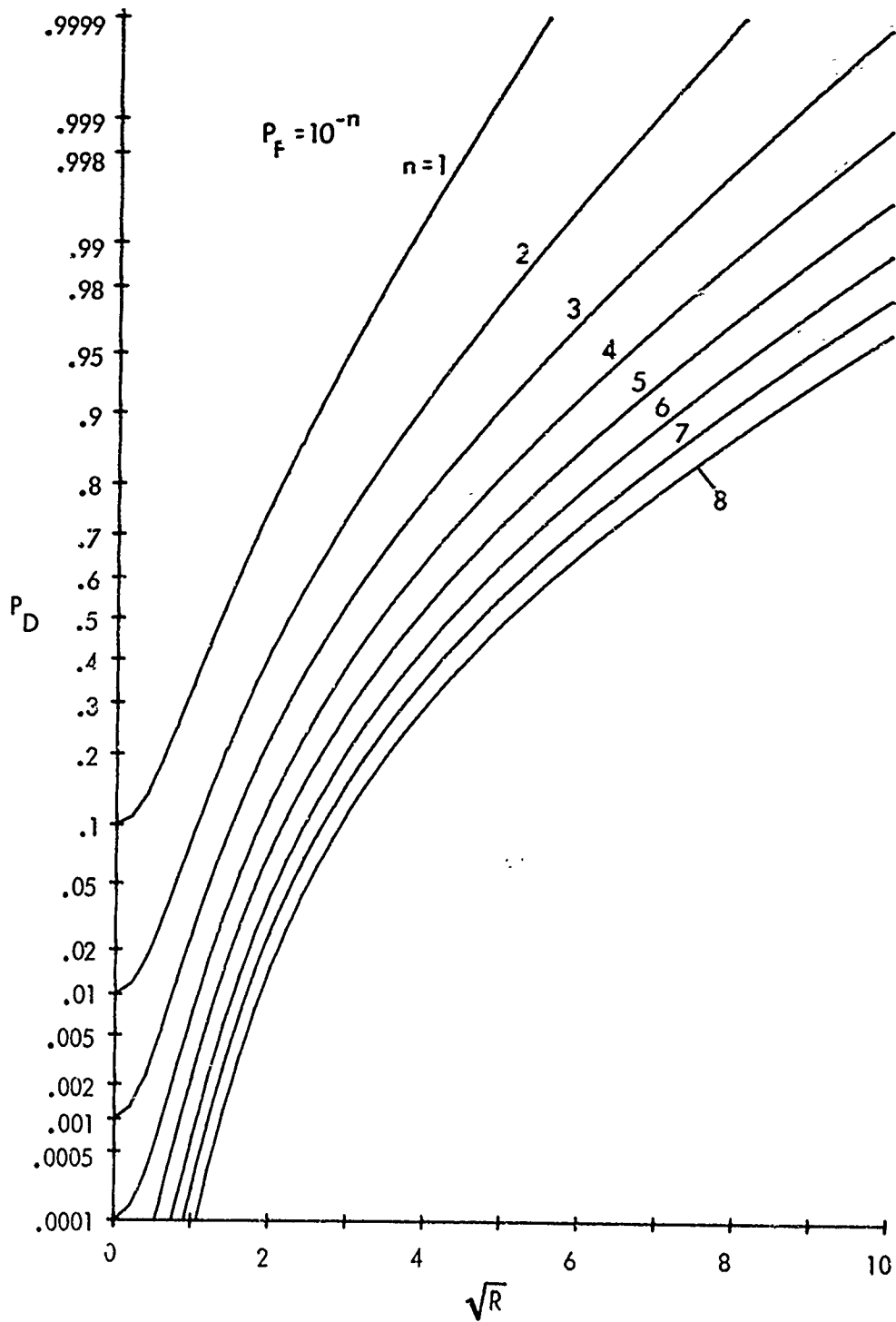


Fig. 4C.  $f = 0$   
 Fig. 4. Detection Probability; LF,  $\beta = 1$

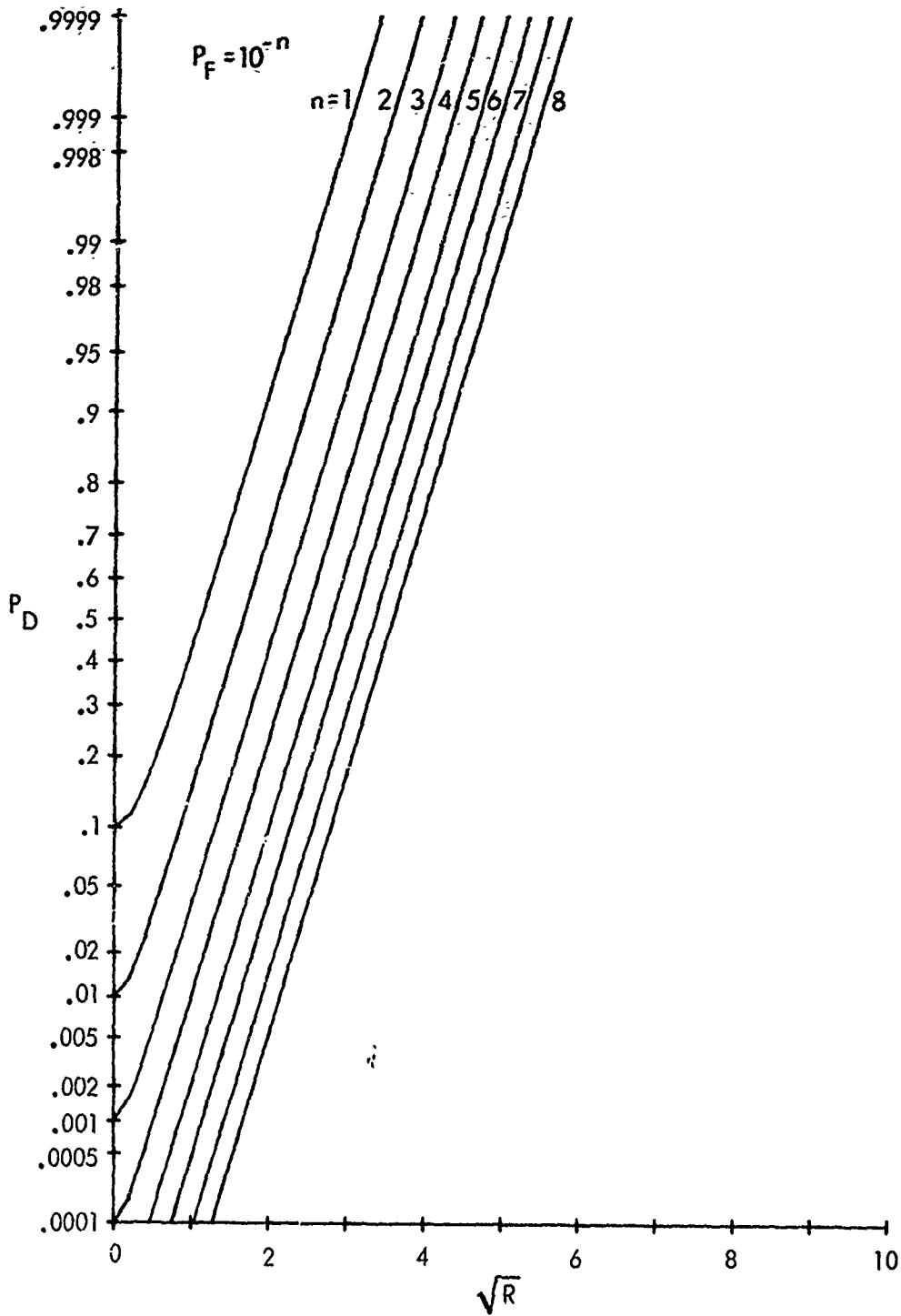


Fig. 5A.  $f = 1$   
 Fig. 5. Detection Probability; LF,  $\beta = 2$

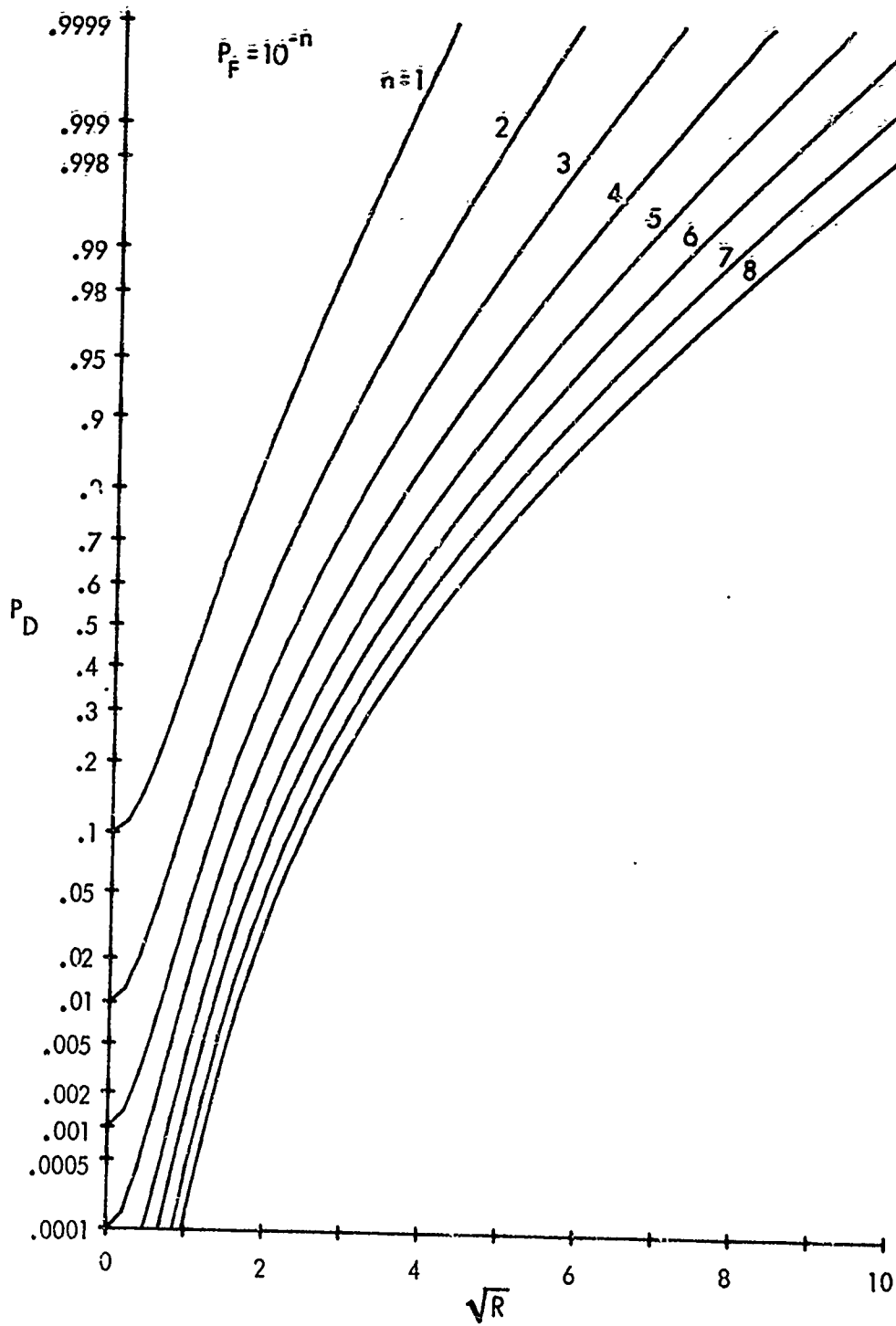


Fig. 5B.  $f = .2$   
 Fig. 5. Detection Probability; LF,  $\beta = 2$

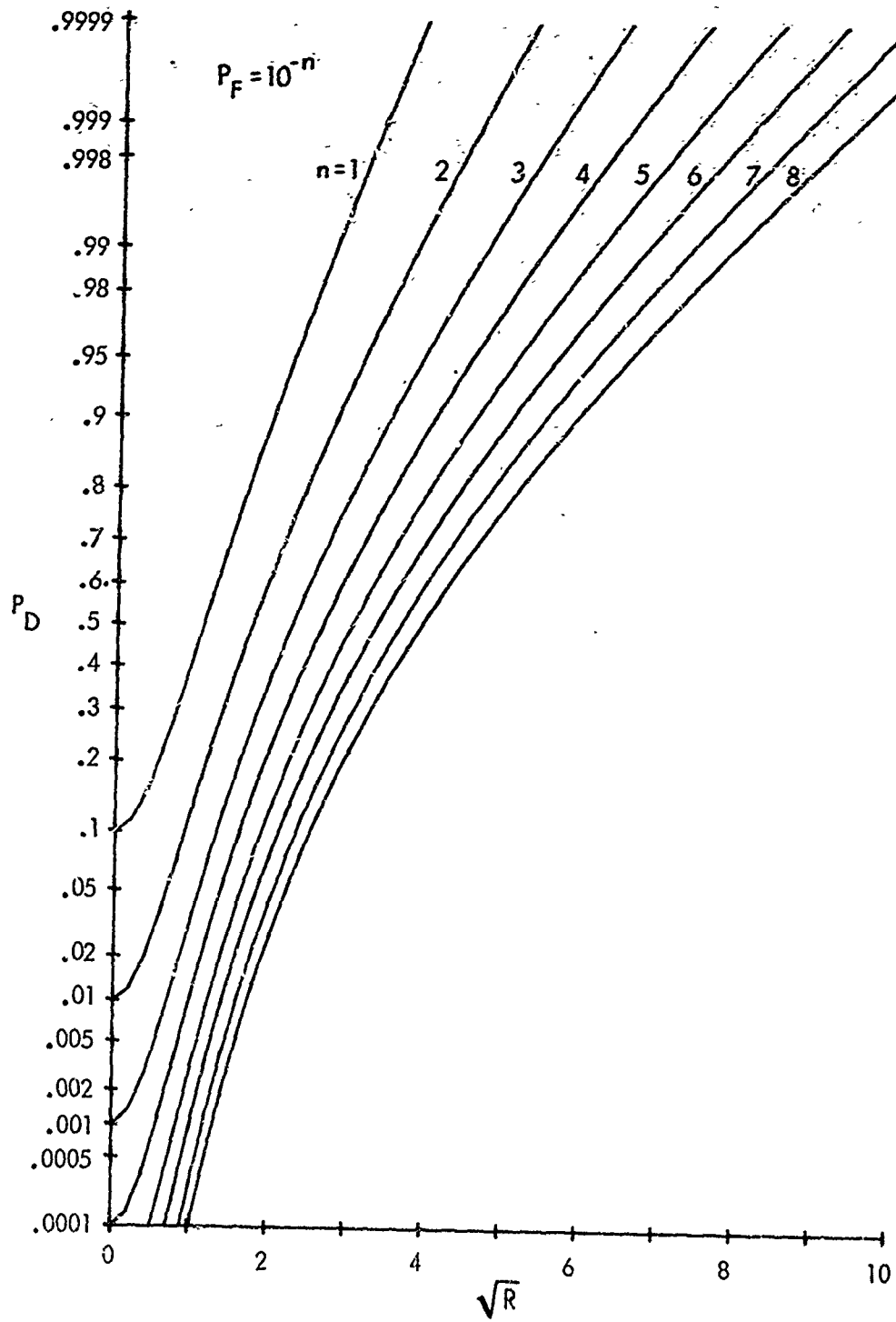


Fig. 5C.  $f = 0$   
Fig. 5. Detection Probability; LF,  $\beta = 2$

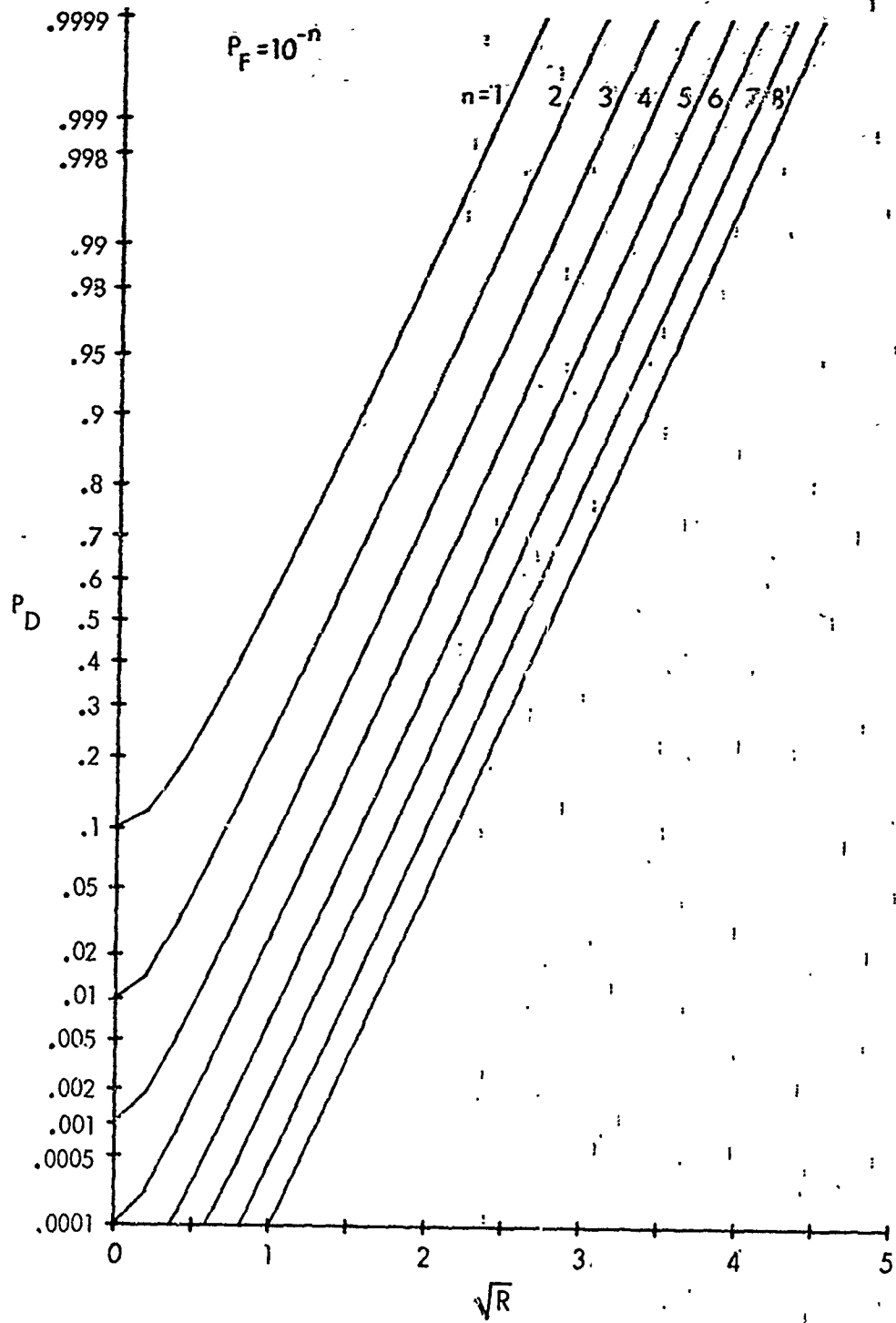


Fig. 6A.  $f = 1$   
 Fig. 6. Detection Probability; LF,  $\beta = 4$

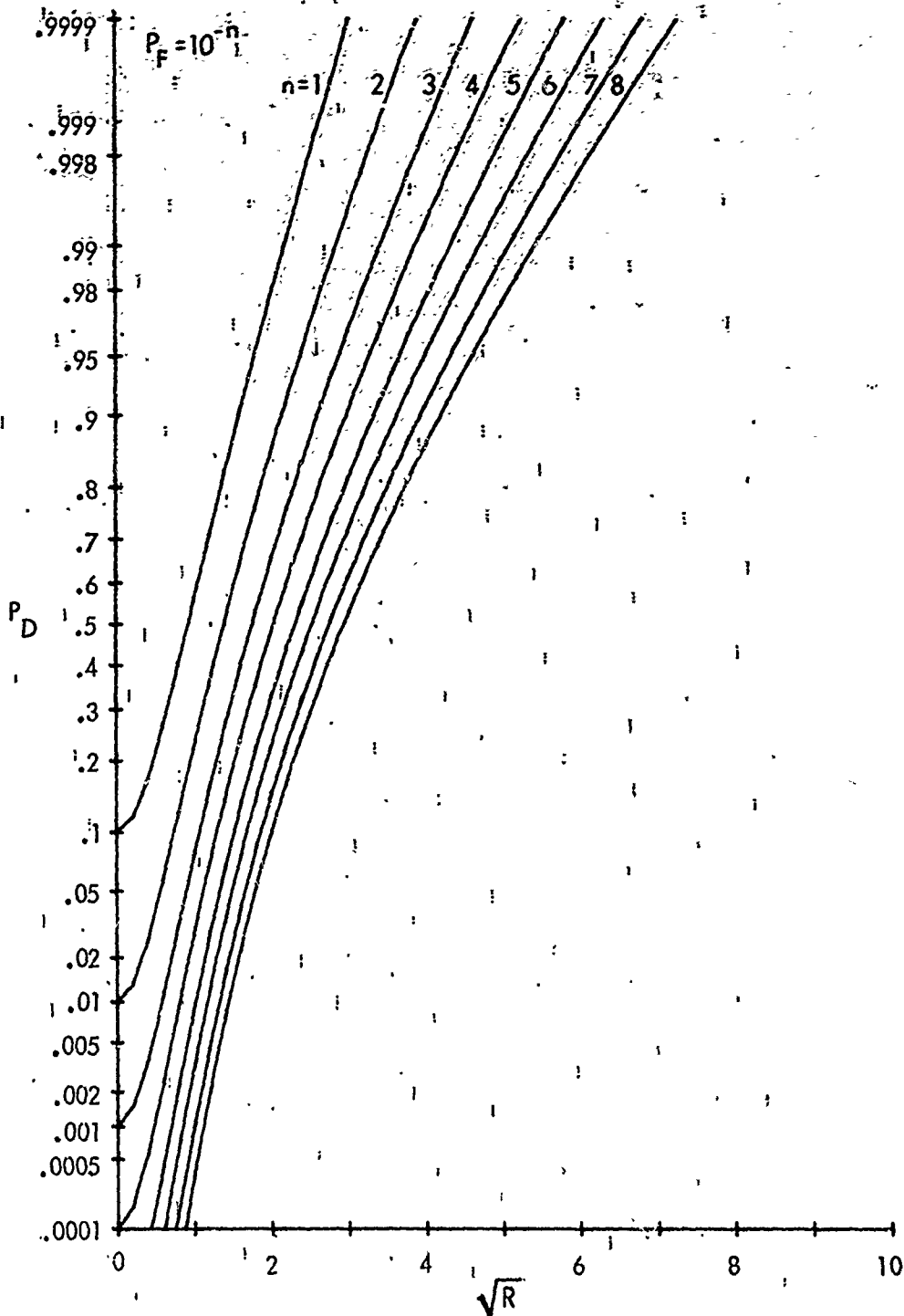


Fig. 6B.  $f = .2$

Fig. 6. Detection Probability; LF,  $\beta = 4$

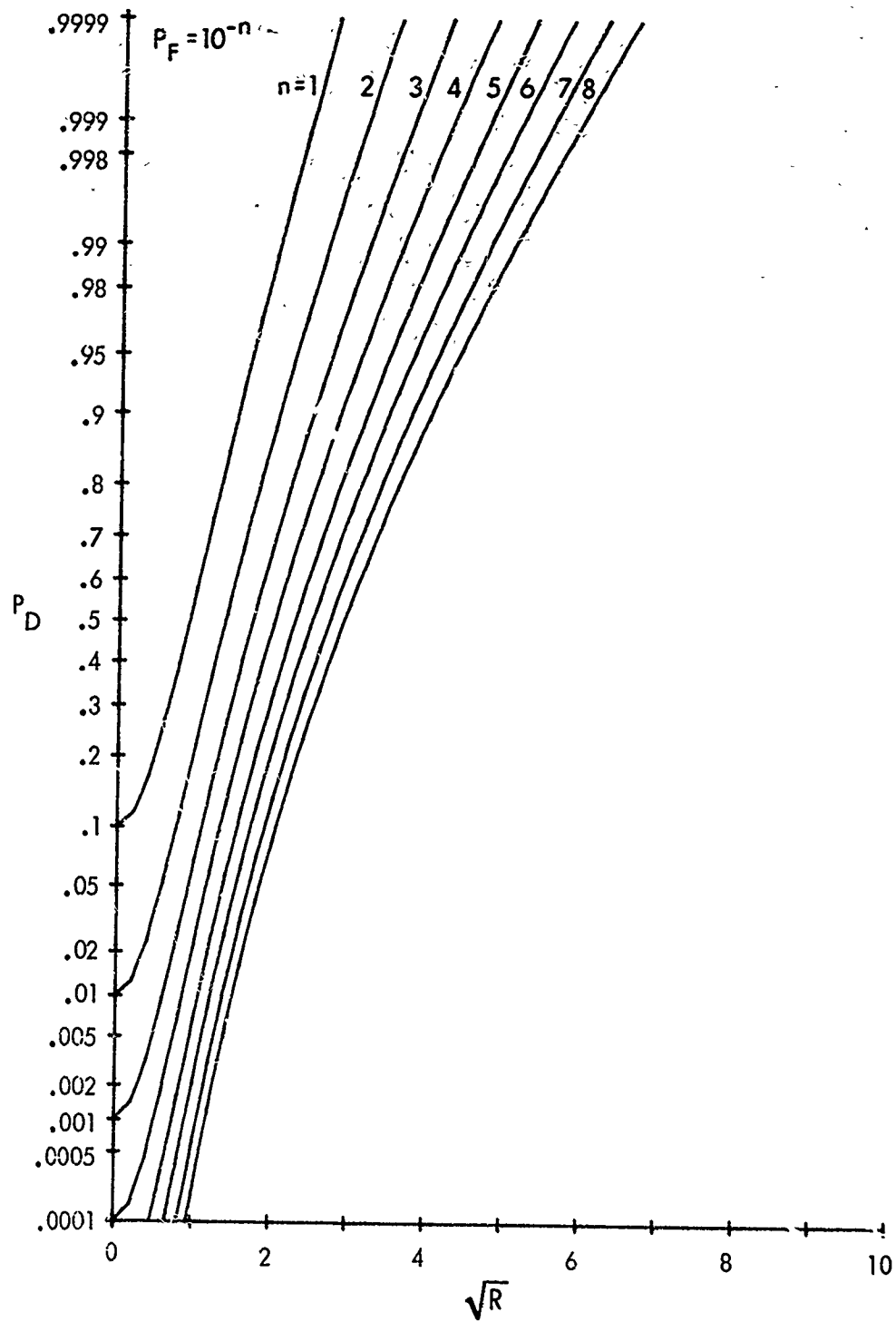


Fig. 6C.  $f = 0$   
Fig. 6. Detection Probability; LF,  $\beta = 4$

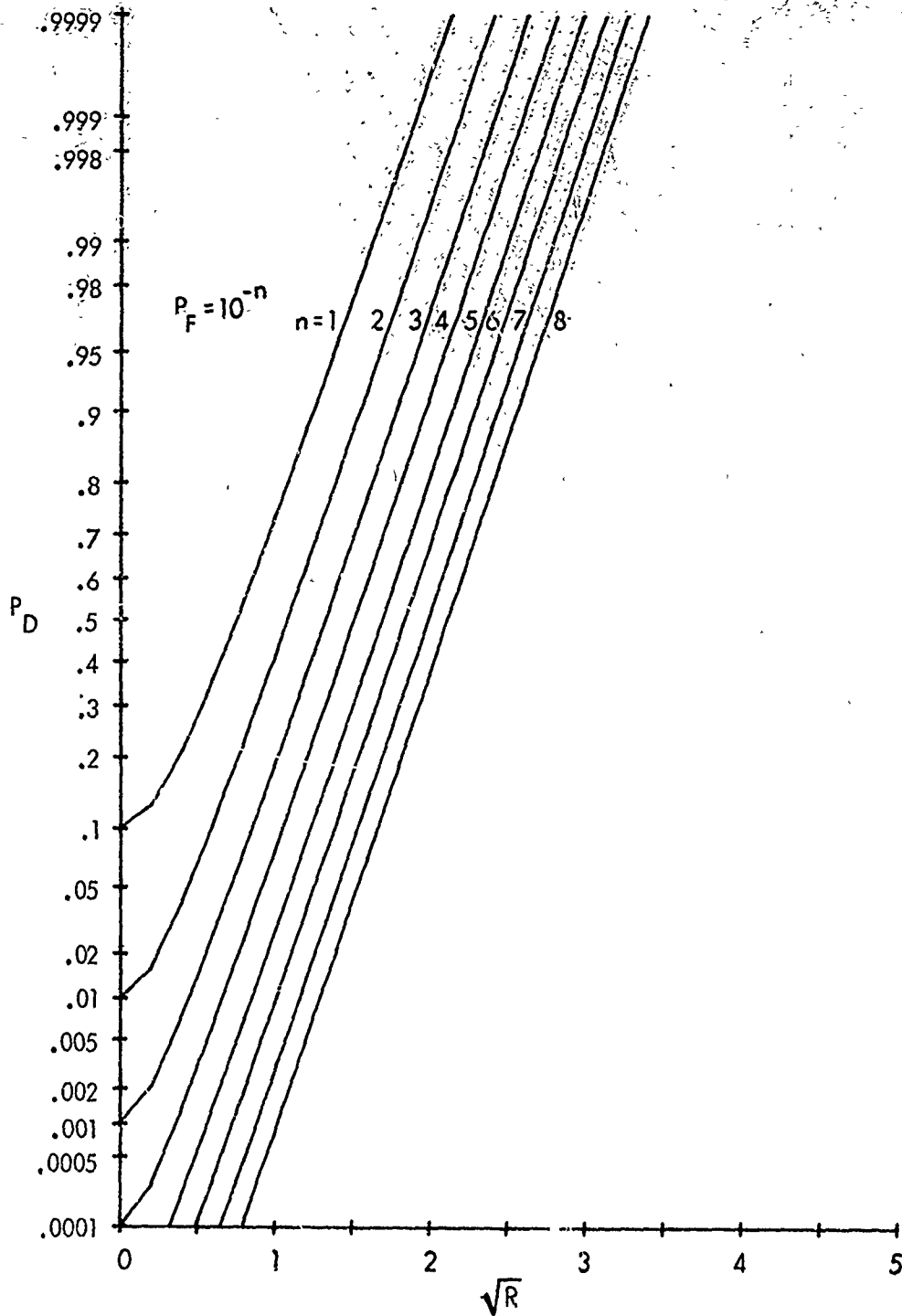


Fig. 7A.  $f = 1$   
 Fig. 7. Detection Probability; LF,  $\beta = 8$

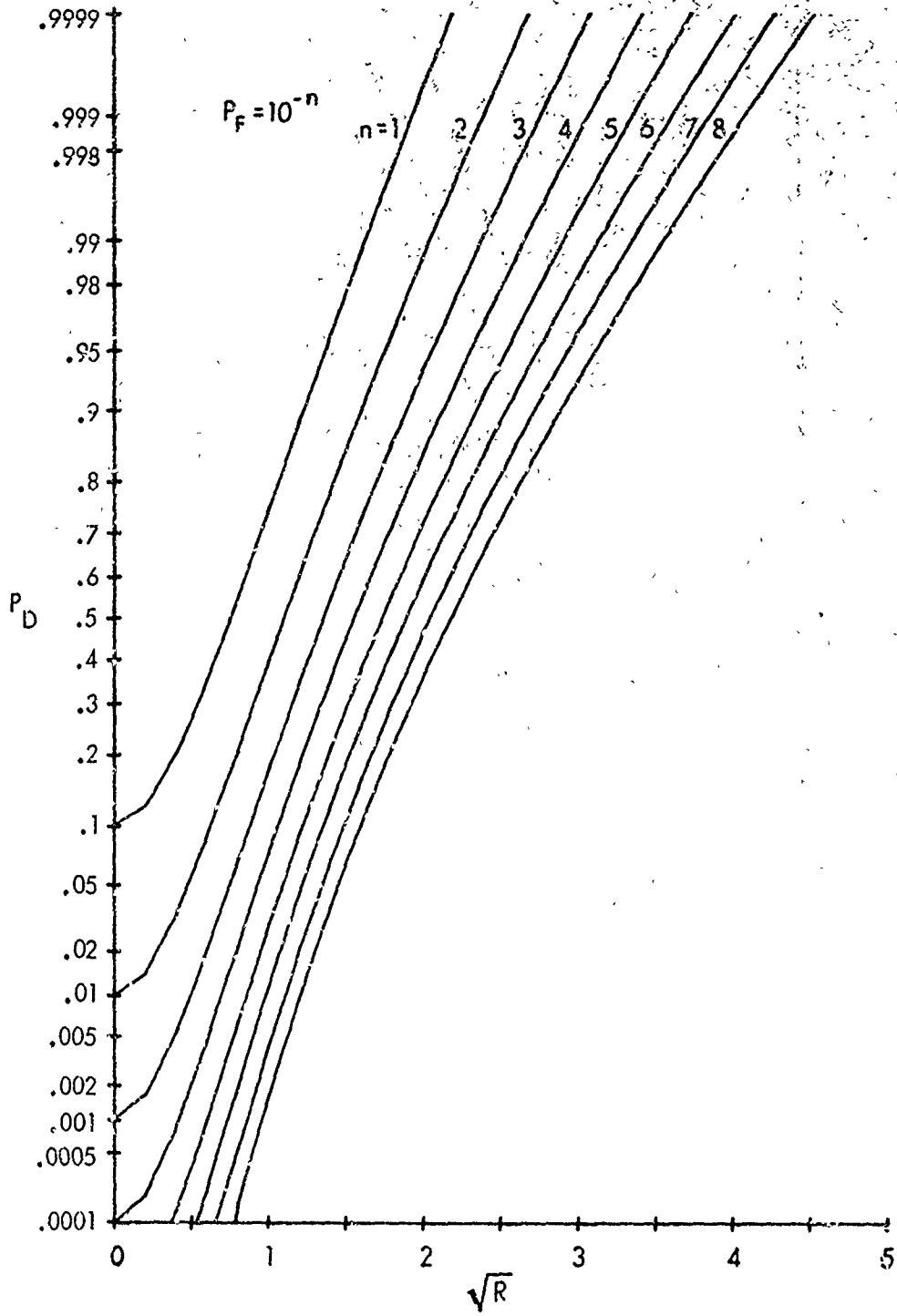


Fig. 7B.  $f = .2$   
Fig. 7. Detection Probability; LF,  $\beta = 8$

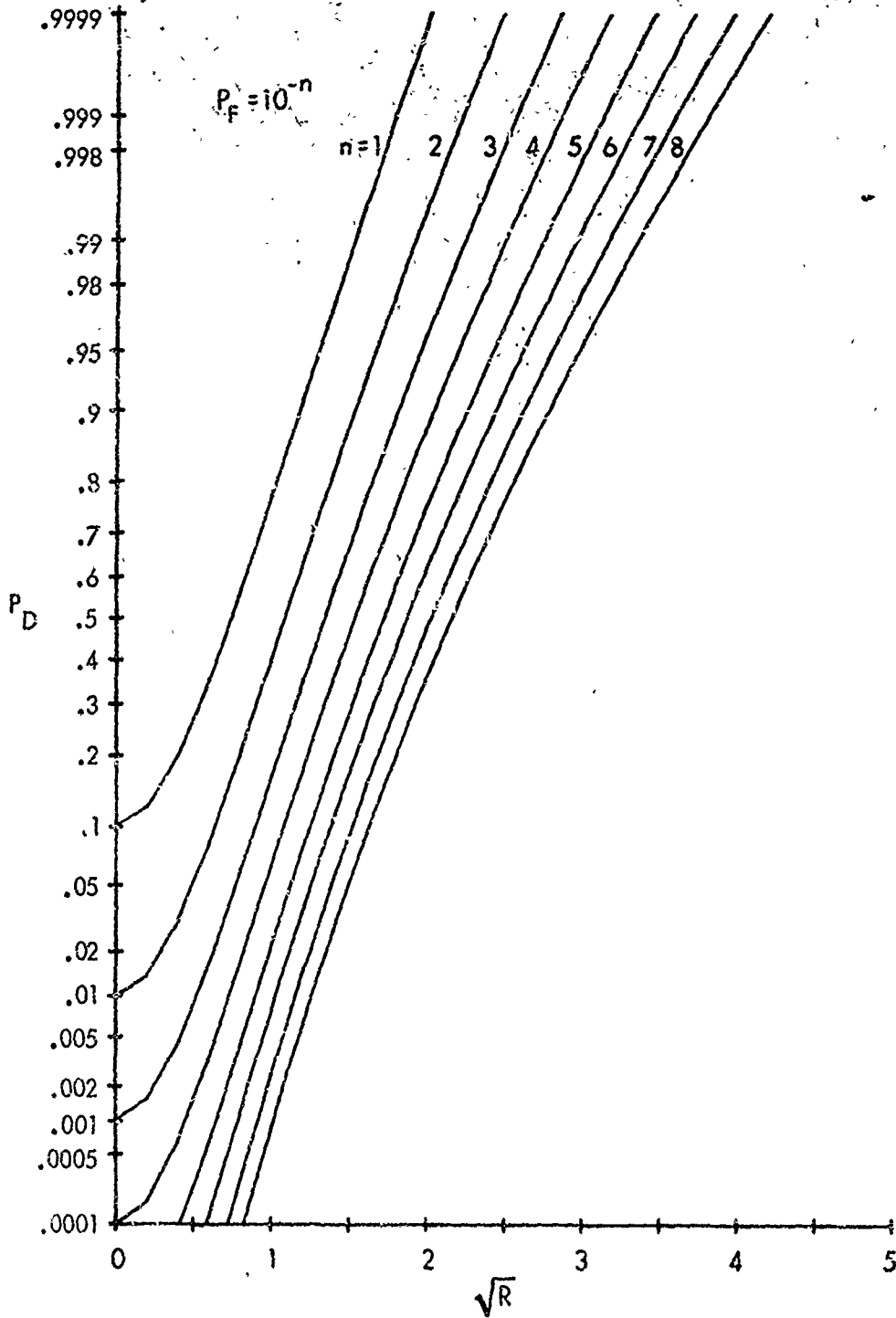


Fig. 7C.  $f = 0$   
 Fig. 7. Detection Probability; LF,  $\beta = 8$ .

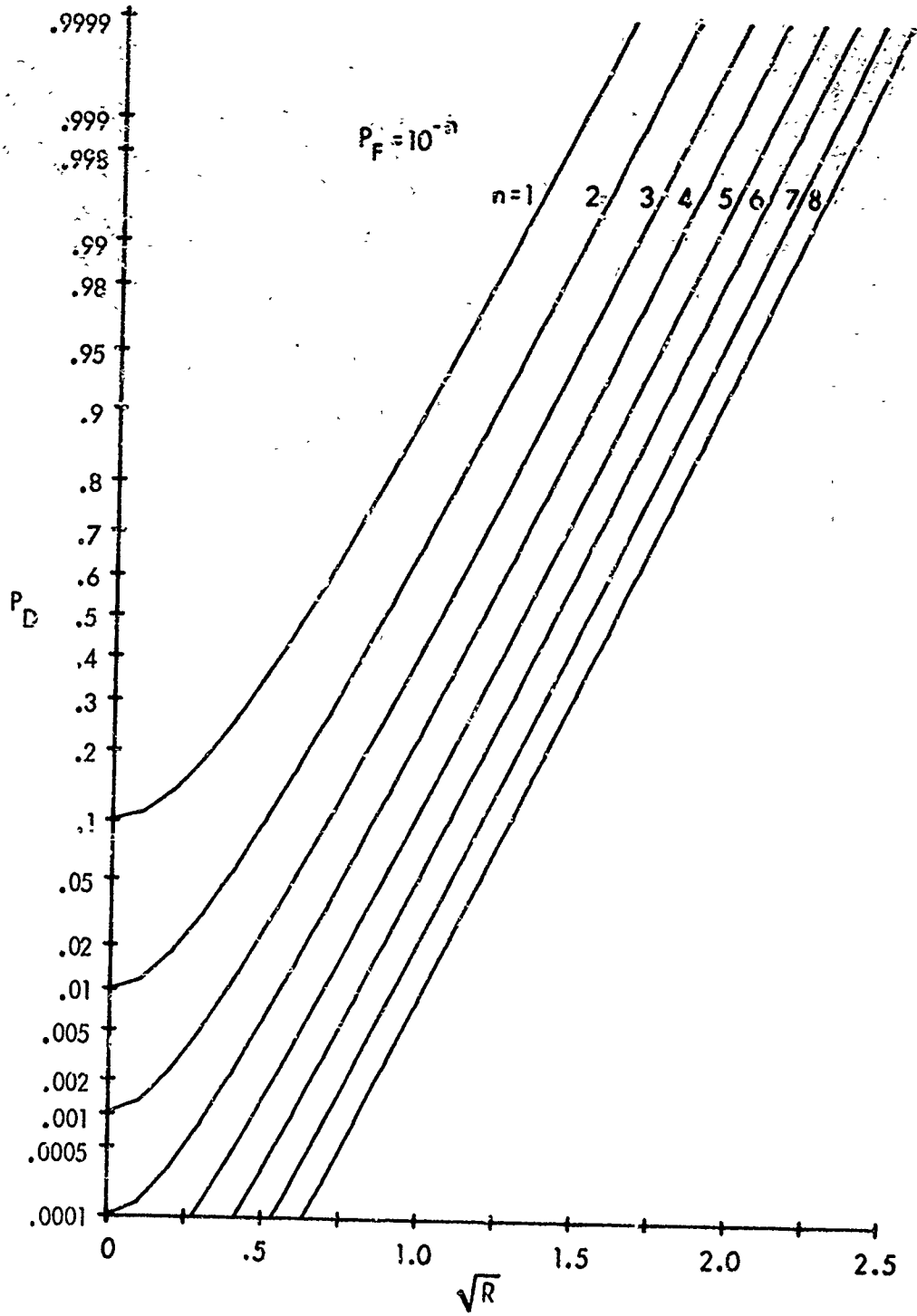


Fig. 8A.  $f = 1$   
Fig. 8. Detection Probability; LF,  $\beta = 16$

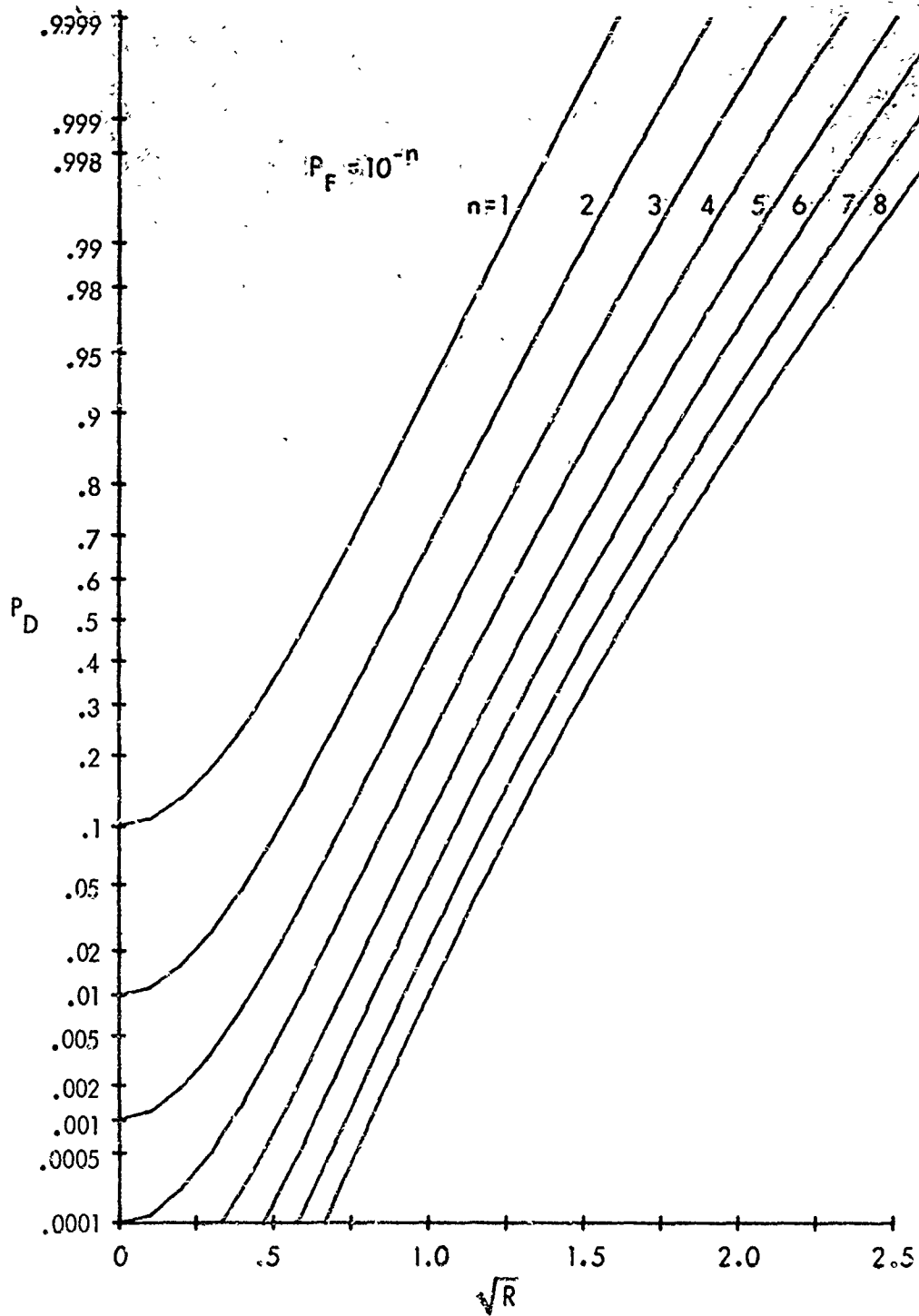


Fig. 8B.  $f = .2$   
 Fig. 8. Detection Probability; LF,  $\beta = 16$

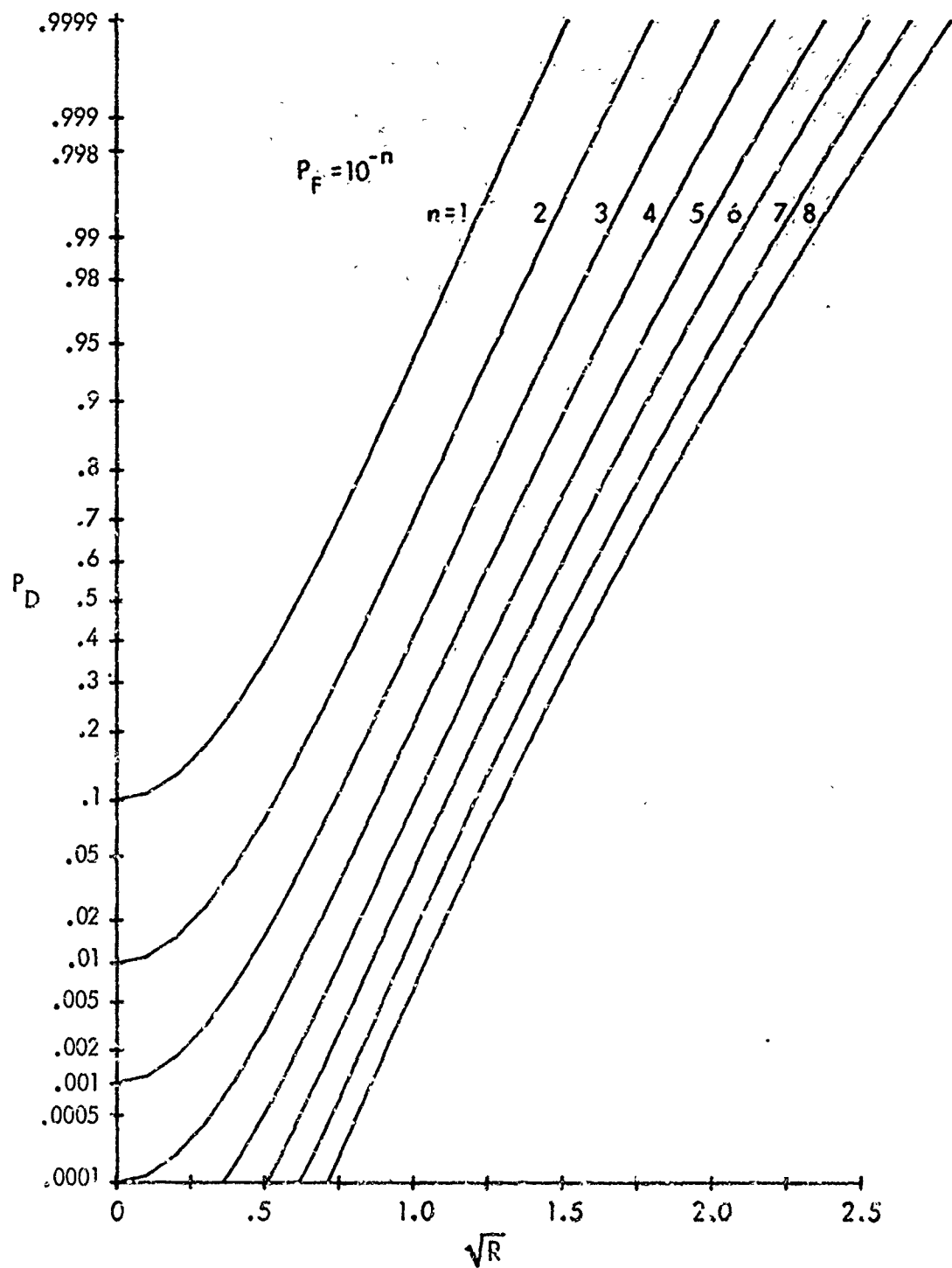


Fig. 8C.  $f = 0$   
 Fig. 8. Detection Probability; LF,  $\beta = 16$

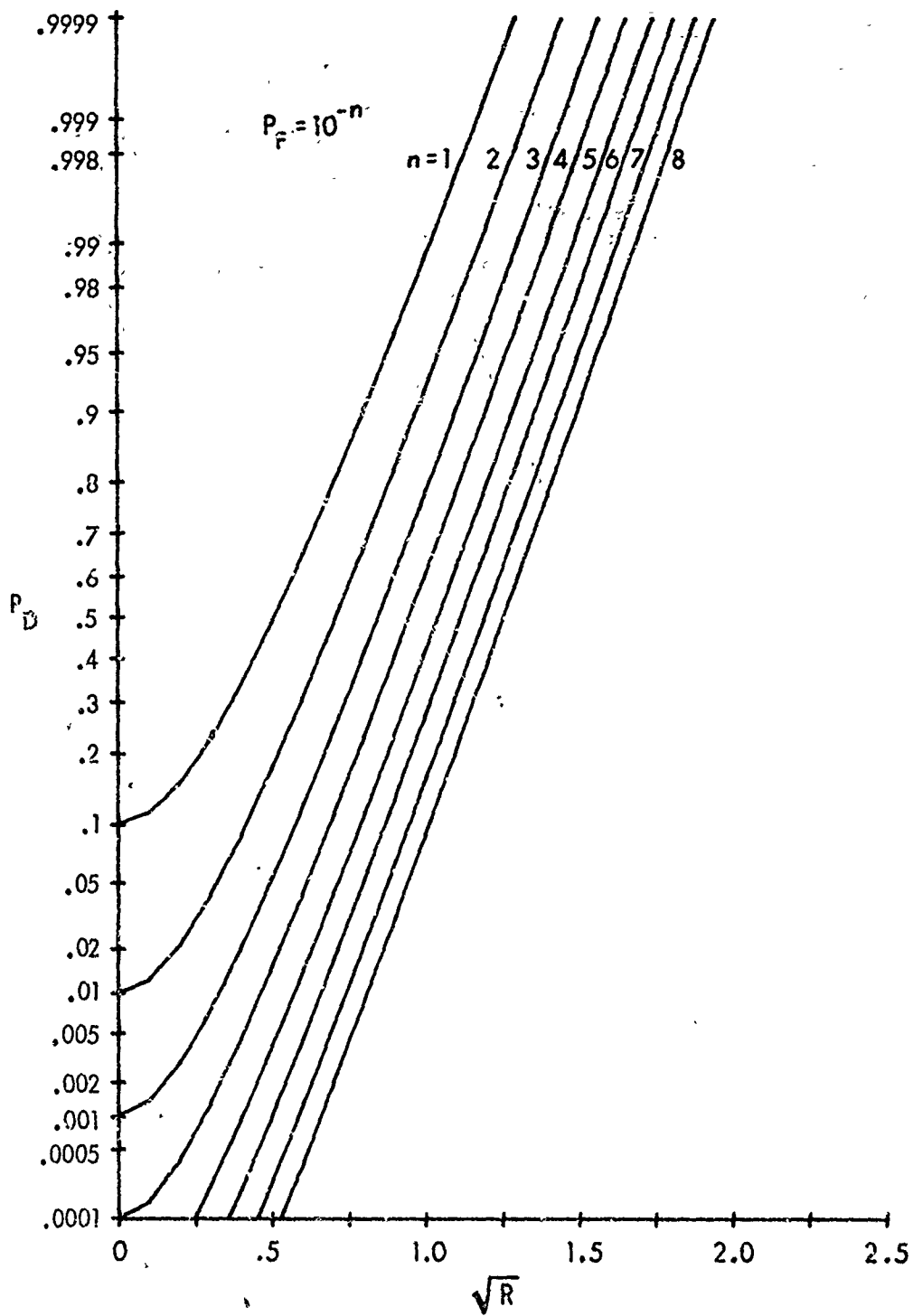


Fig. 9A.  $f = 1$   
 Fig. 9. Detection Probability; LF,  $\beta = 32$

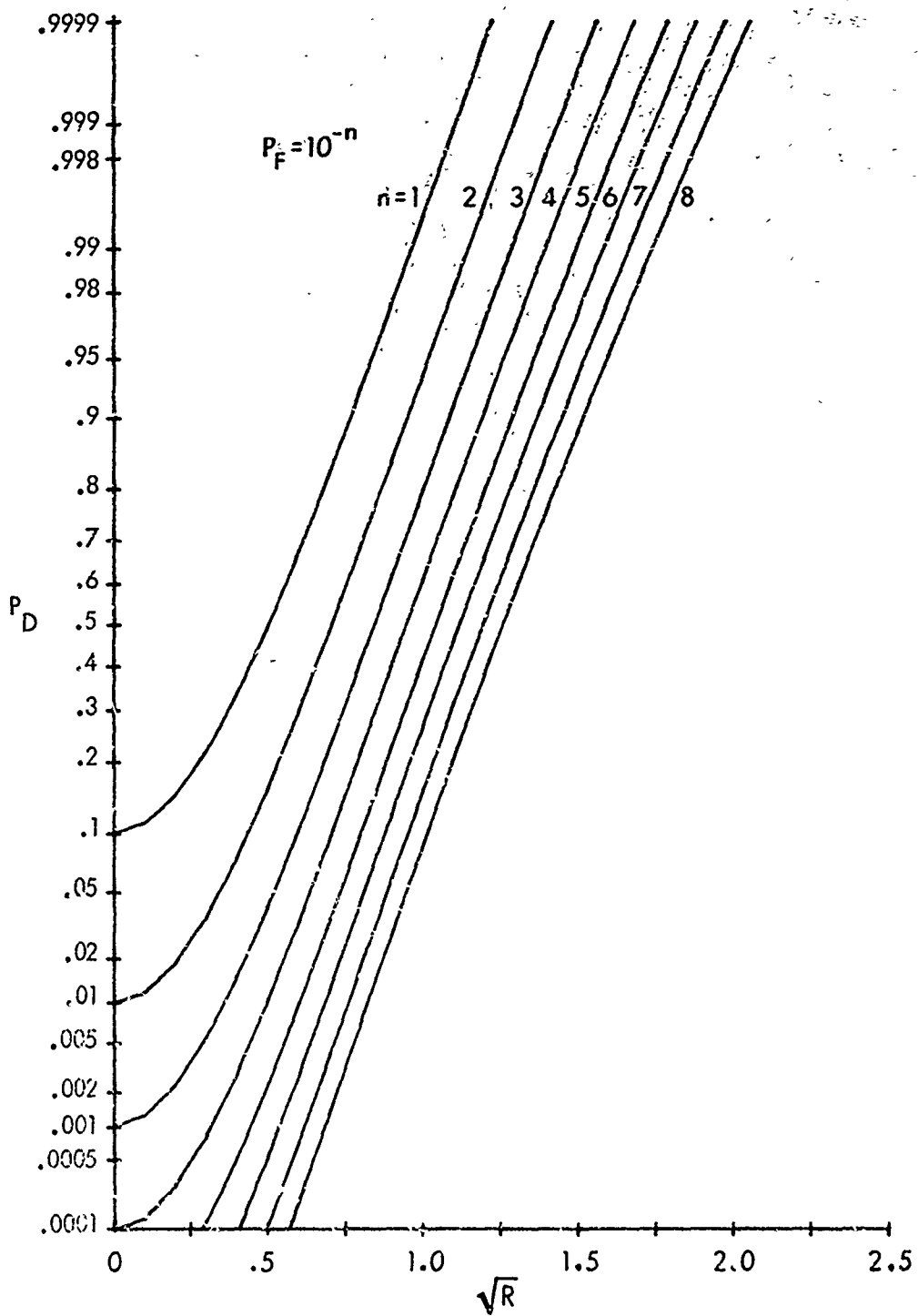


Fig. 9B.  $f = .2$   
 Fig. 9. Detection Probability; LF,  $\beta = 32$

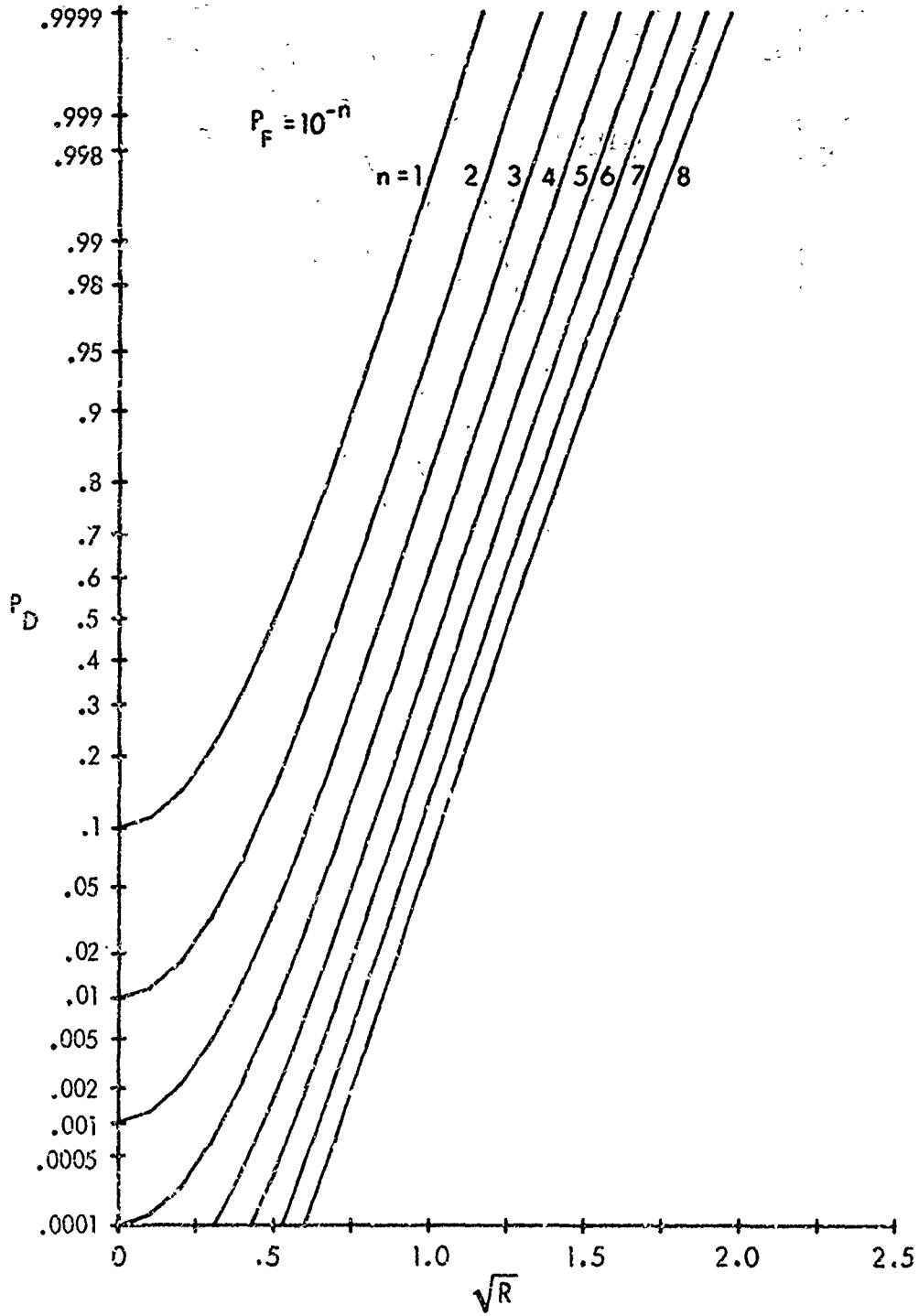


Fig. 9C.  $f = 0$   
Fig. 9. Detection Probability; LF,  $\beta = 32$

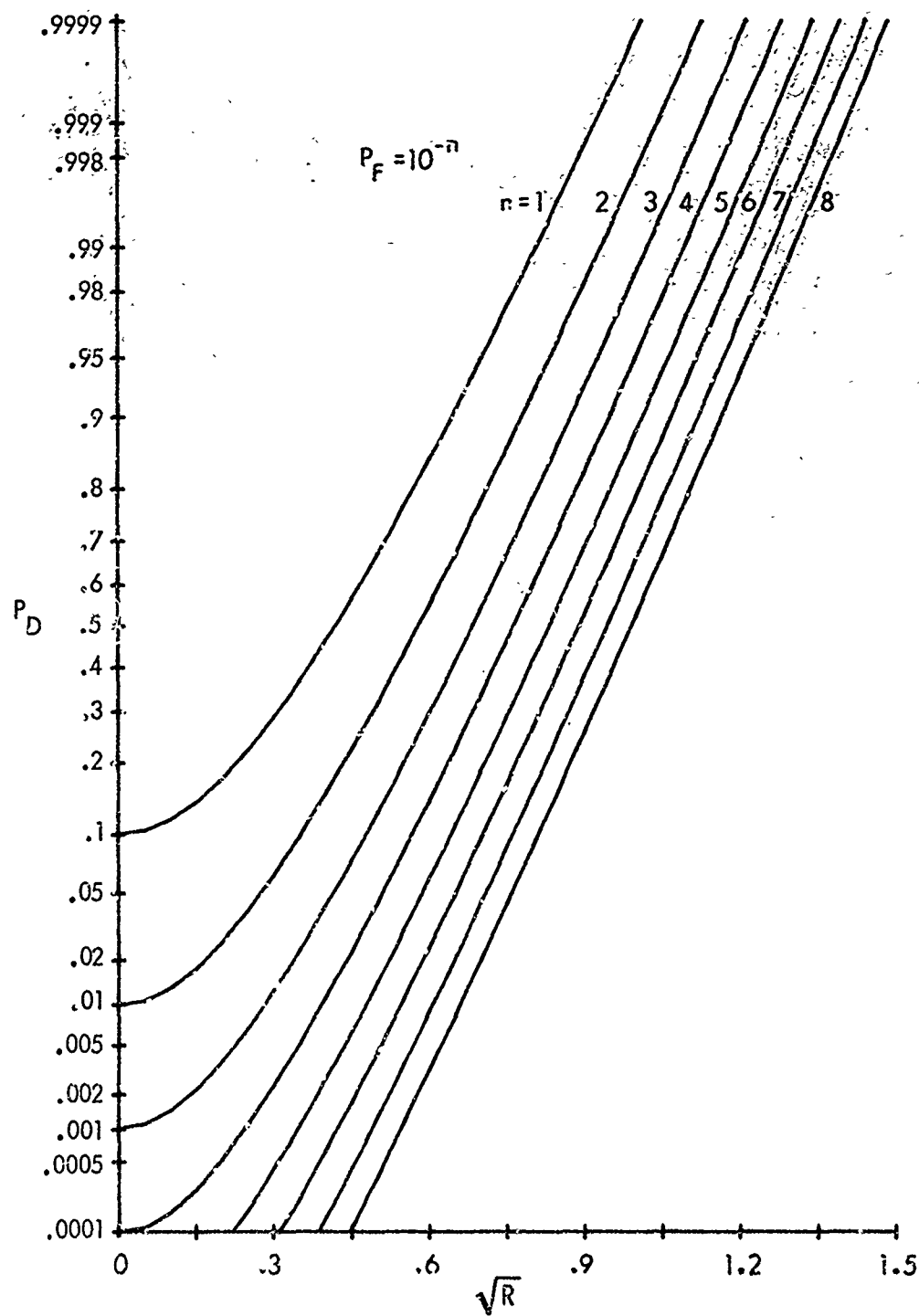


Fig. 10A.  $f = 1$   
 Fig. 10. Detection Probability; LF,  $\beta = 64$

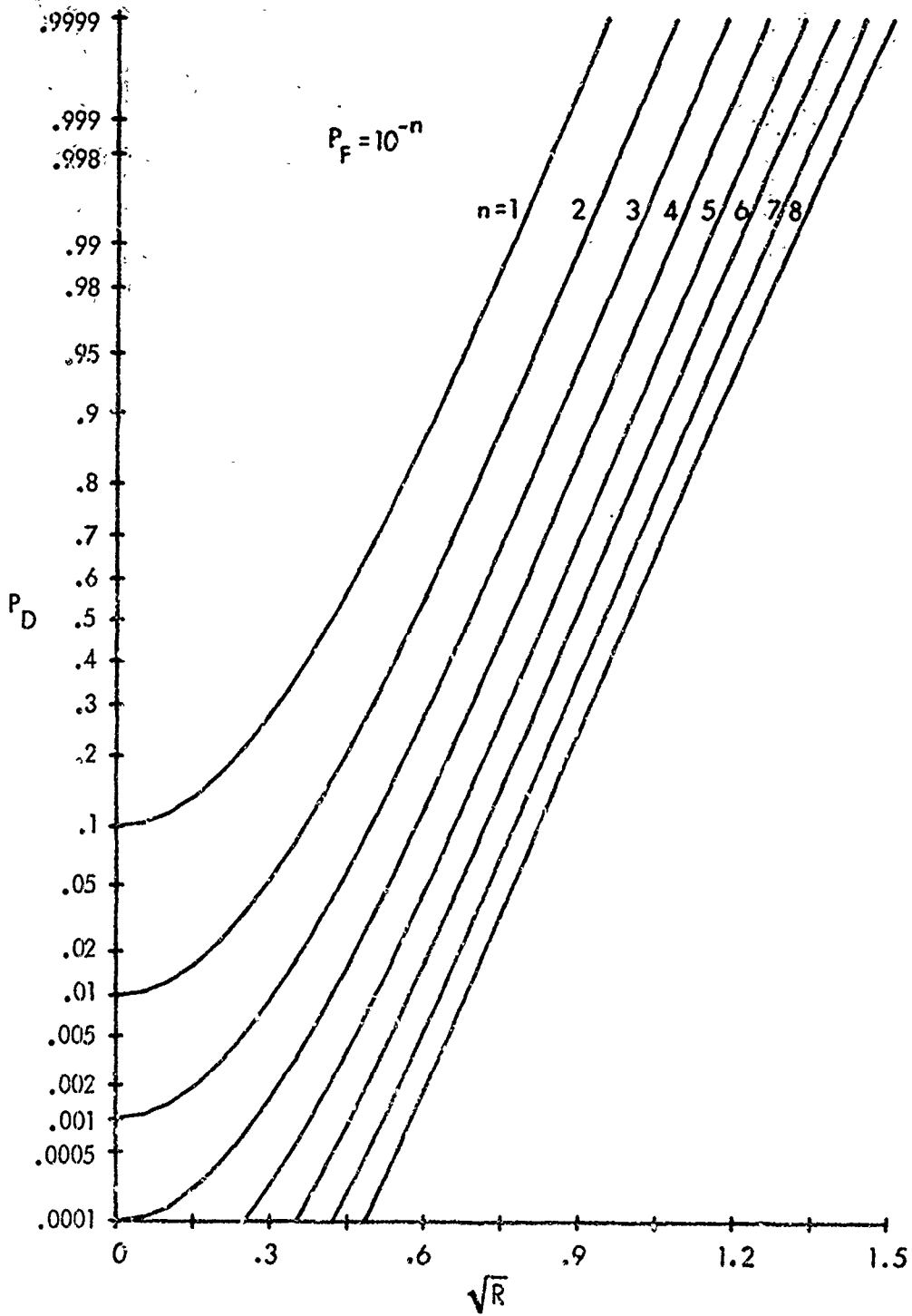


Fig. 10B.  $f = .2$   
 Fig. 10. Detection Probability; LF,  $\beta = 64$

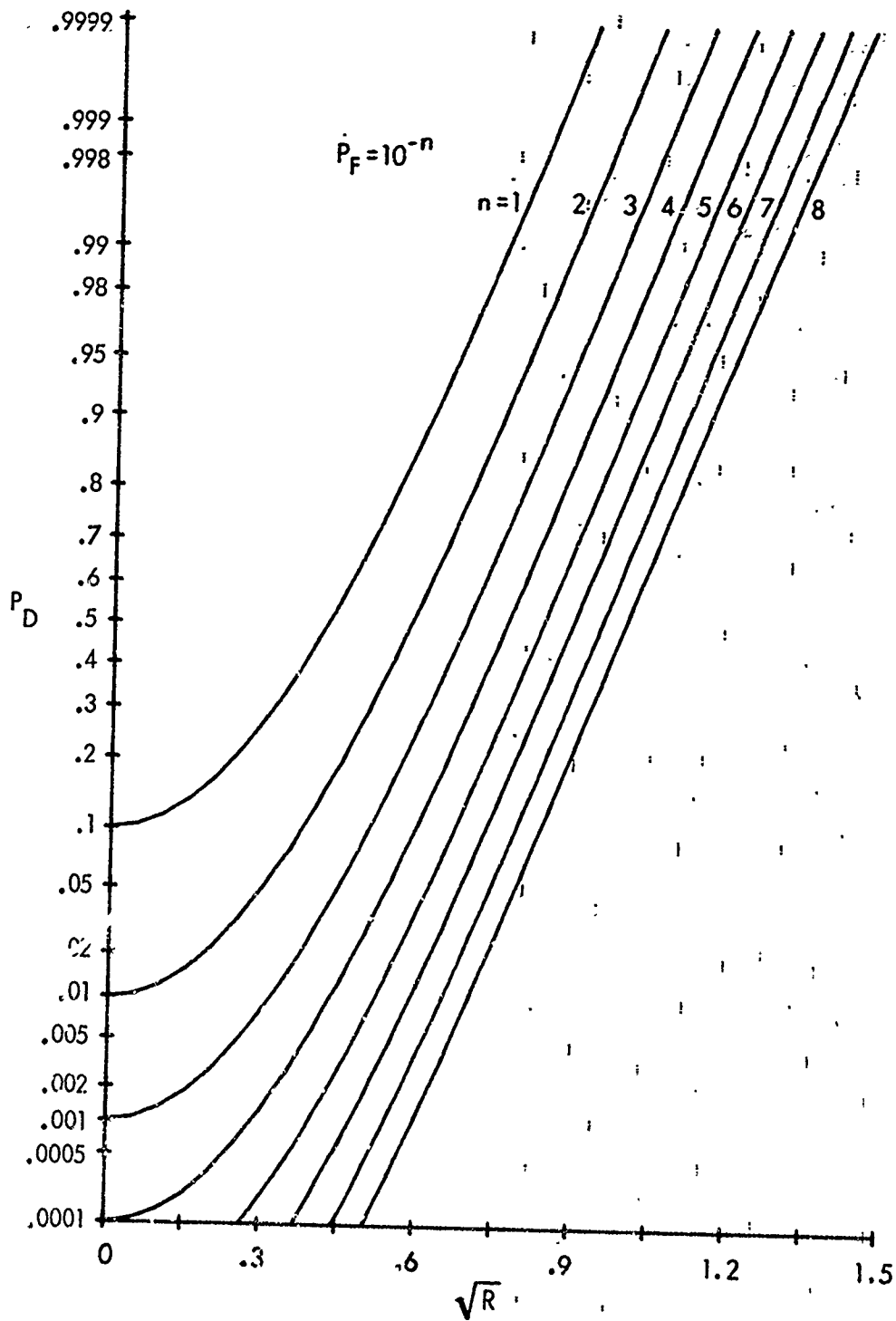


Fig. 10C,  $f = 0$   
 Fig. 10. Detection Probability; I.F,  $\beta = 64$

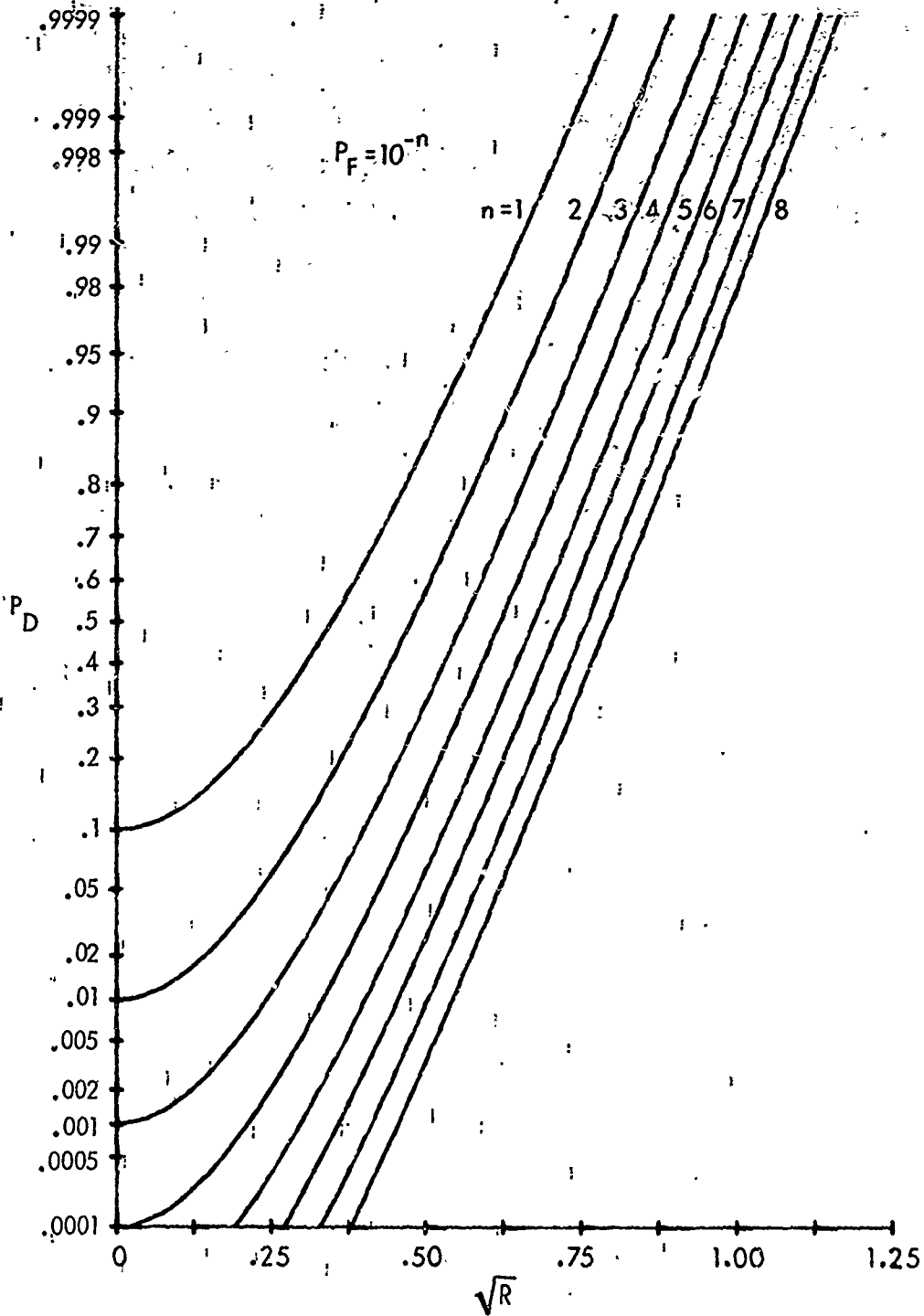


Fig. 11A.  $f = 1$   
 Fig. 11. Detection Probability; LF,  $\beta = 128$

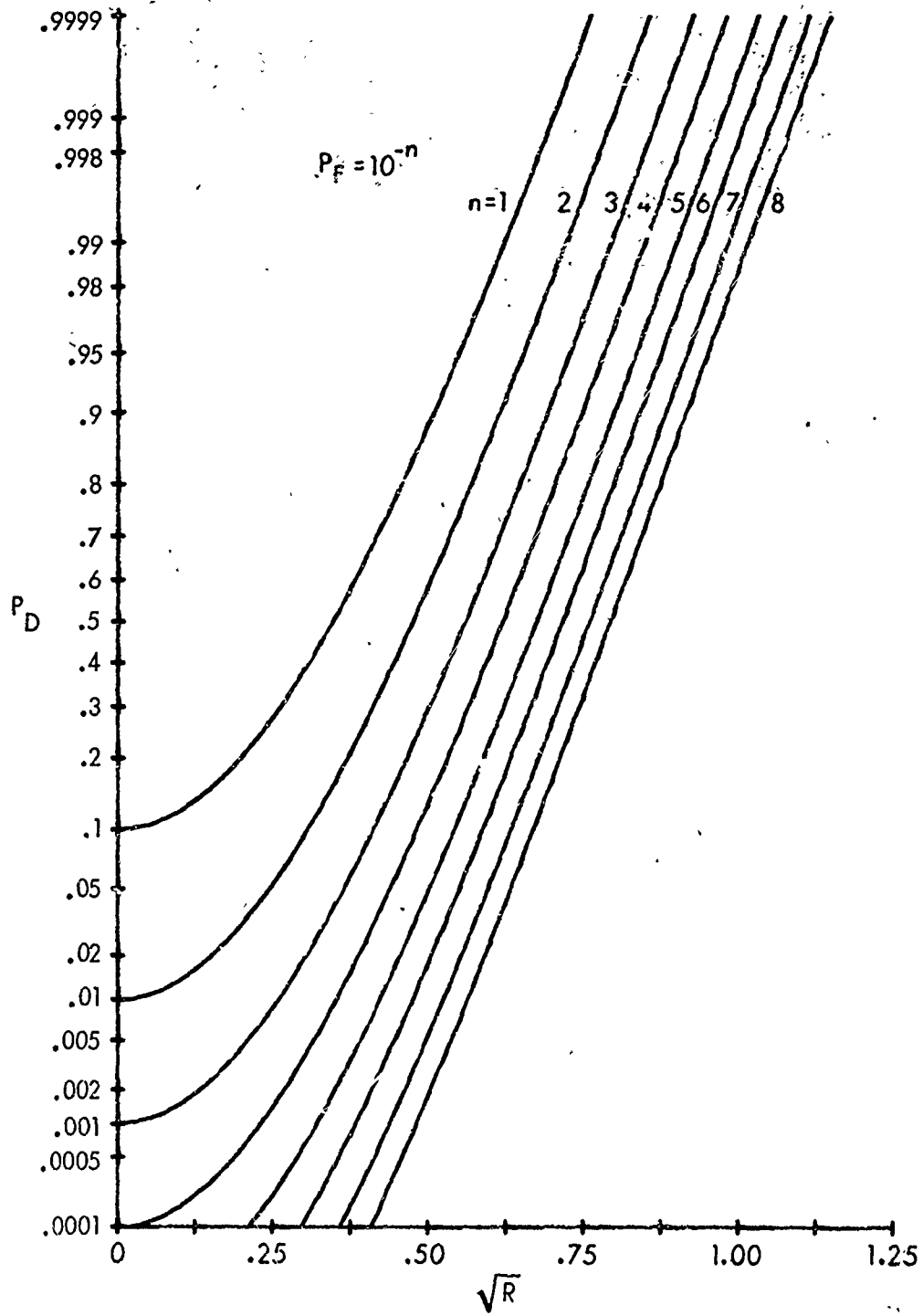


Fig. 11B.  $f = .2$   
Fig. 11. Detection Probability; LF,  $\beta = 128$

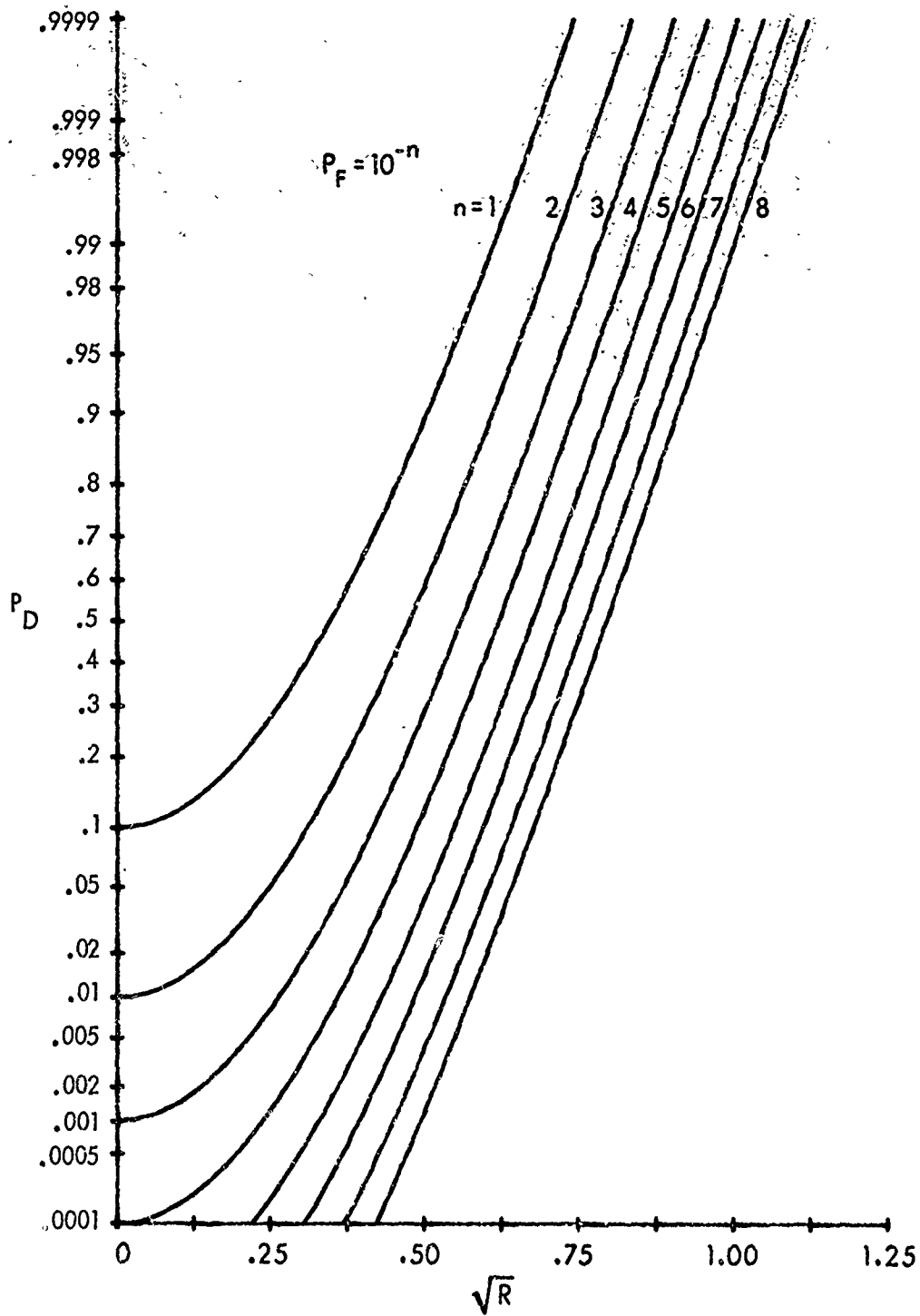


Fig. 11C.  $f = 0$   
 Fig. 11. Detection Probability; LF,  $\beta = 128$

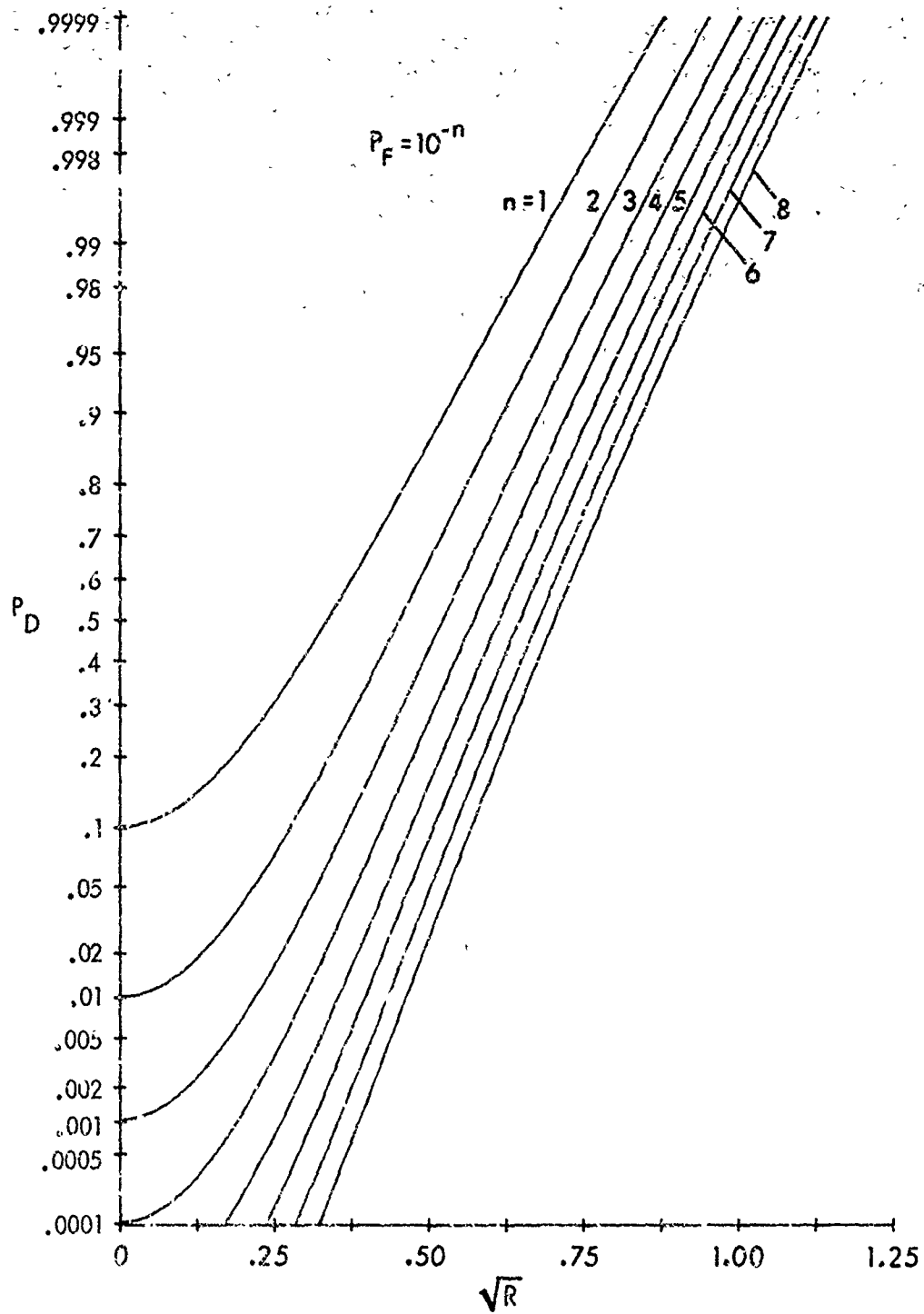


Fig. 12A.  $f = 1$   
Fig. 12. Detection Probability; LF,  $\beta = 128$ , Gaussian Assumption

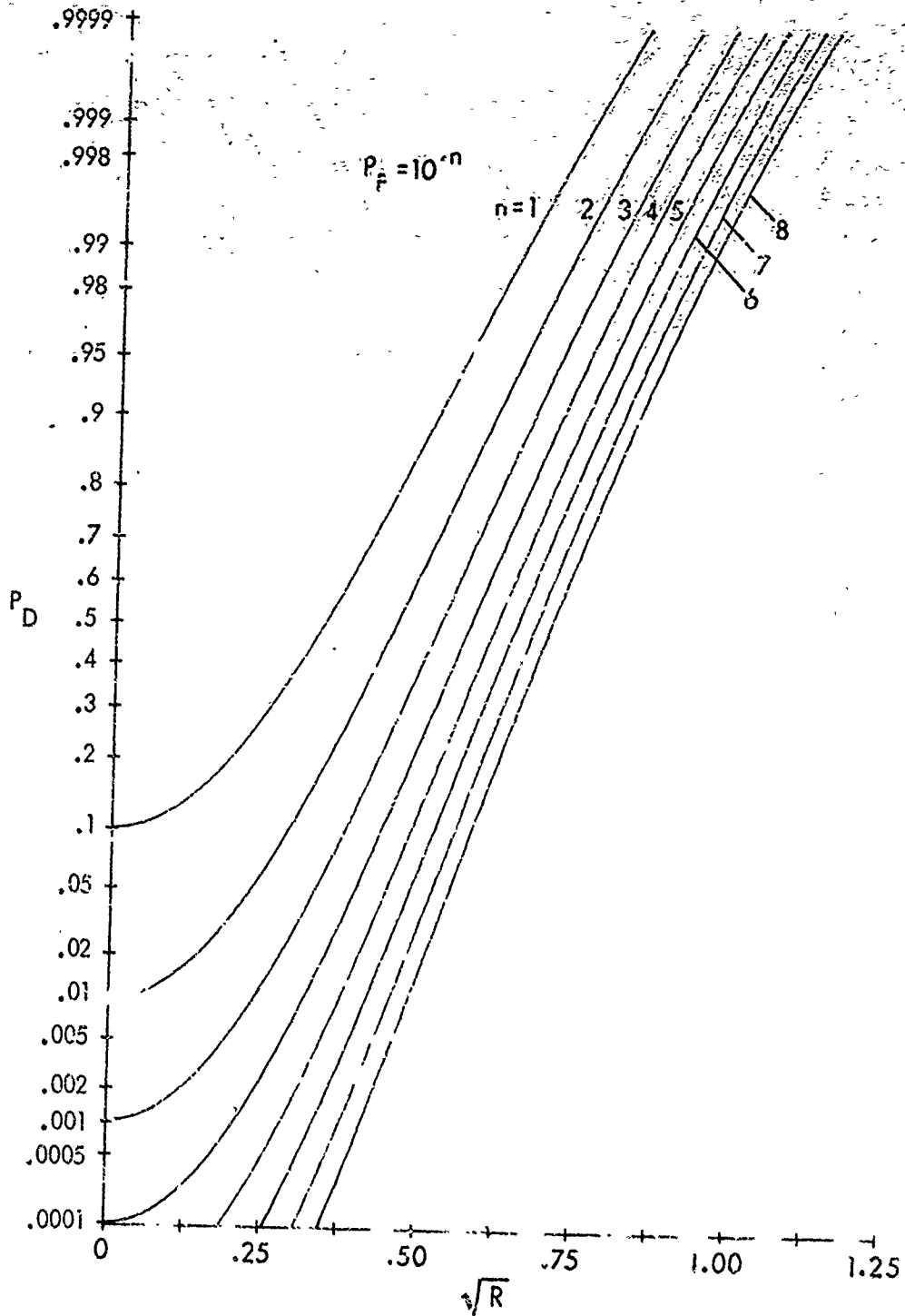


Fig. 12B.  $f = .2$   
 Fig. 12. Detection Probability; L.F,  $\beta = 126$ , Gaussian Assumption

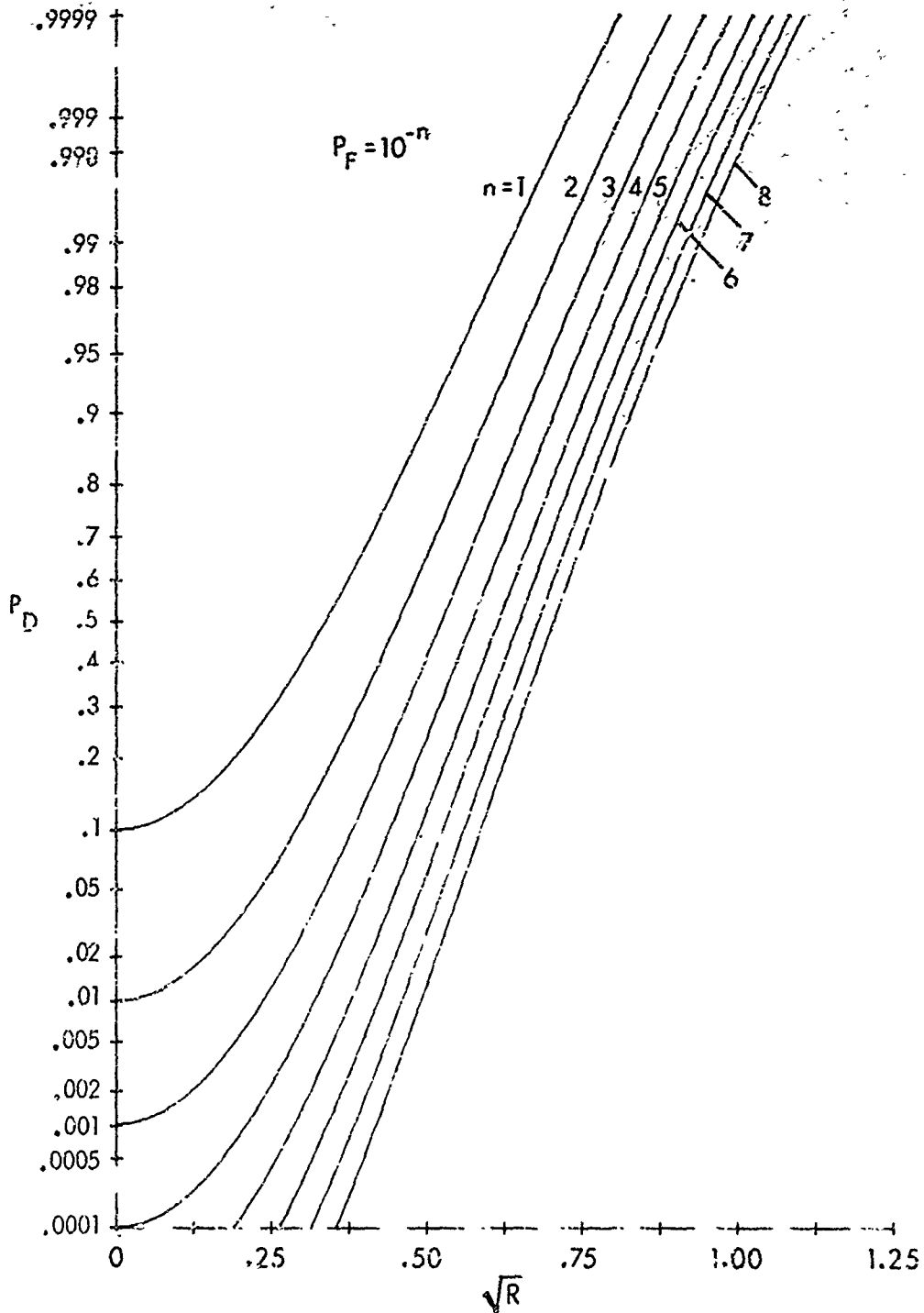


Fig. 12C.  $f = 0$   
 Fig. 12. Detection Probability; LF,  $\beta = 128$ , Gaussian Assumption

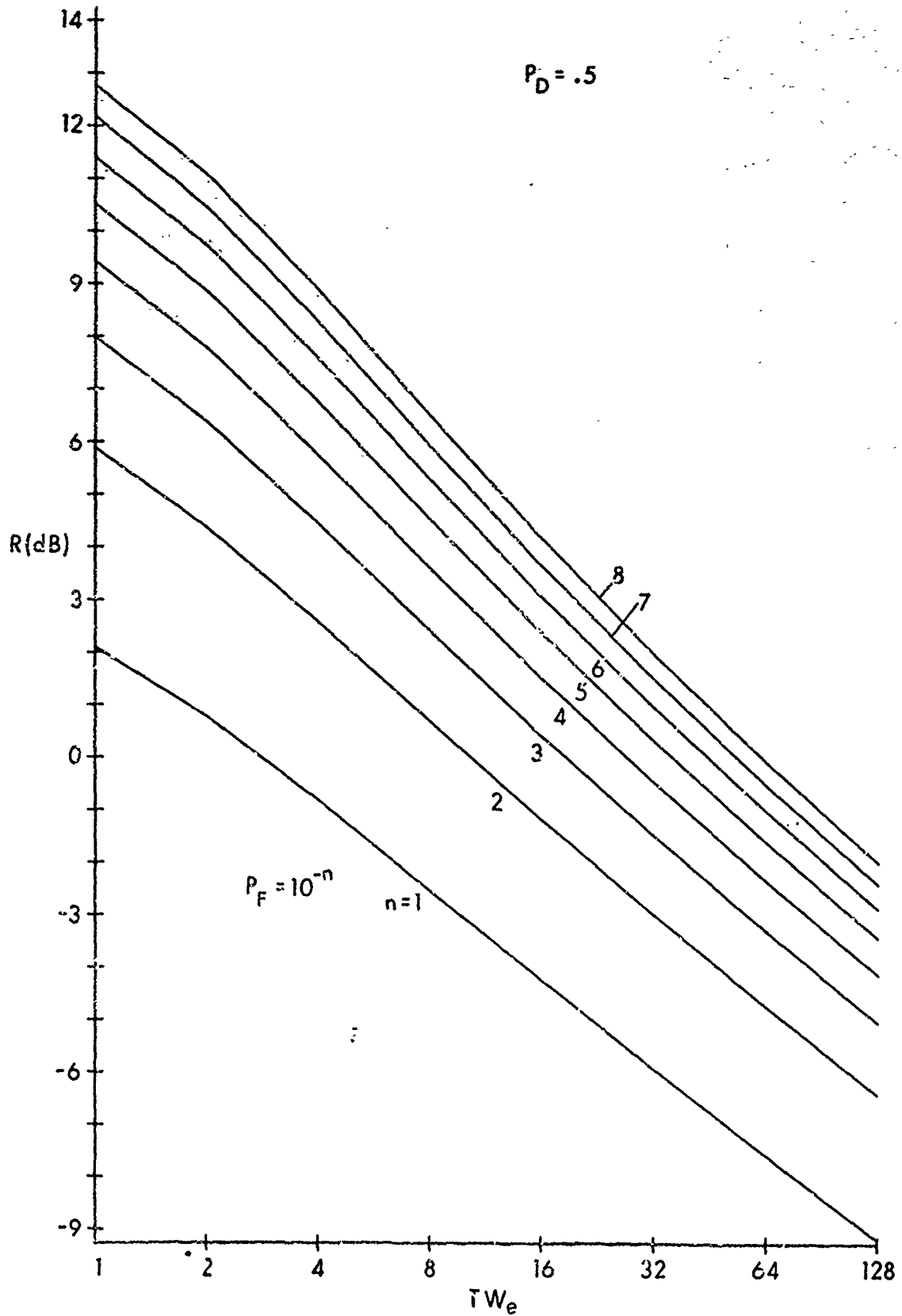


Fig. 13A.  $f = 1$

Fig. 13. Required Signal-to-Noise Ratio; L.F

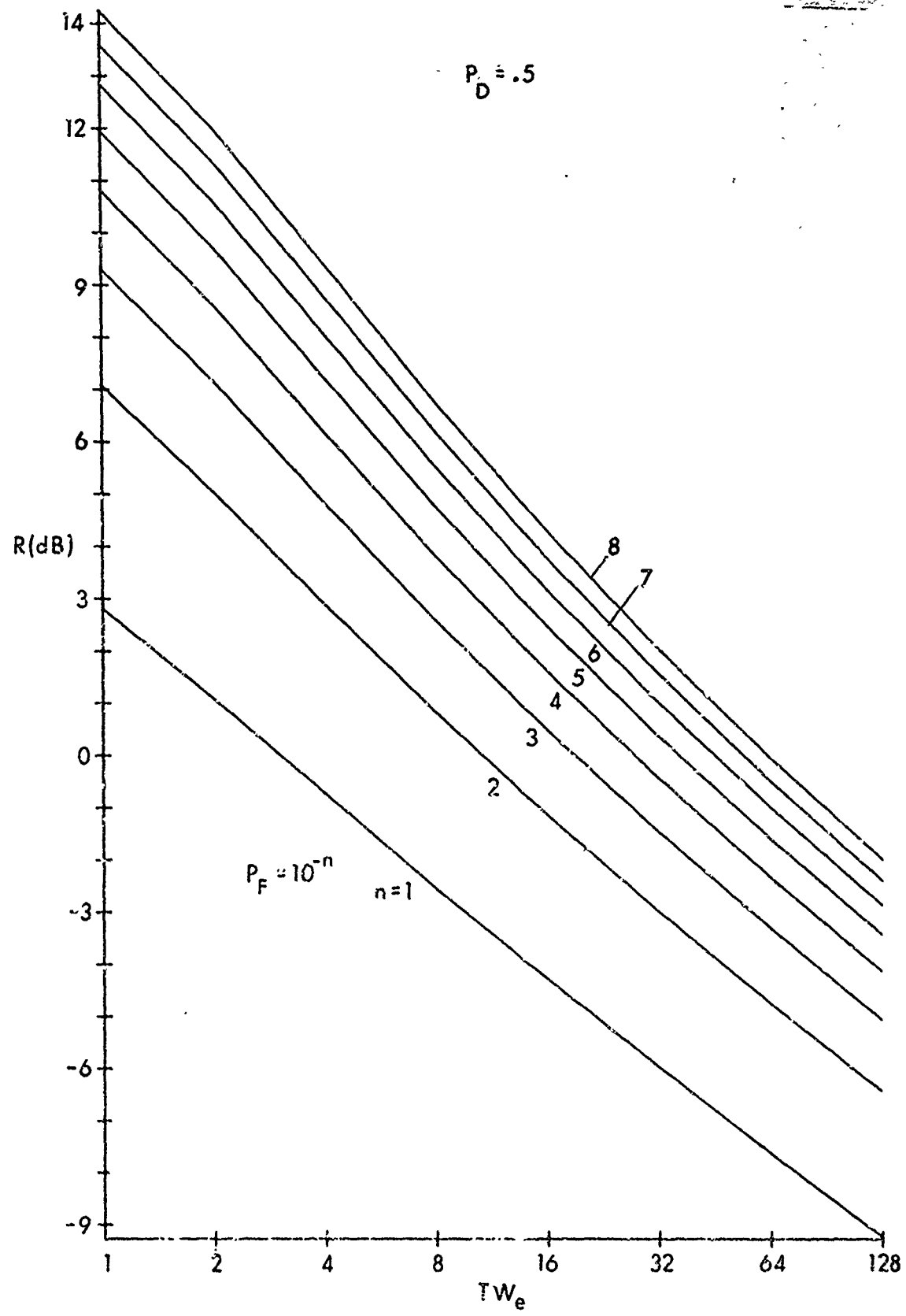


Fig. 13B.  $f = .2$   
Fig. 13. Required Signal-to-Noise Ratio; LF

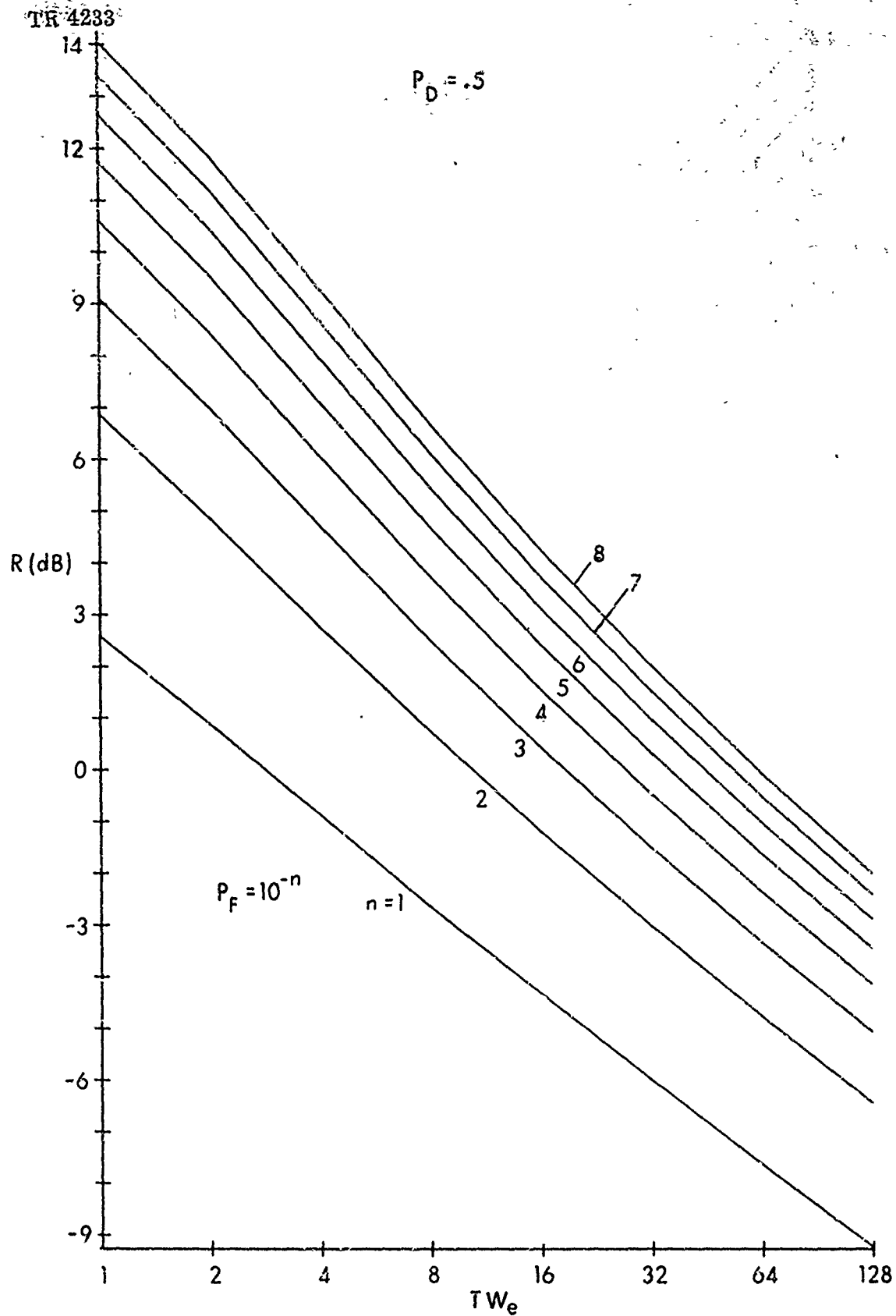


Fig. 13C. 1 - 0

Fig. 13. Required Signal-to-Noise Ratio; LF

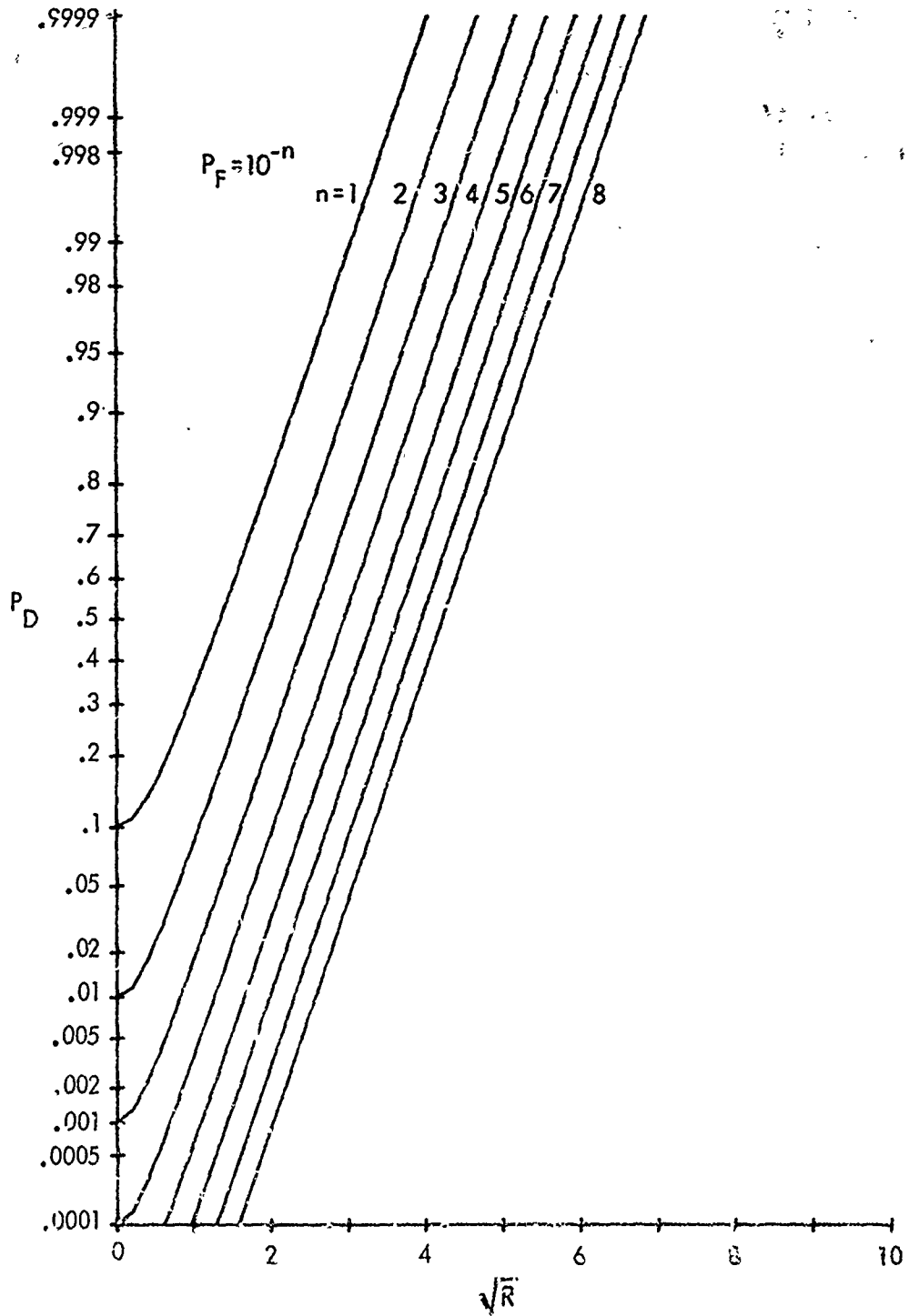


Fig. 14A.  $f = 1$   
 Fig. 14. Detection Probability; NR,  $\hat{\beta} = 0$

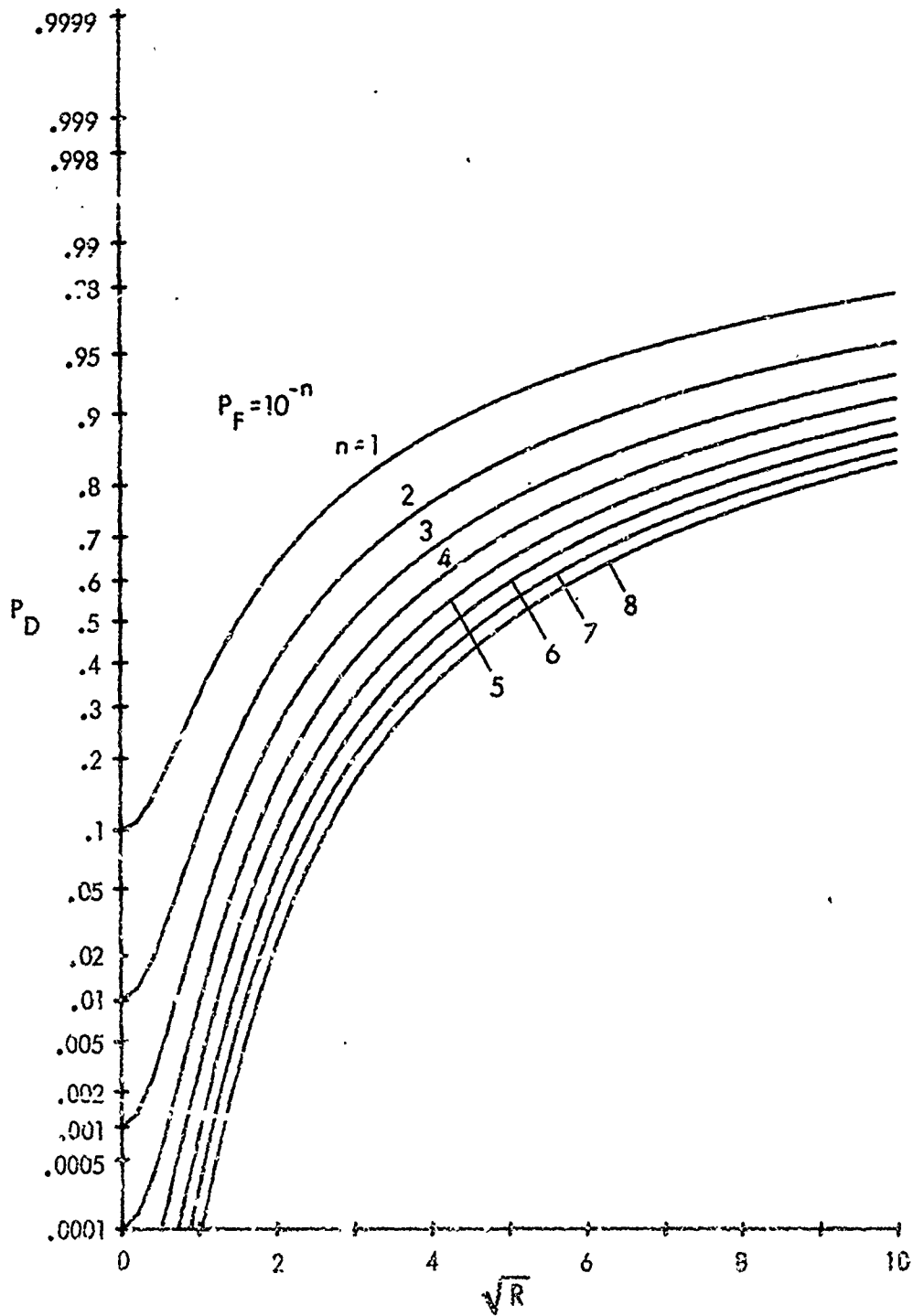


Fig. 14B.  $f = .2$   
 Fig. 14. Detection Probability: NR,  $\hat{\beta} = 0$

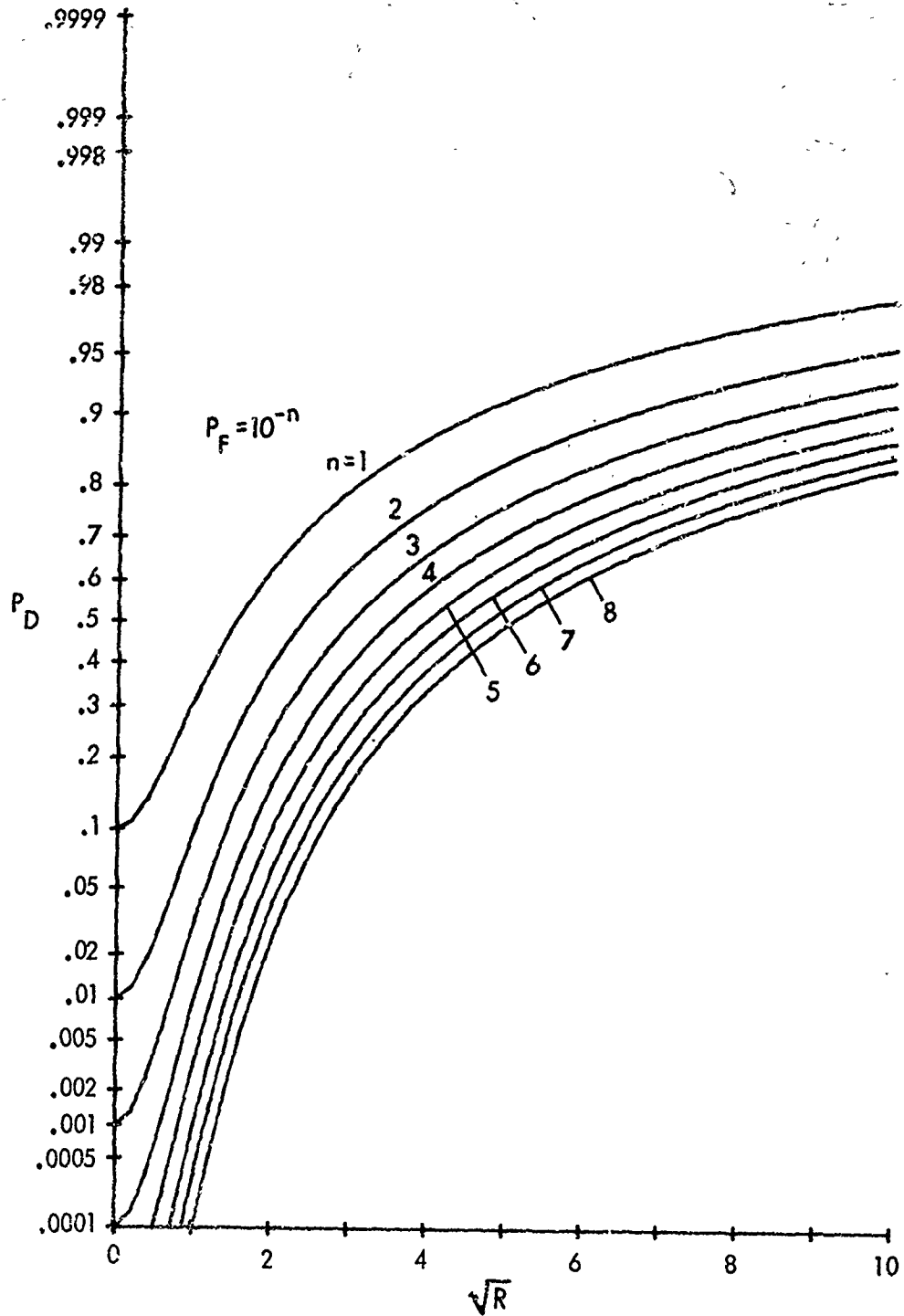


Fig. 14C.  $f = 0$   
 Fig. 14. Detection Probability; NB,  $\hat{\beta} = 0$

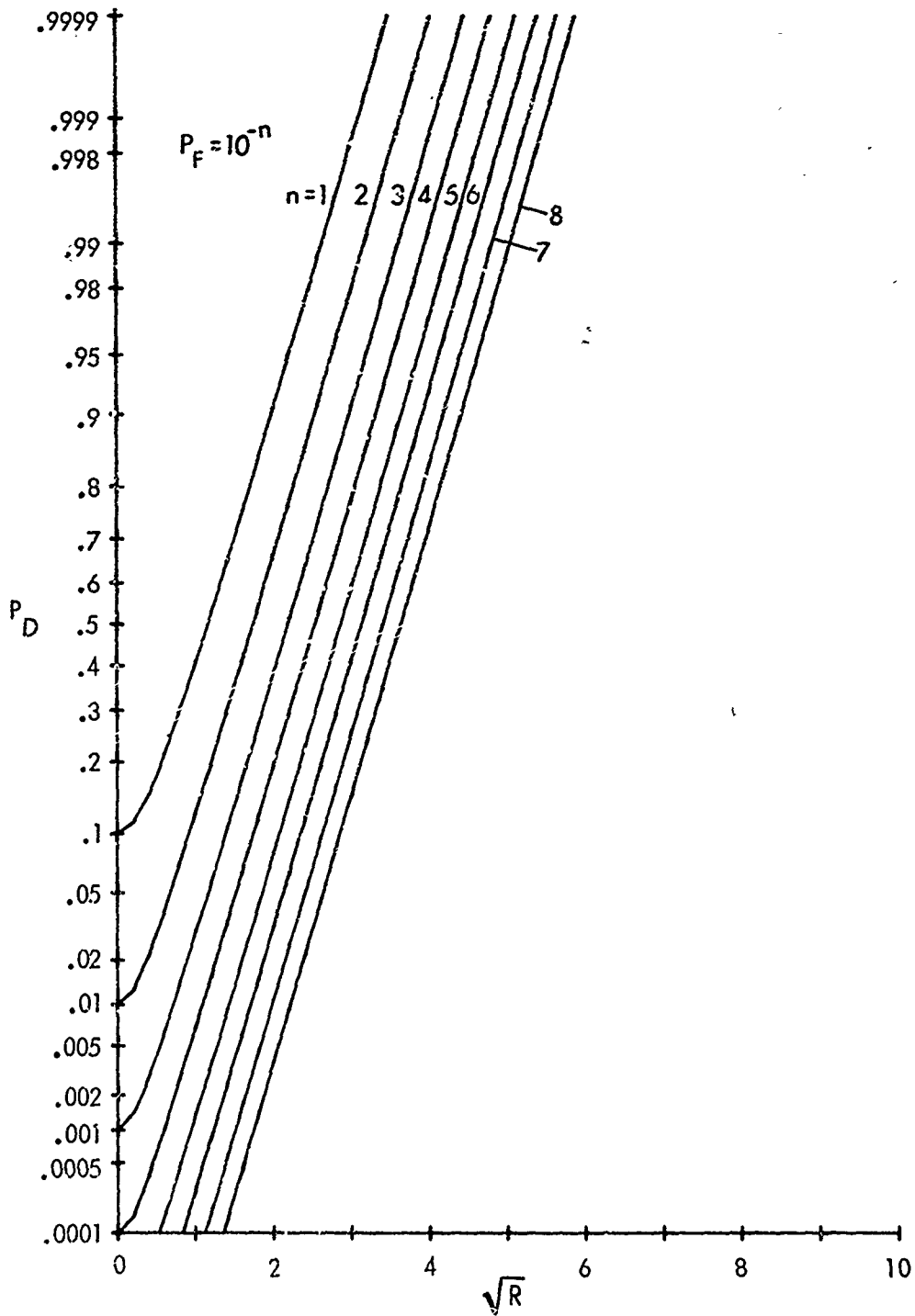


Fig. 15A.  $f = 1$   
 Fig. 15. Detection Probability; NB,  $\hat{\beta} = 1$

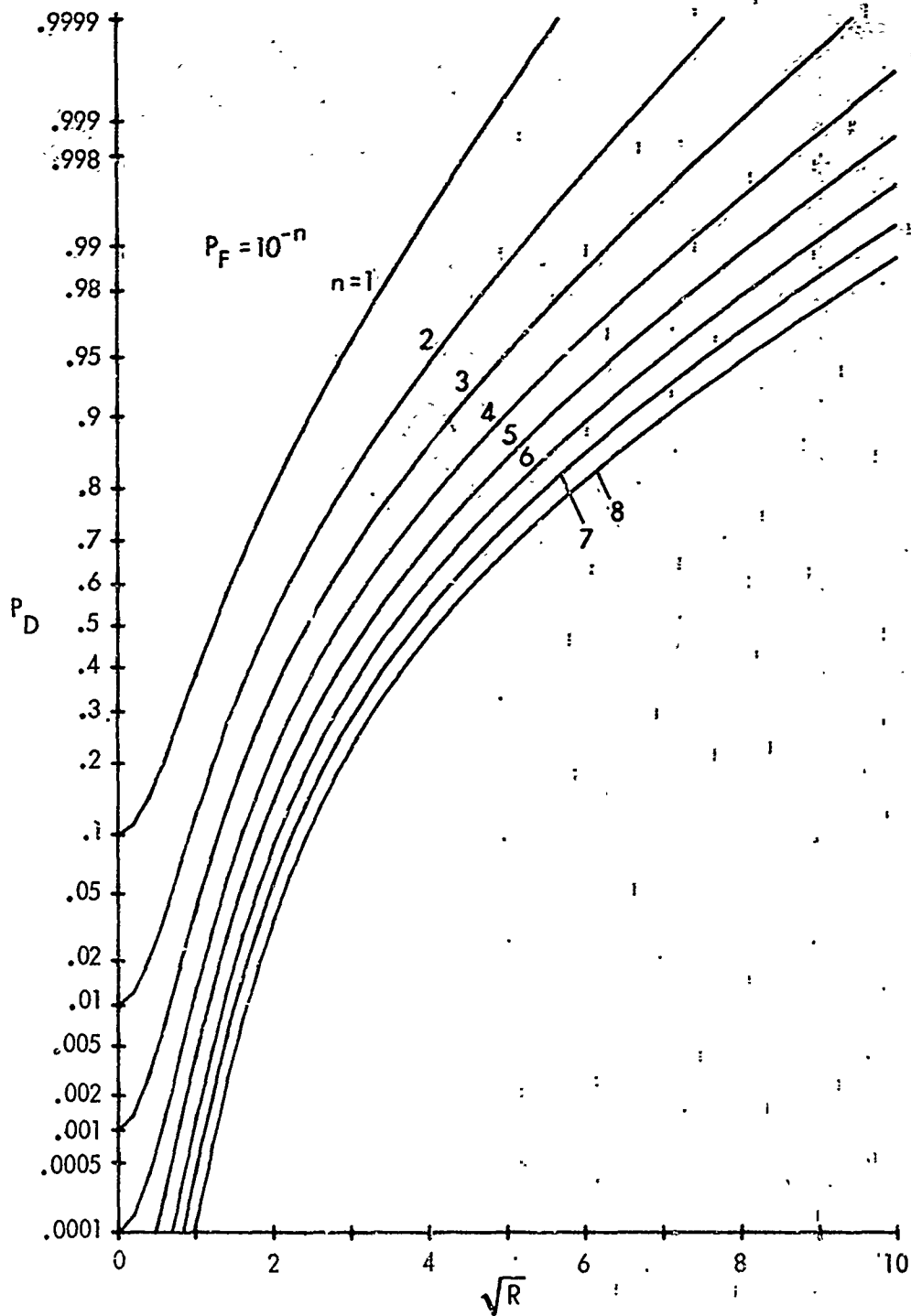


Fig. 15B.  $f = .2$   
 Fig. 15. Detection Probability; NB,  $\hat{\beta} = 1$

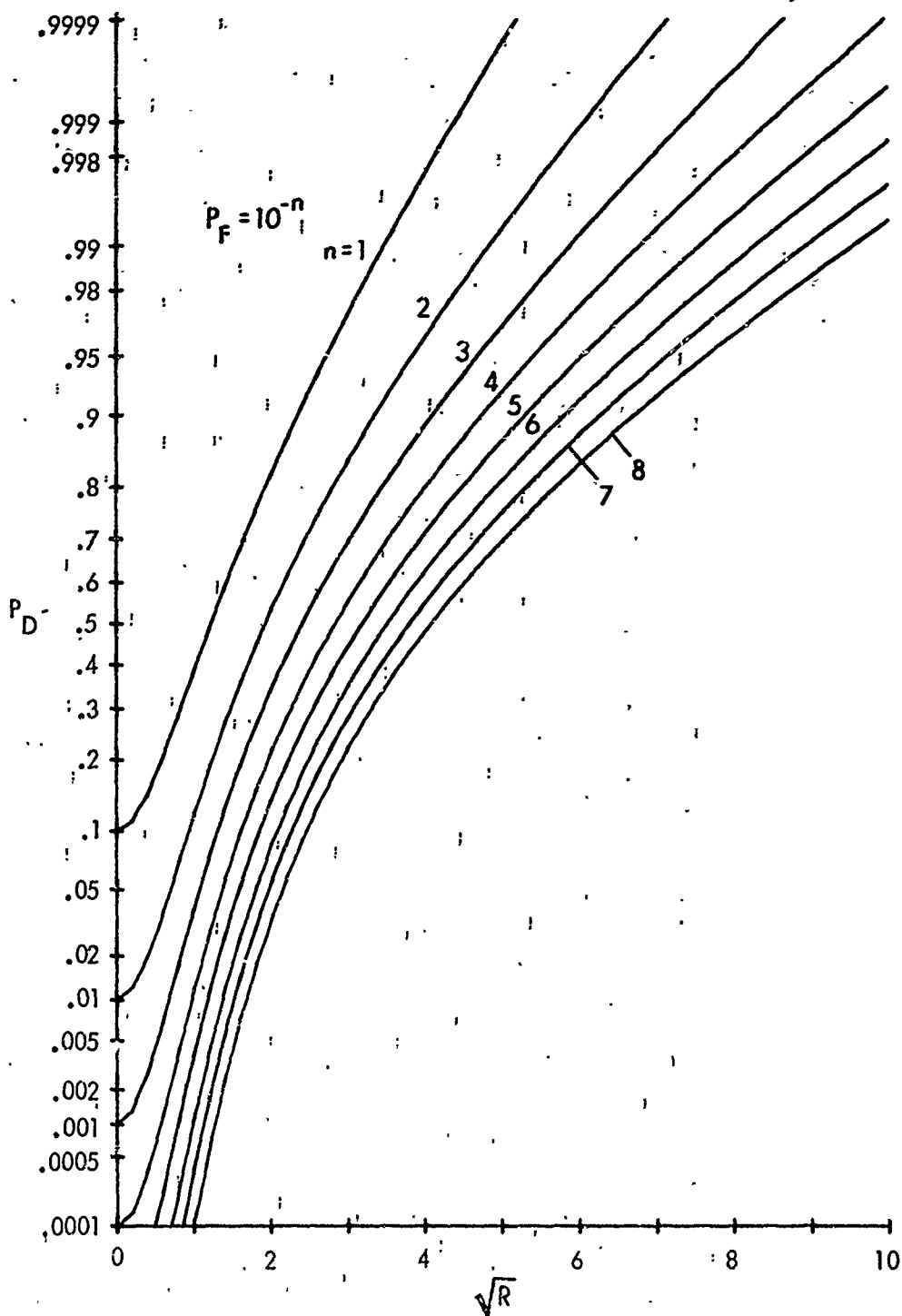


Fig. 15C.  $f = 0$   
 Fig. 15. Detection Probability; NB,  $\hat{\beta} = 1$

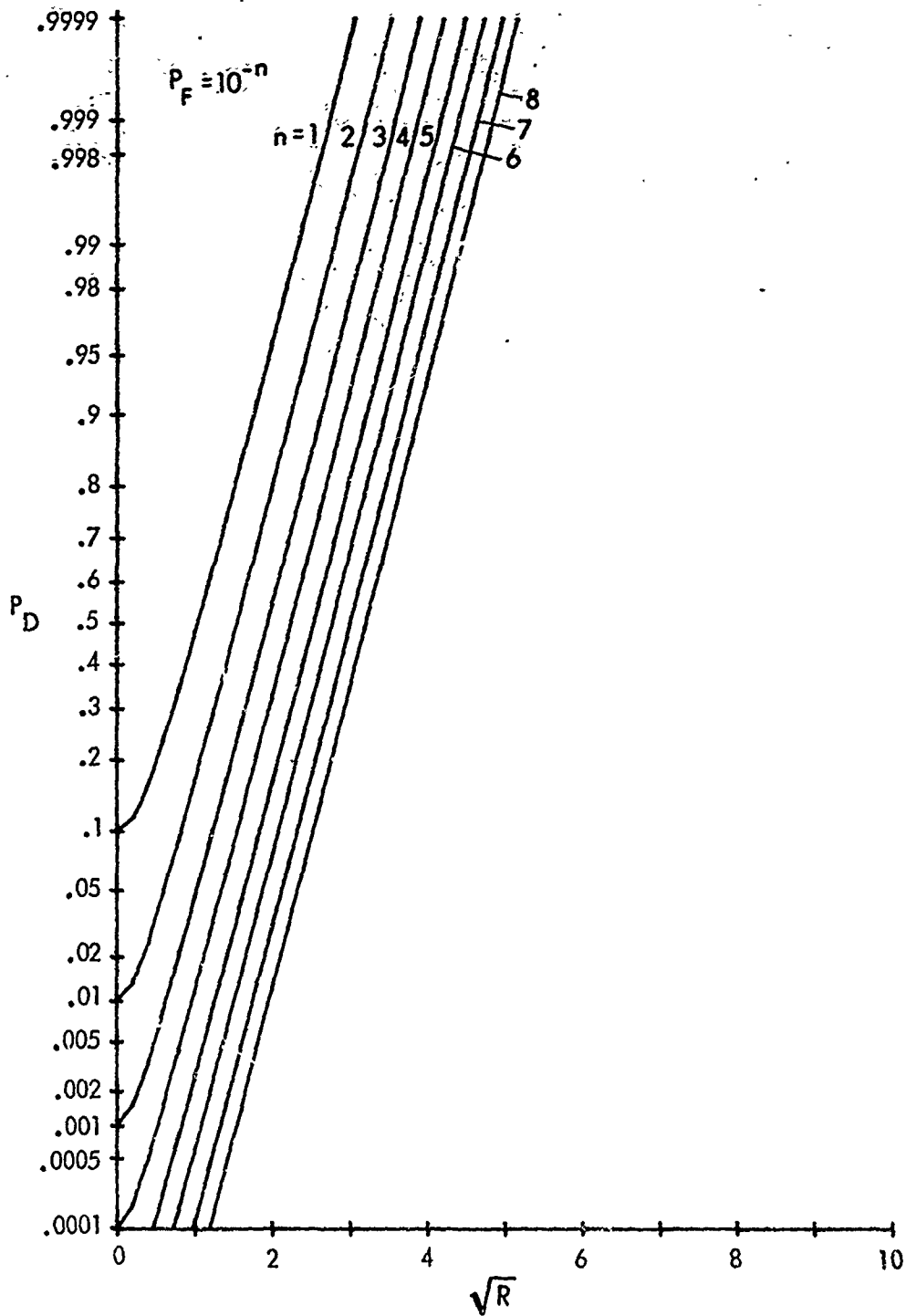


Fig. 16A.  $f = 1$   
 Fig. 16. Detection Probability; NB,  $\hat{\beta} = 2$

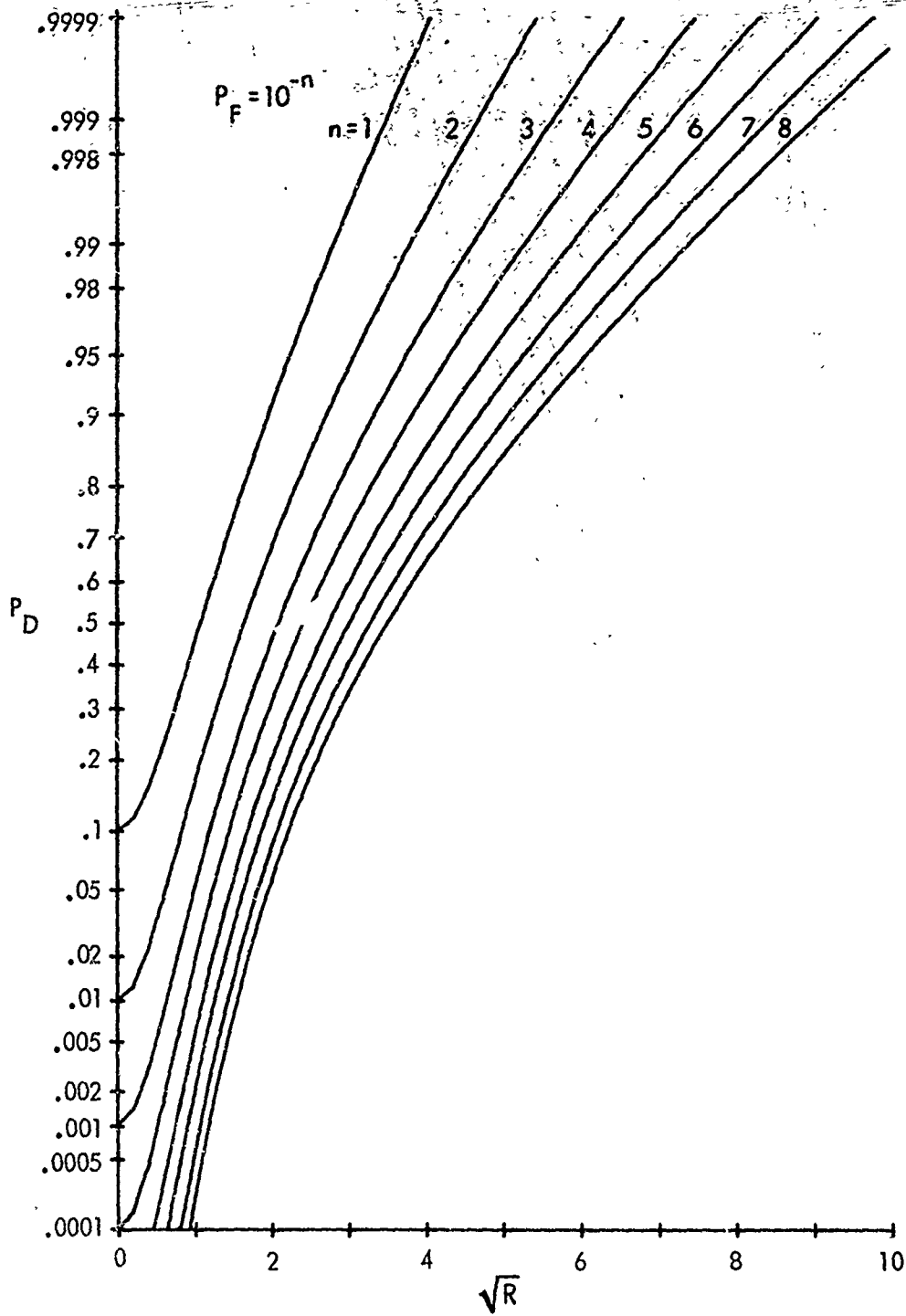


Fig. 16B.  $f = .2$   
 Fig. 16. Detection Probability; NB,  $\hat{\beta} = 2$

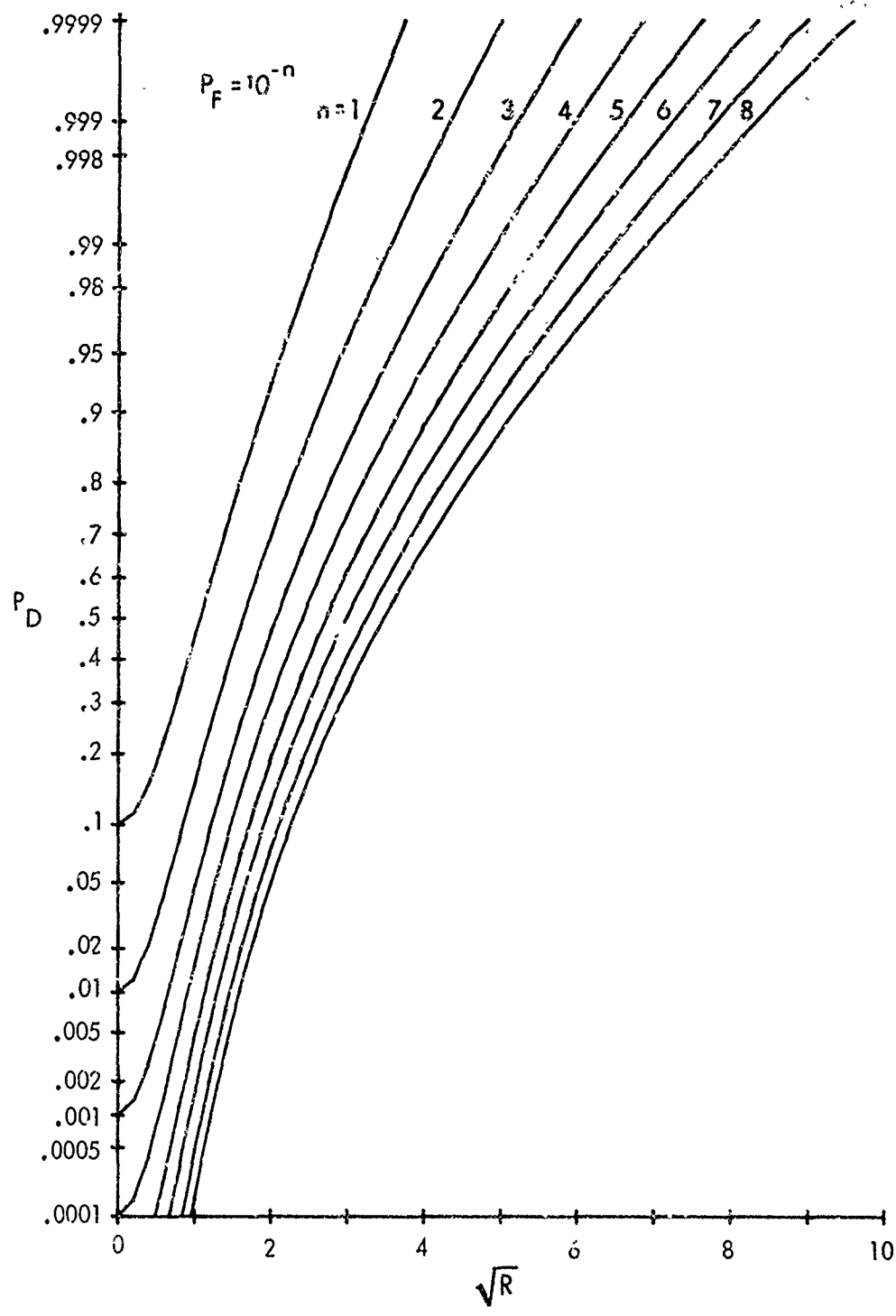


Fig. 16C.  $f = 0$   
Fig. 16. Detection Probability; NB,  $\hat{\beta} = 2$

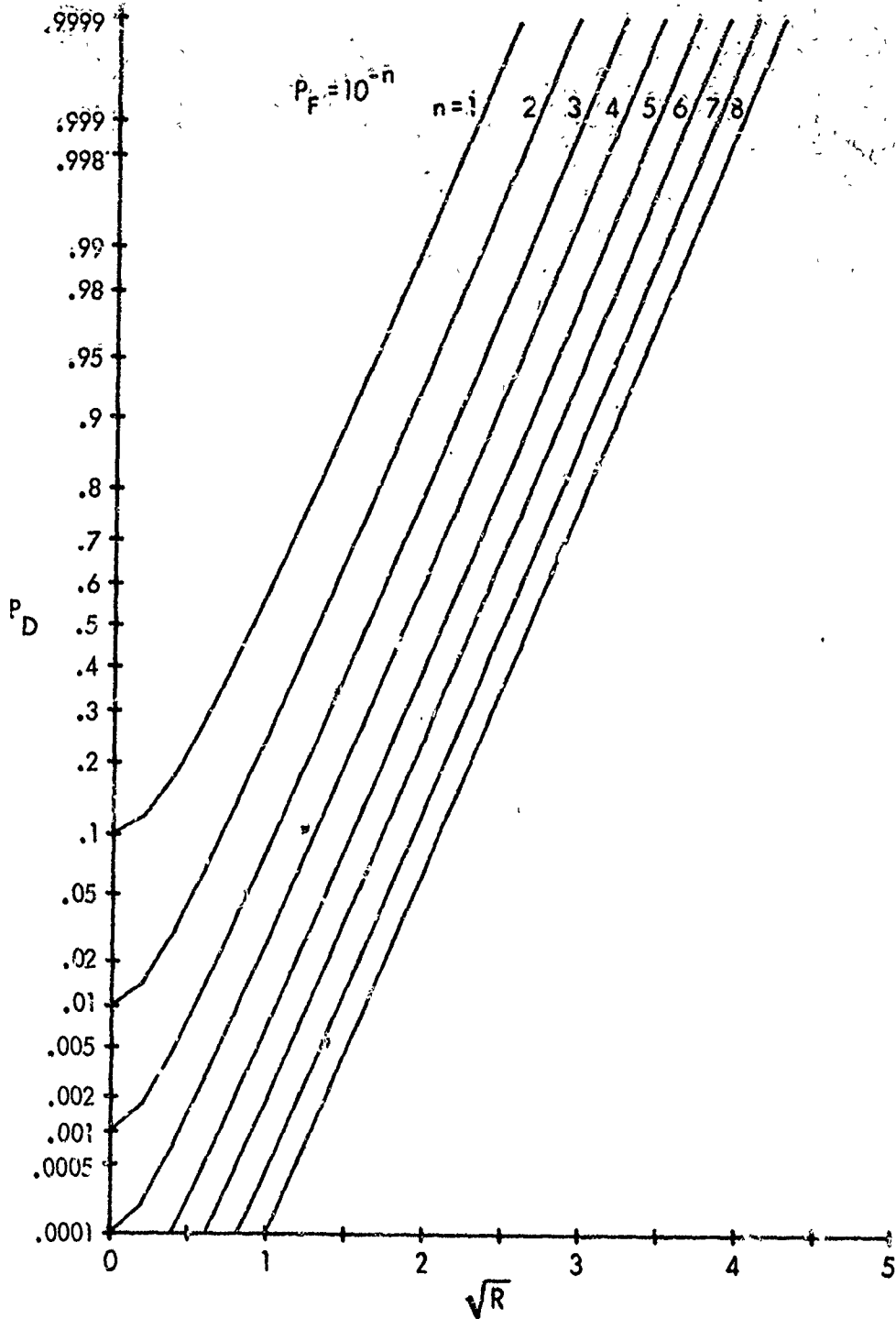


Fig. 17A.  $f = 1$   
Fig. 17. Detection Probability; NB,  $\hat{\beta} = 4$

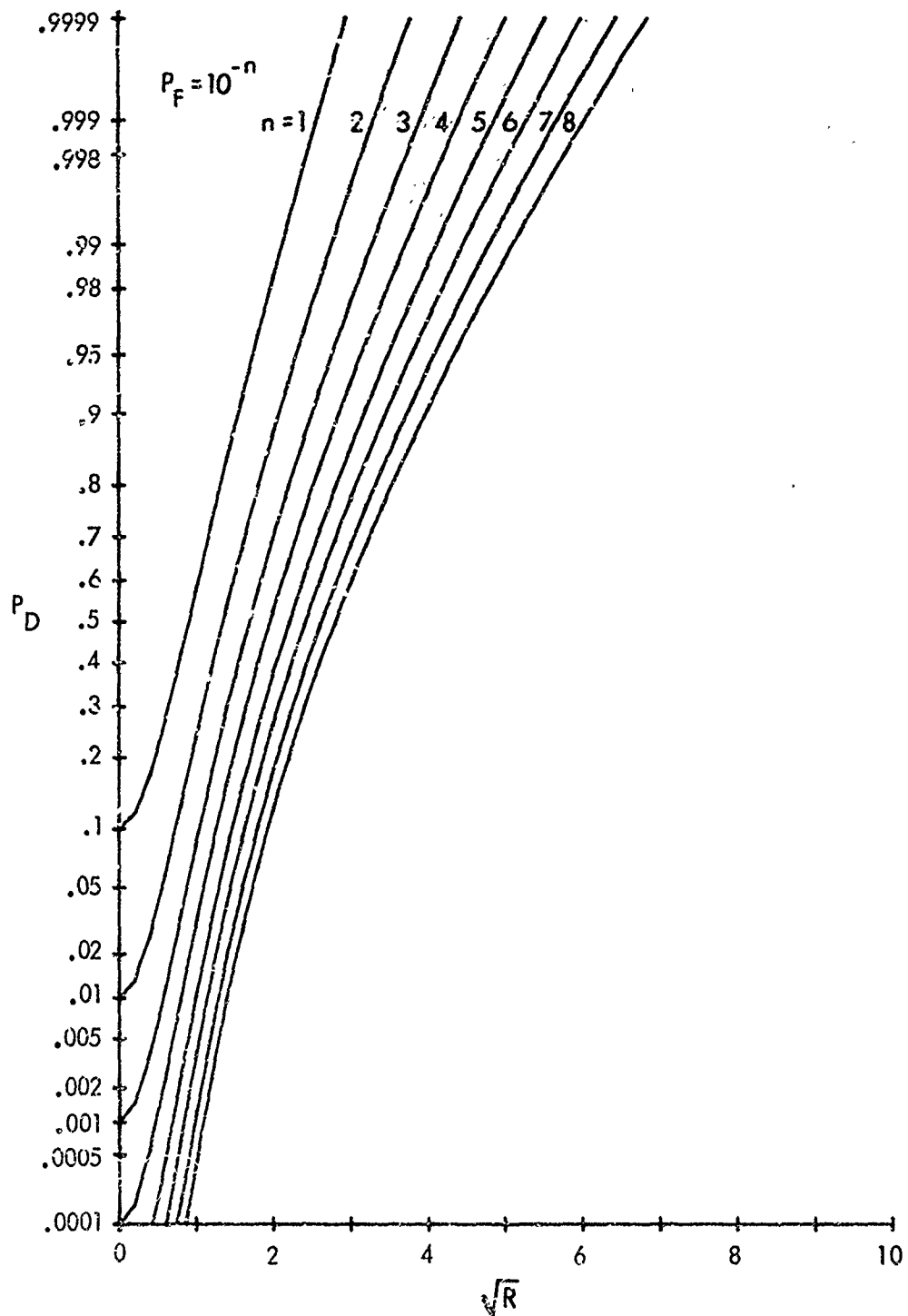


Fig. 17B.  $f = .2$   
 Fig. 17. Detection Probability; NB,  $\hat{\beta} = 4$

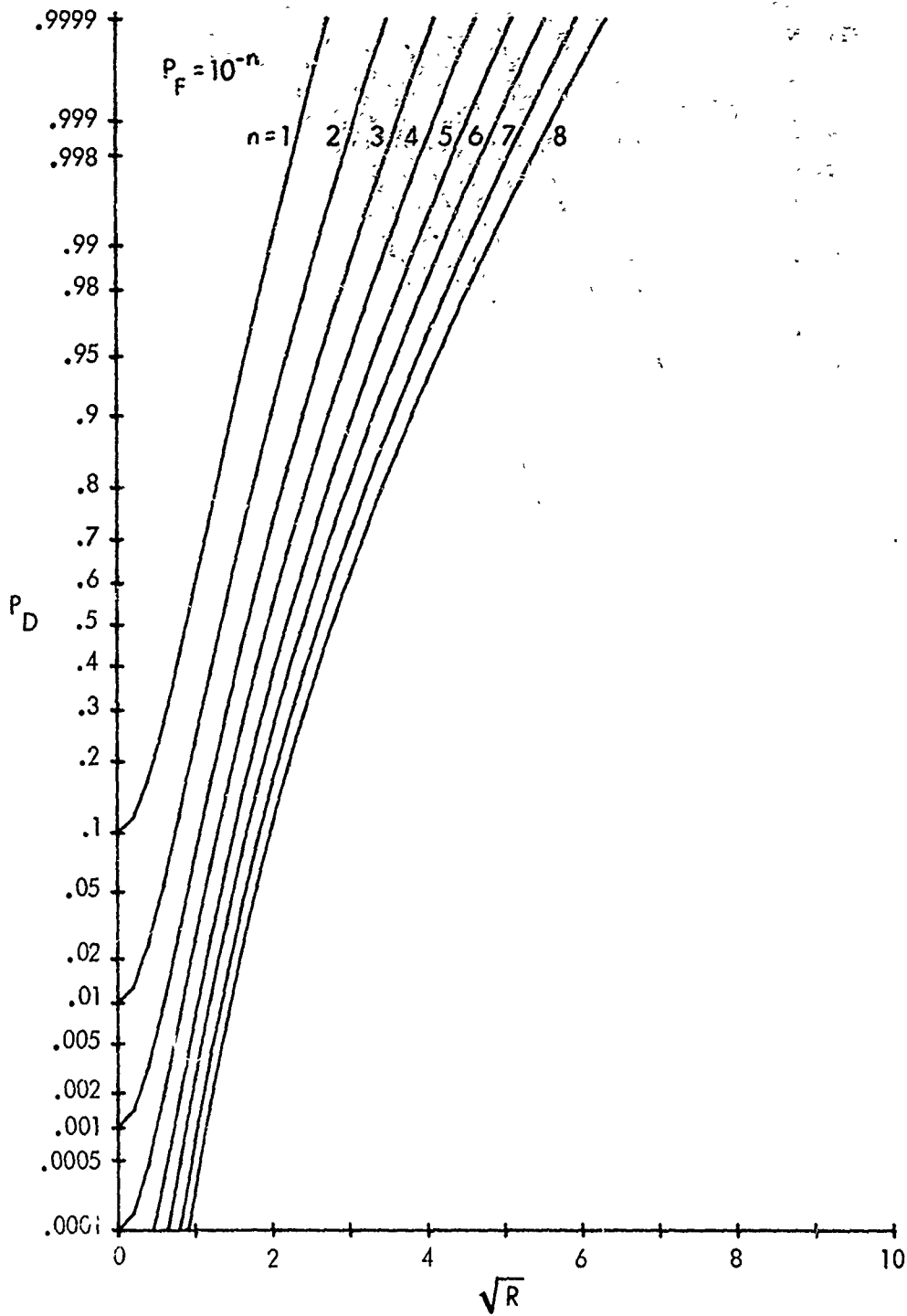


Fig. 17C.  $f = 0$   
 Fig. 17. Detection Probability; NB,  $\hat{\beta} = 4$

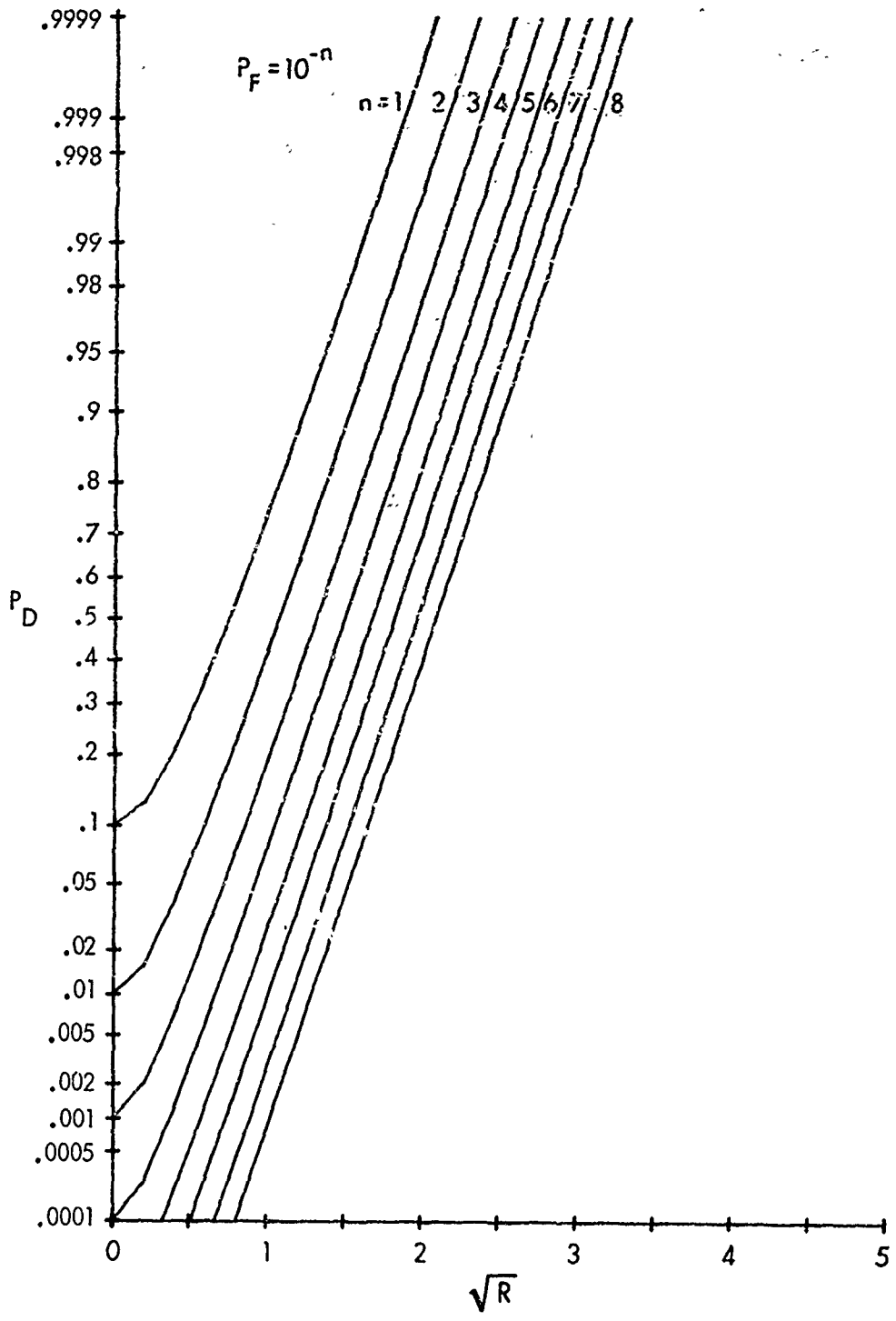


Fig. 18A.  $f = 1$   
Fig. 18. Detection Probability; NB,  $\hat{\beta} = 8$

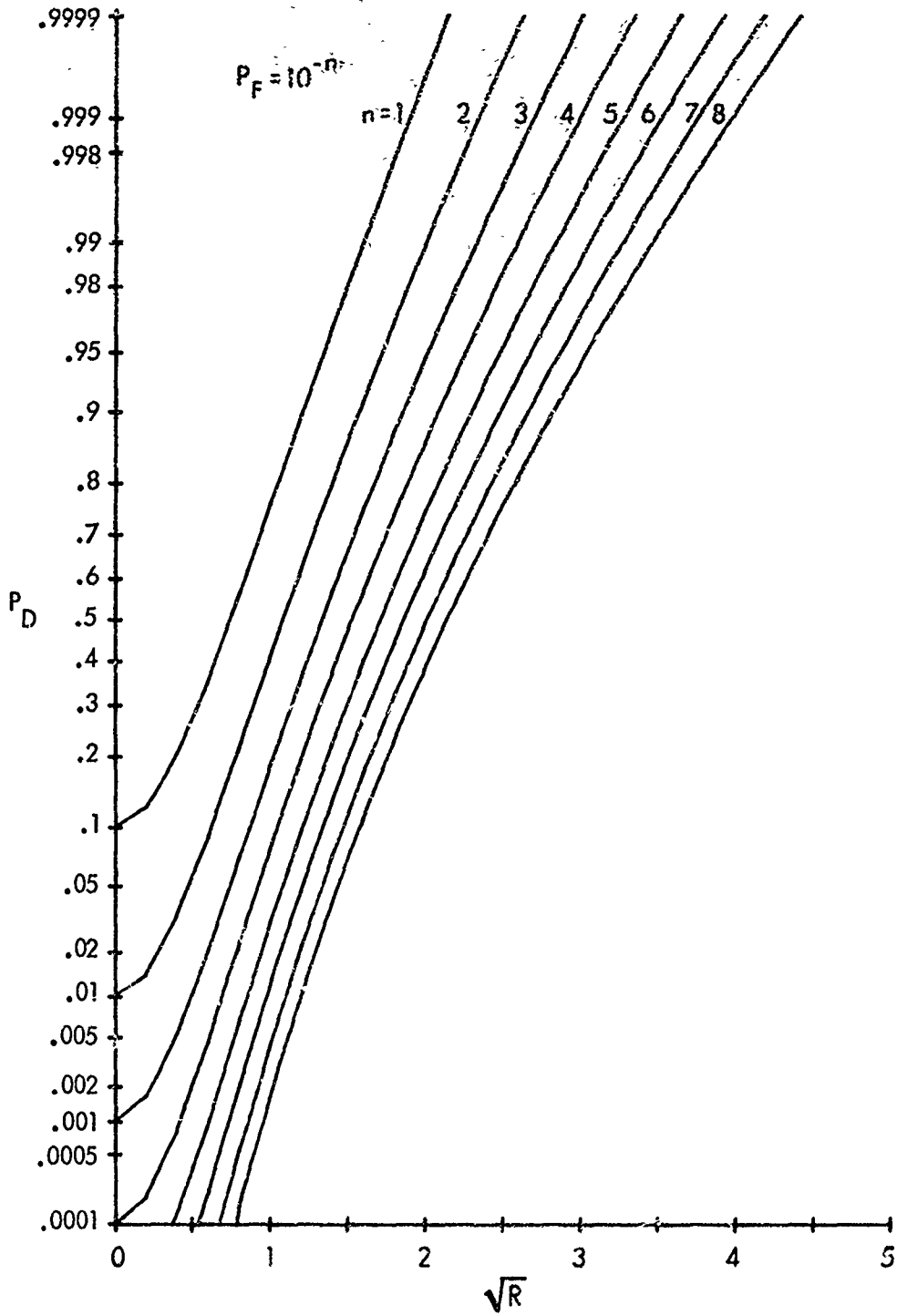


Fig. 18B.  $f = .2$   
 Fig. 18. Detection Probability; NB,  $\hat{\beta} = 8$

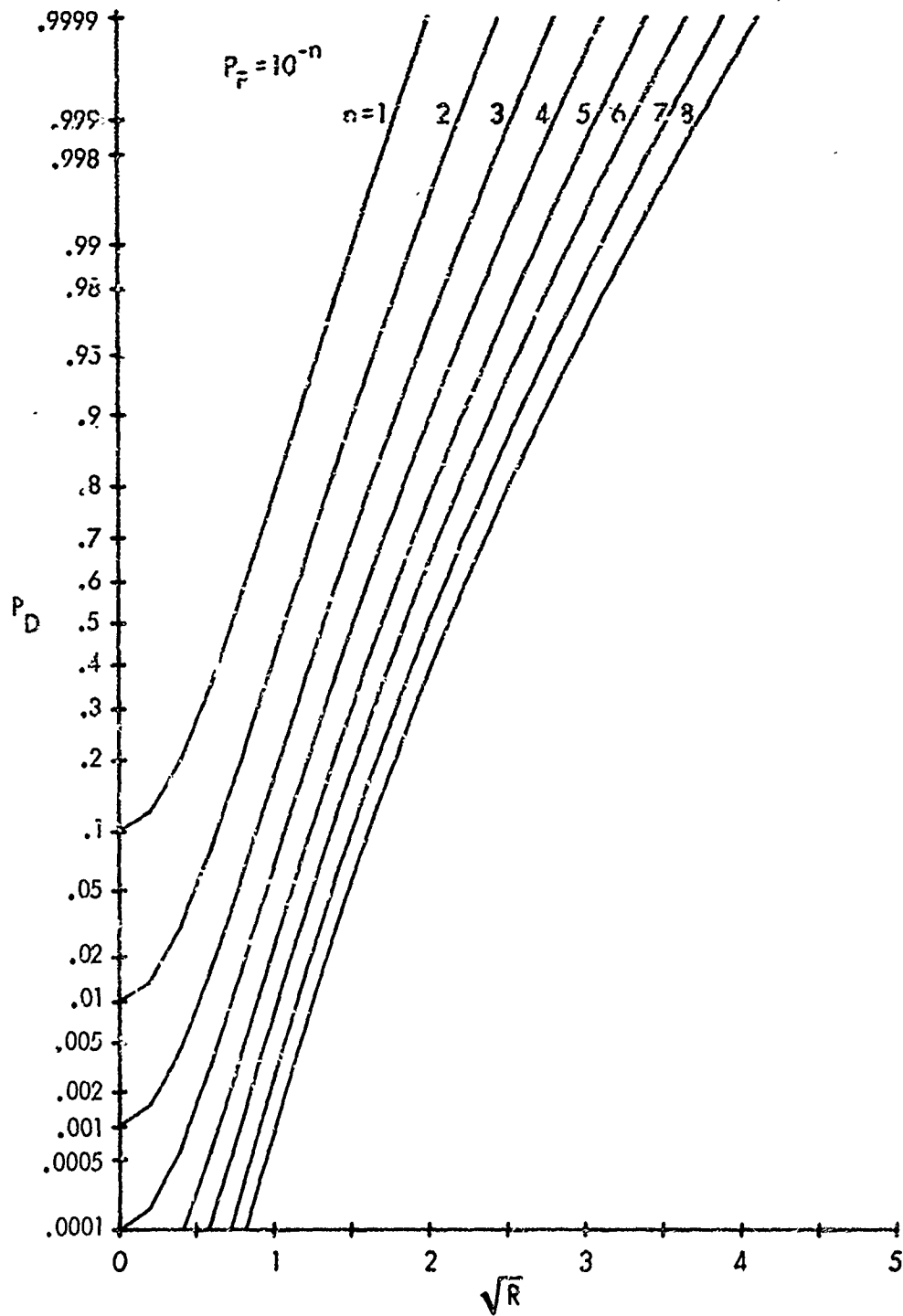


Fig. 18C.  $f = 0$   
 Fig. 18. Detection Probability; NB,  $\hat{\beta} = 8$

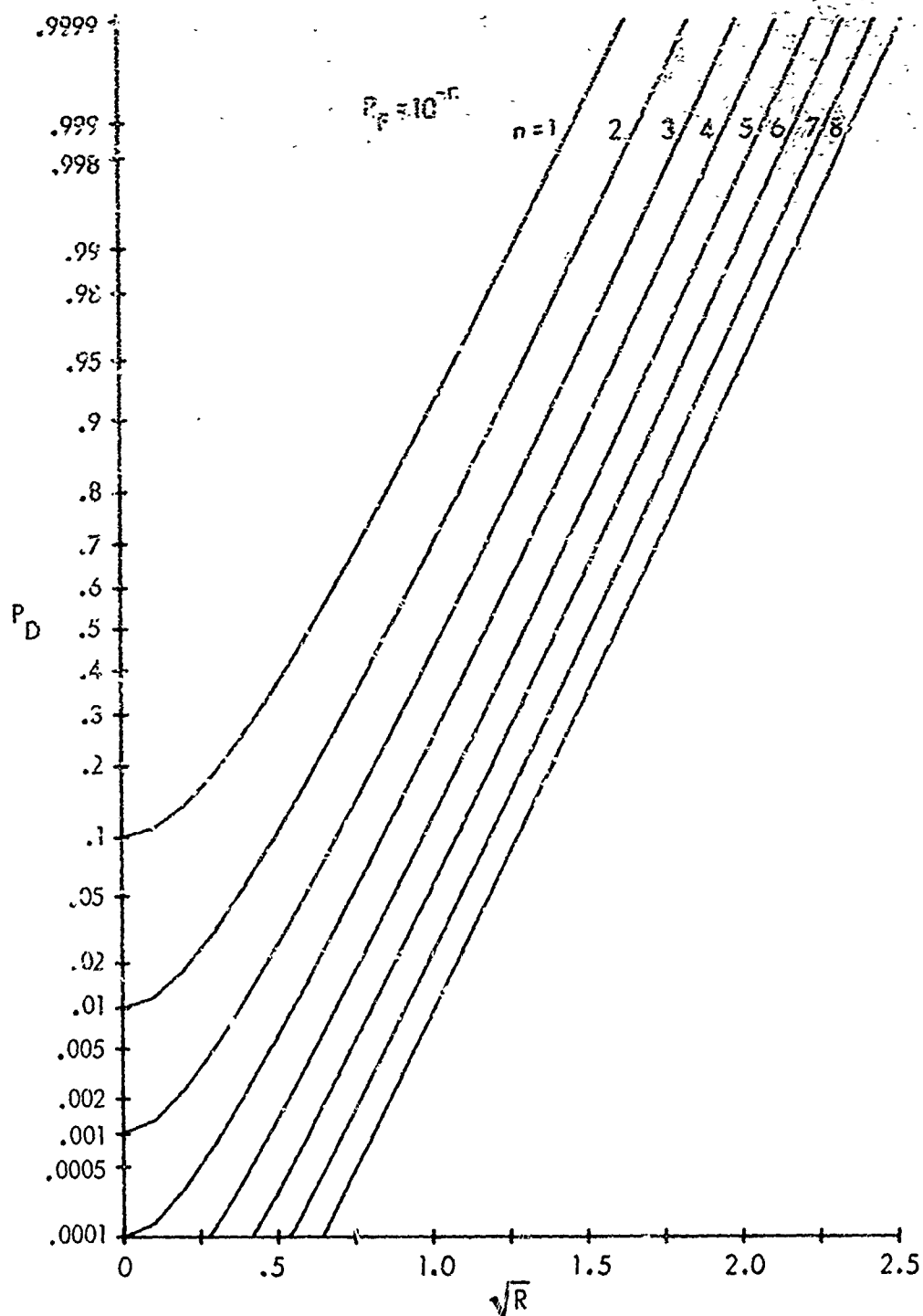


Fig. 19A.  $f = 1$   
Fig. 19. Detection Probability; NB,  $\hat{\beta} = 16$

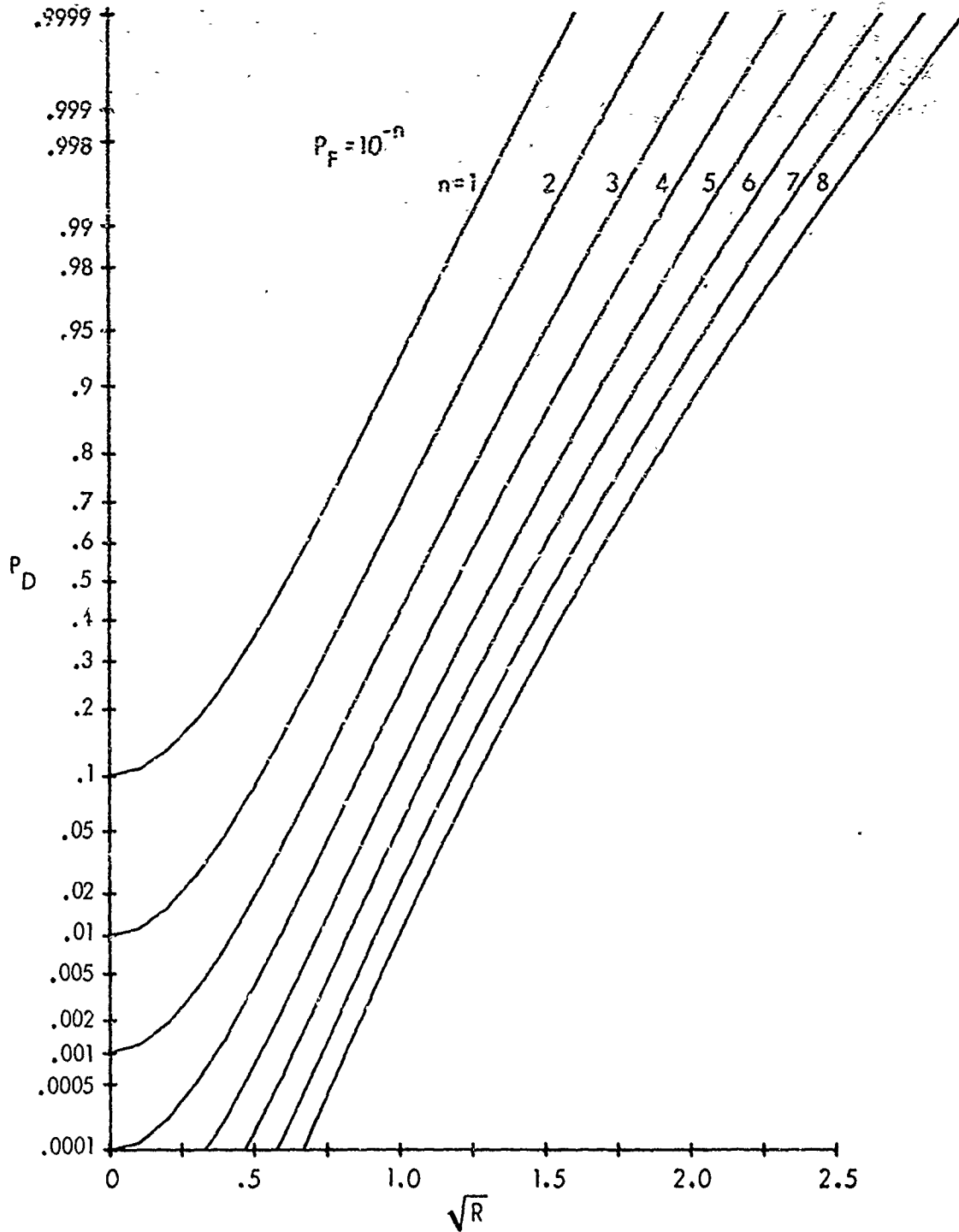


Fig. 19B.  $f = .2$   
 Fig. 19. Detection Probability; NB,  $\hat{\beta} = 16$

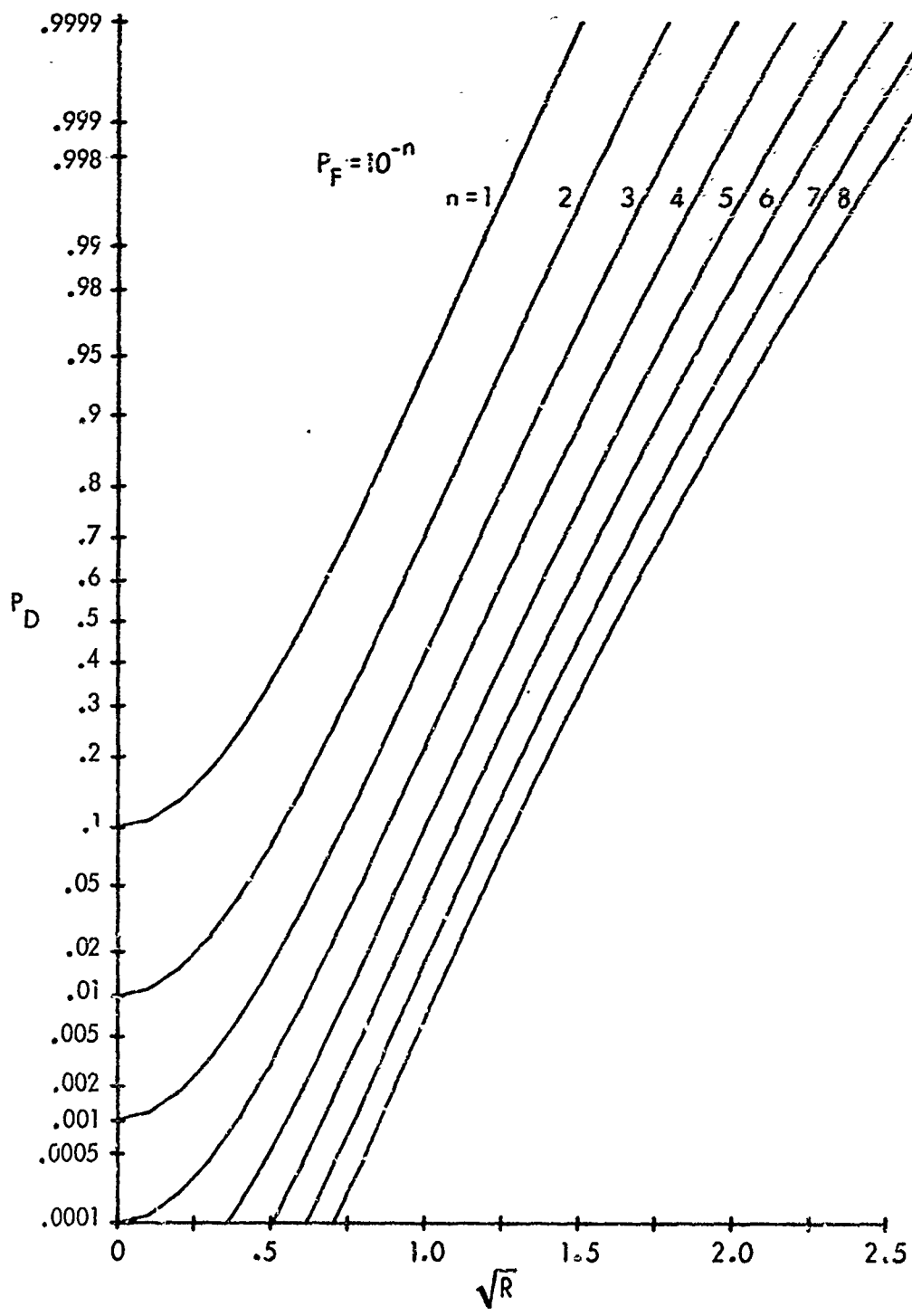


Fig. 19C.  $f = 0$   
 Fig. 19. Detection Probability; NB,  $\hat{\beta} = 16$

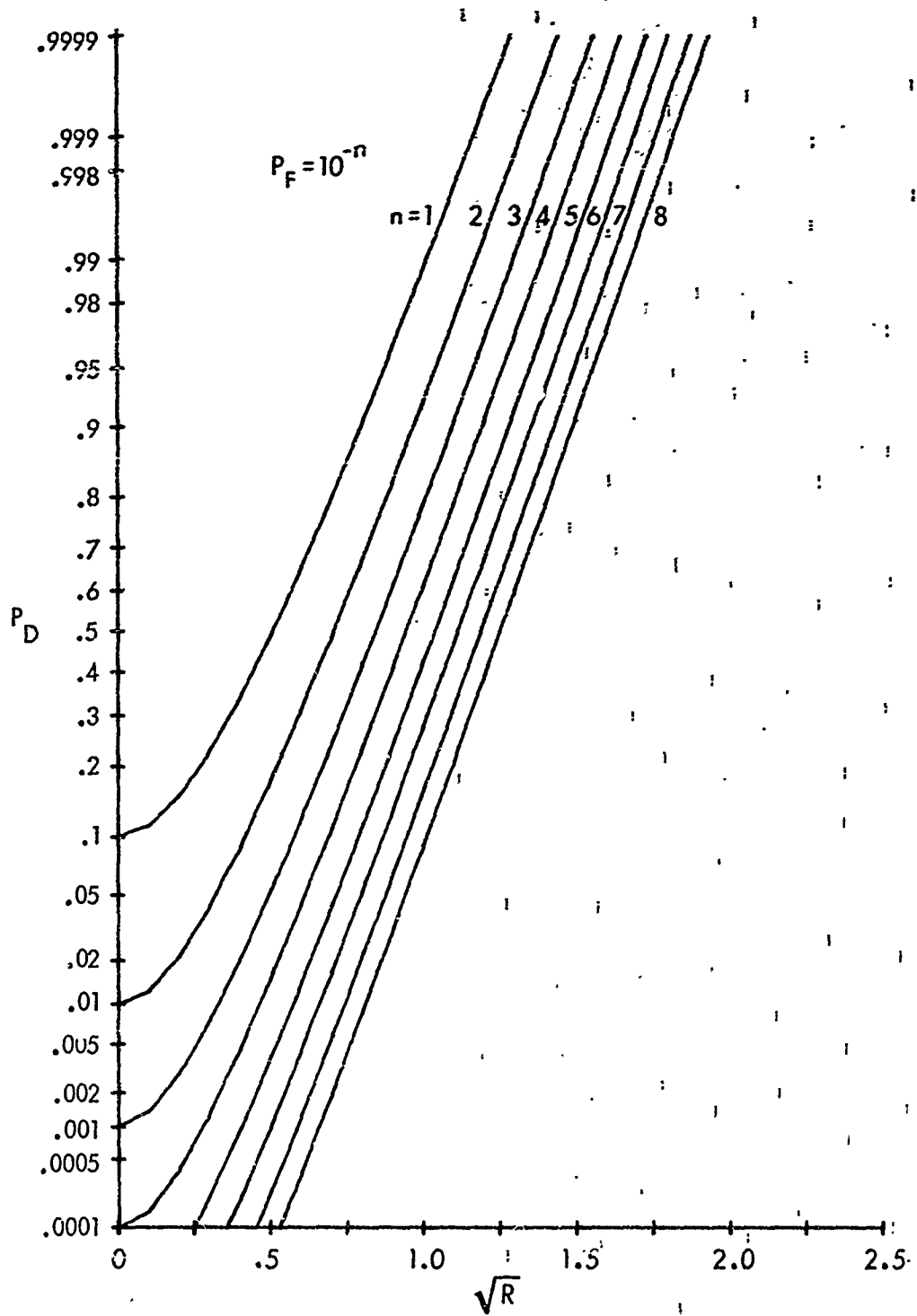


Fig. 20A.  $f = 1$   
Fig. 20. Detection Probability; NB,  $\hat{\beta} = 32$

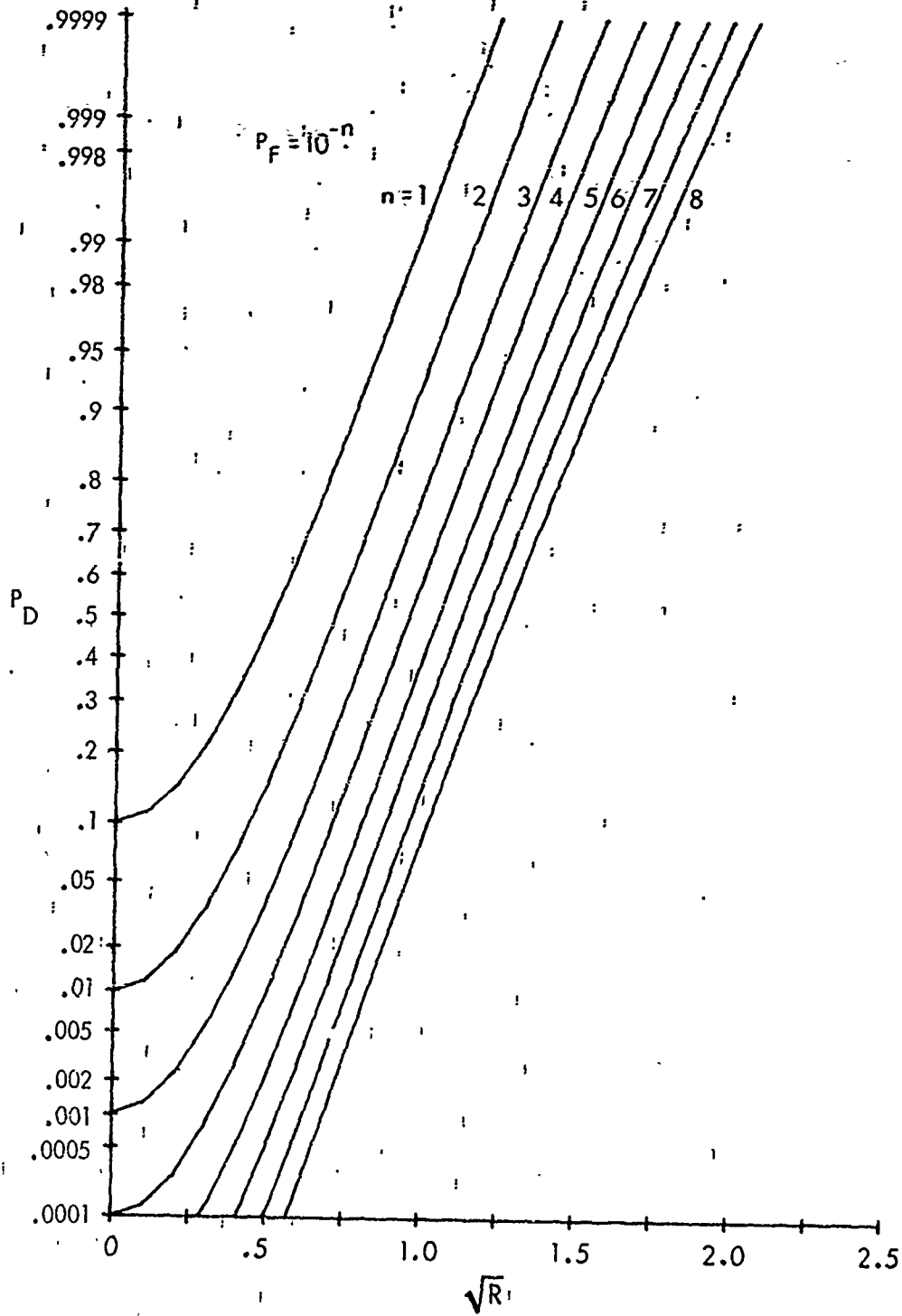


Fig. 20B,  $f = .2$   
 Fig. 20. Detection Probability; NB,  $\hat{\beta} = 32$

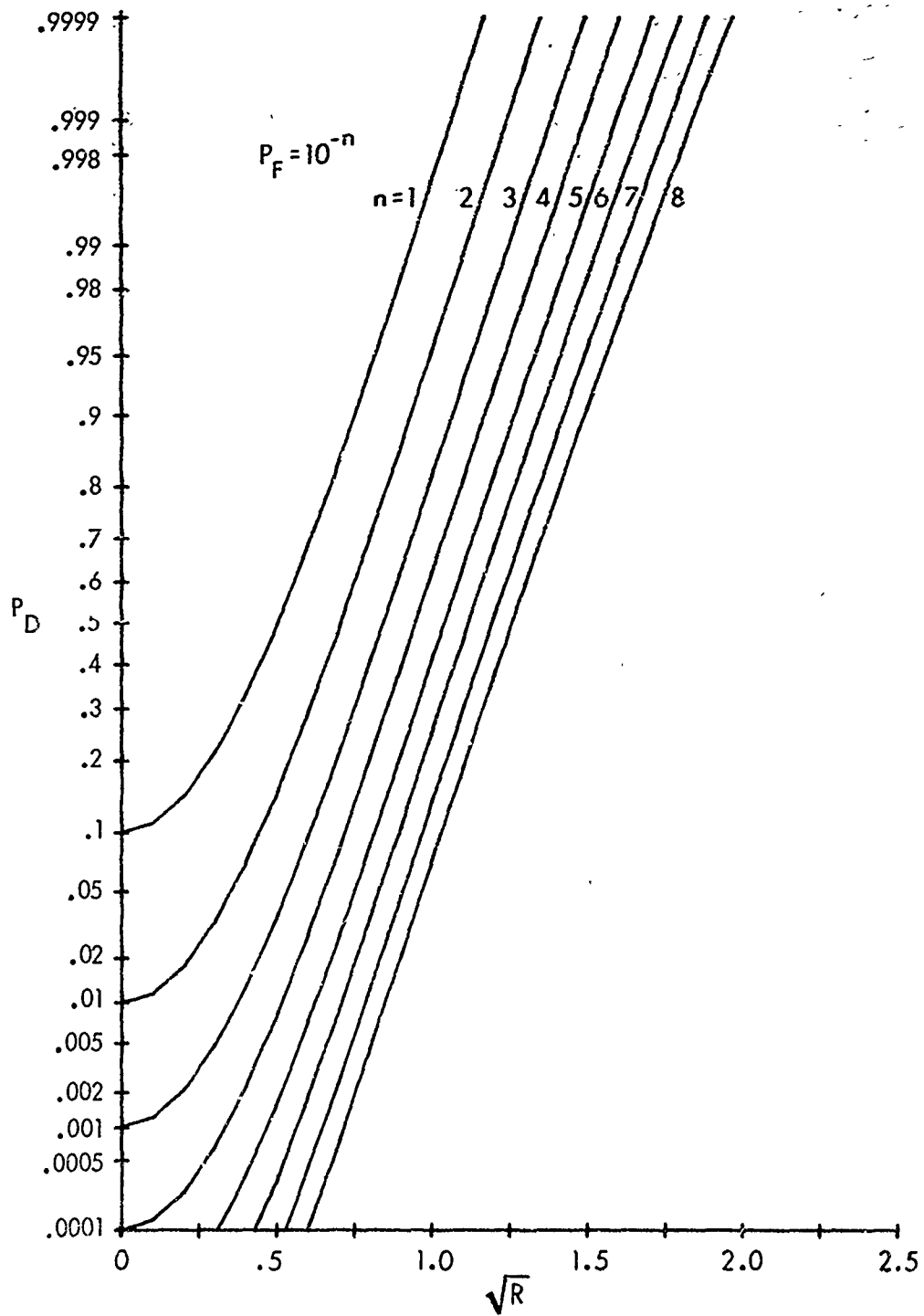


Fig. 20C.  $f = 0$   
 Fig. 20. Detection Probability; NB,  $\hat{\beta} = 32$

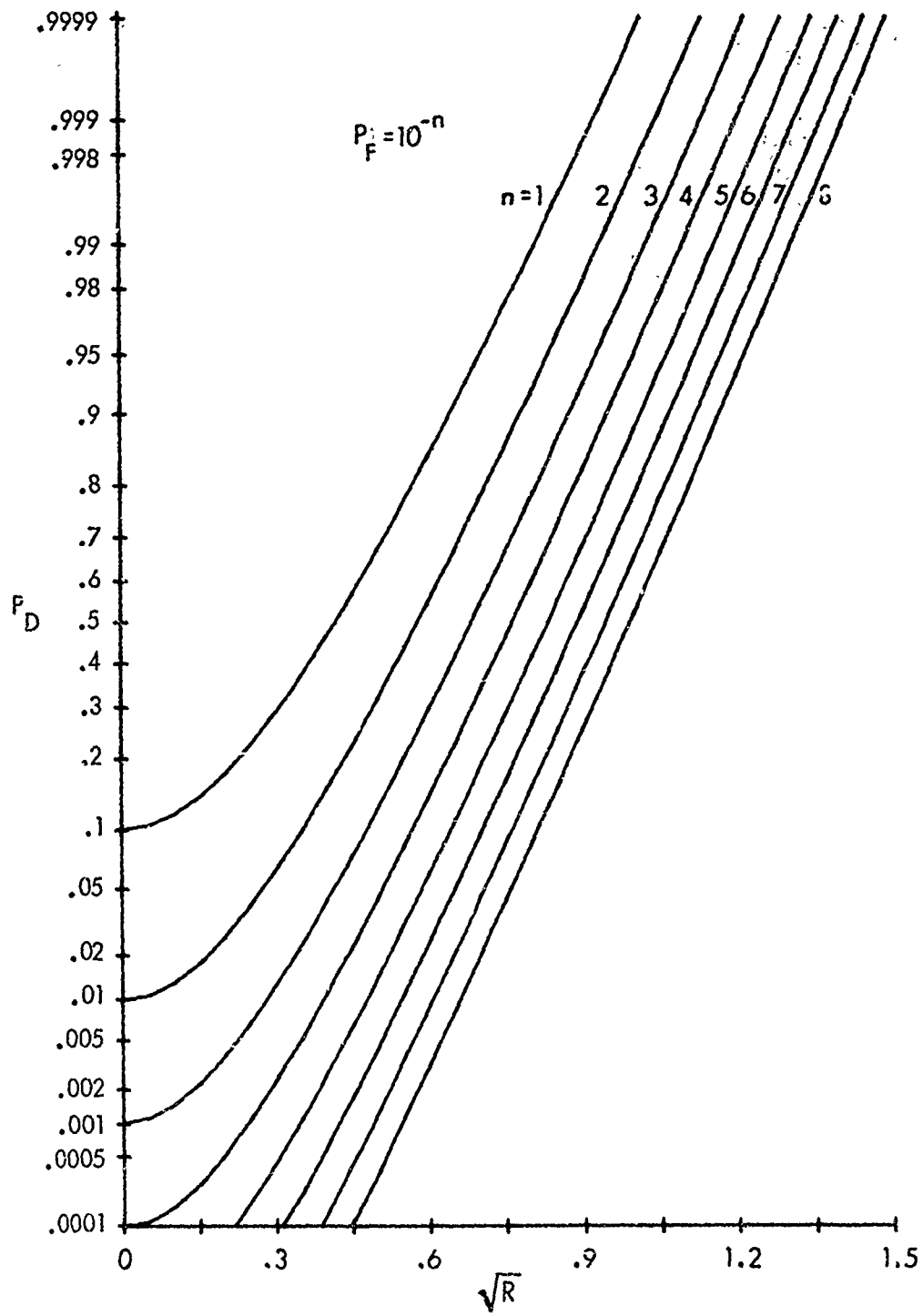


Fig. 21A.  $f = 1$   
 Fig. 21. Detection Probability; NB,  $\hat{\beta} = 64$

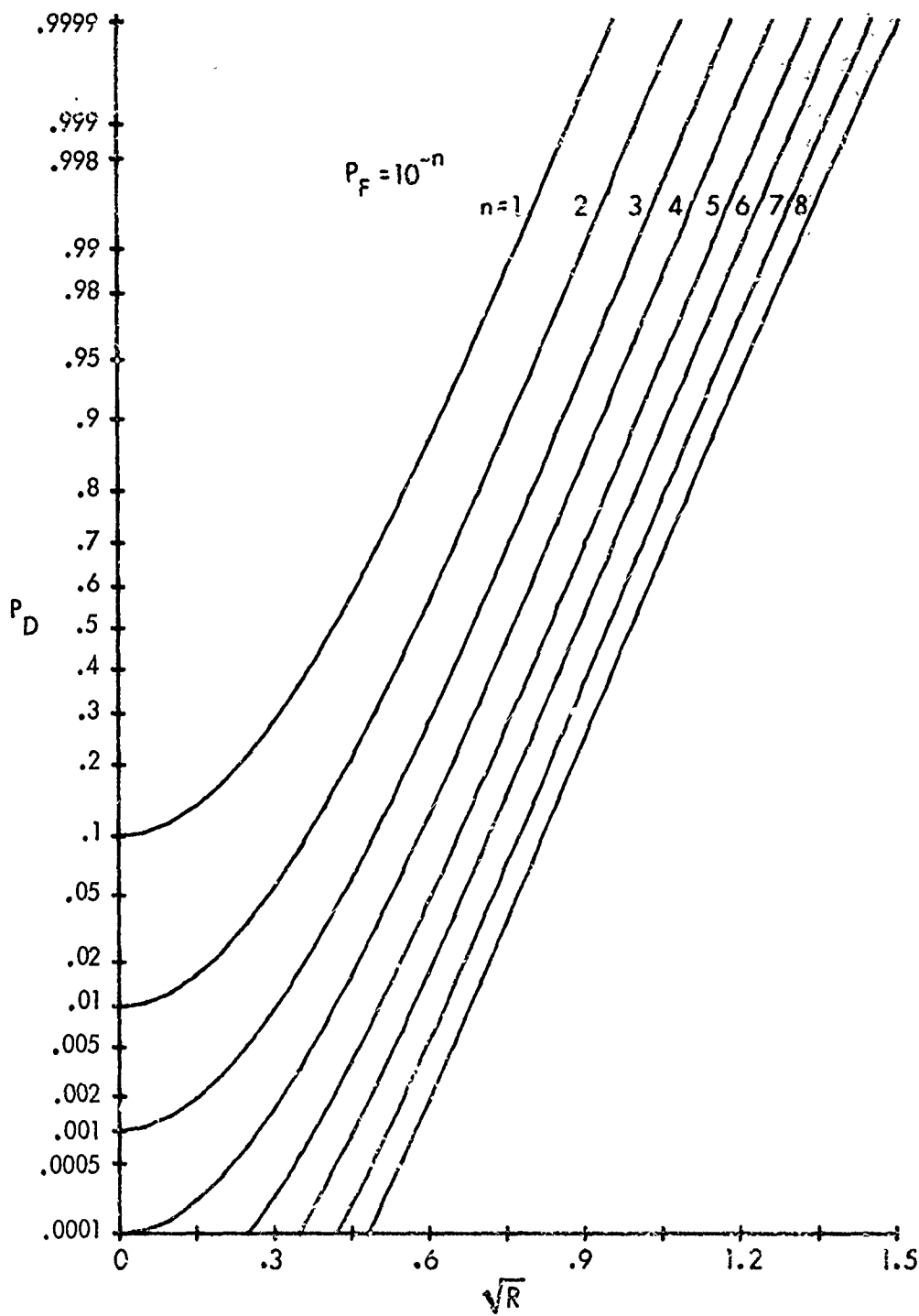


Fig. 21B.  $f = .2$   
 Fig. 21. Detection Probability; NE,  $\hat{\beta} = 64$

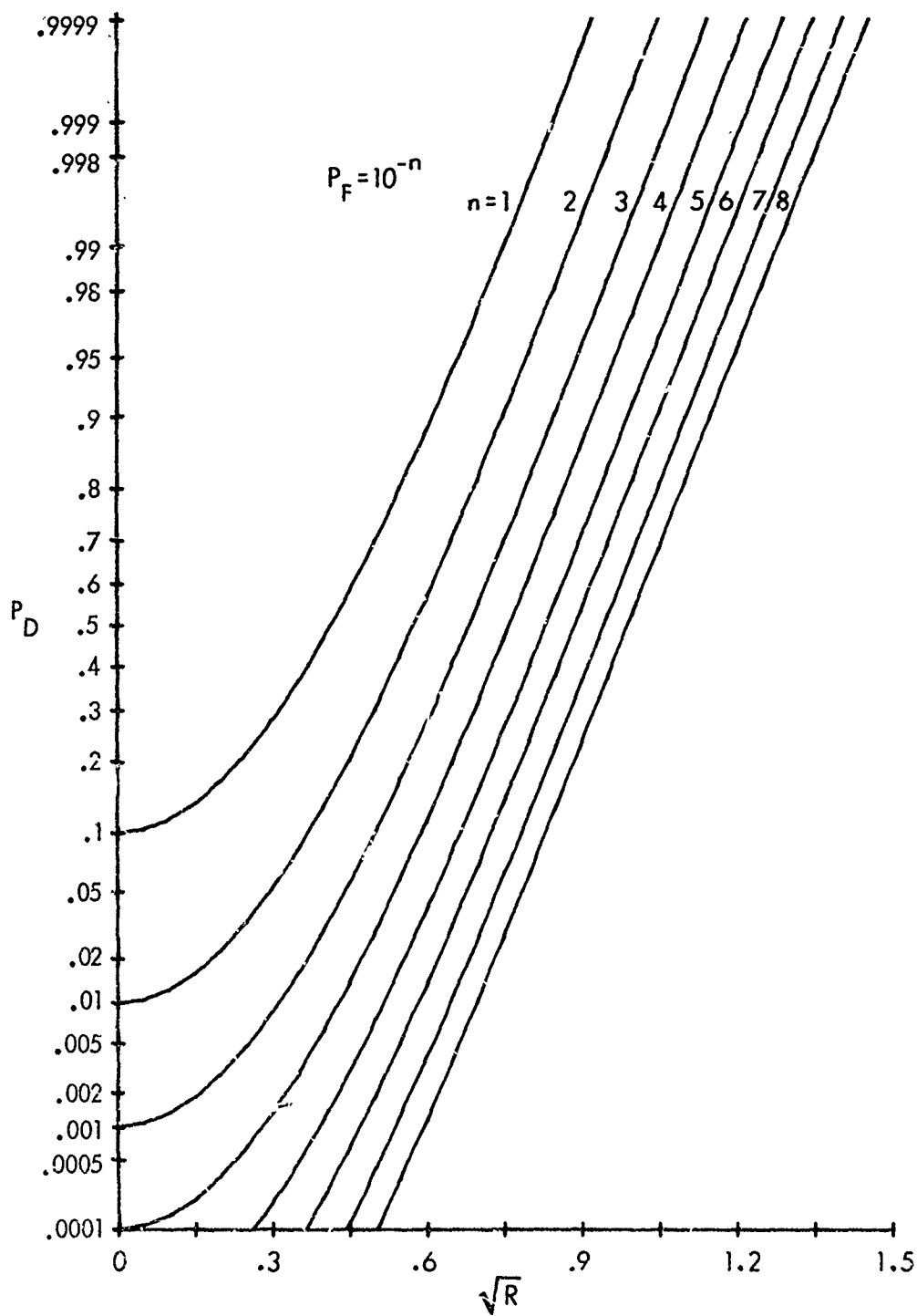


Fig. 21C.  $f = 0$   
 Fig. 21. Detection Probability; NB,  $\hat{\beta} = 64$

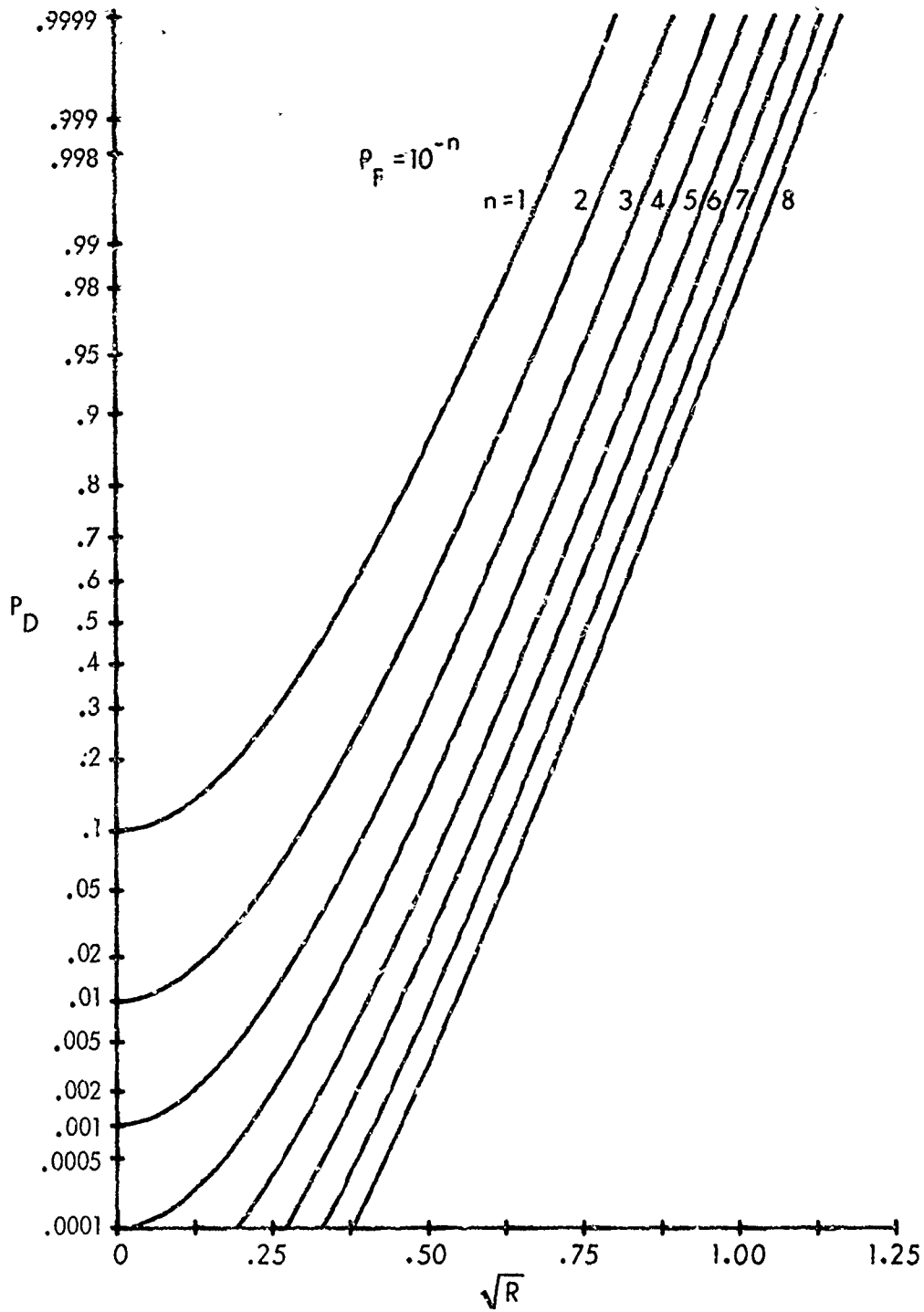


Fig. 22A.  $f = 1$   
 Fig. 22. Detection Probability; NB,  $\hat{\beta} = 128$

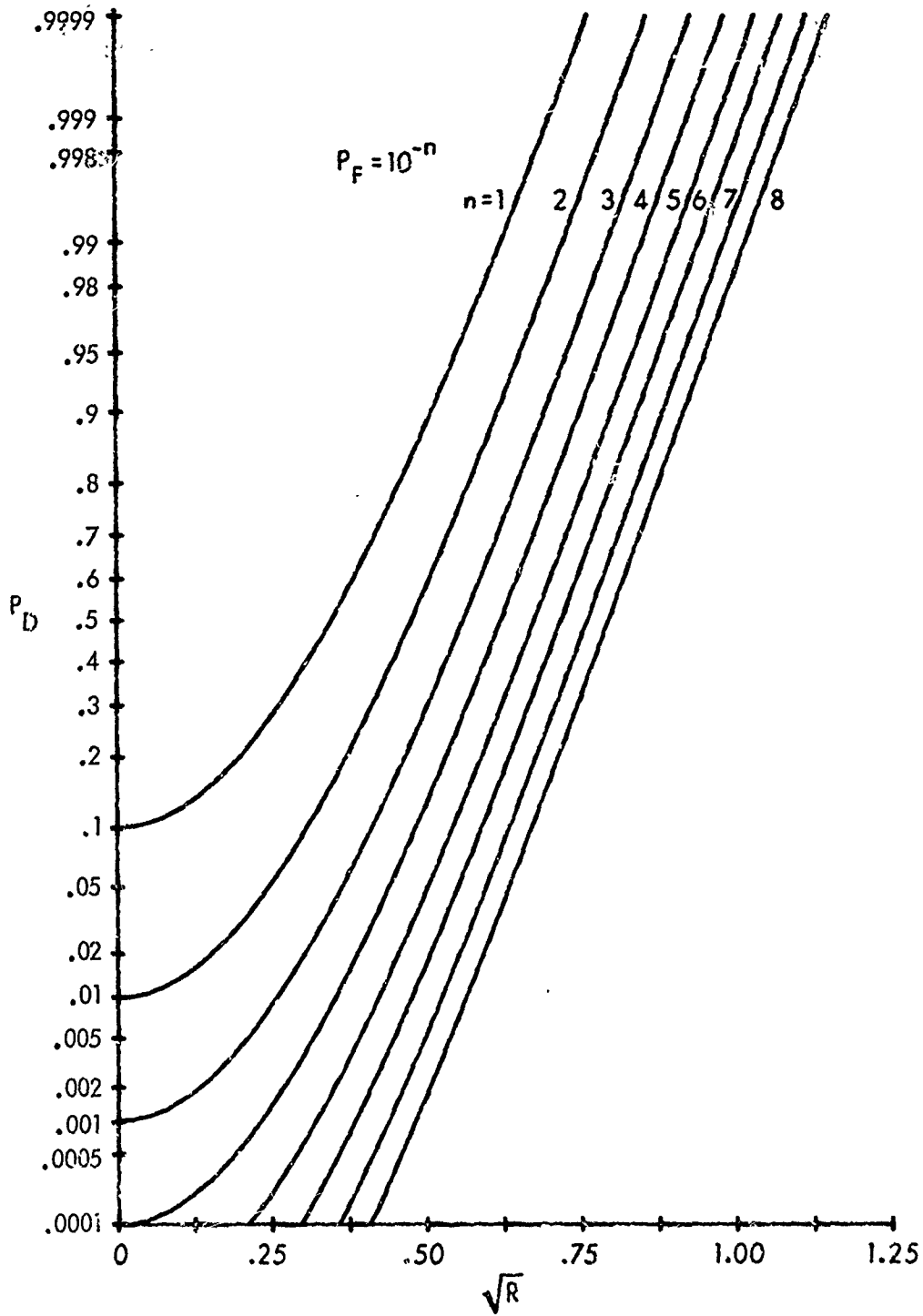


Fig. 22B.  $f = .2$   
 Fig. 22. Detection Probability; NB,  $\hat{\beta} = 128$

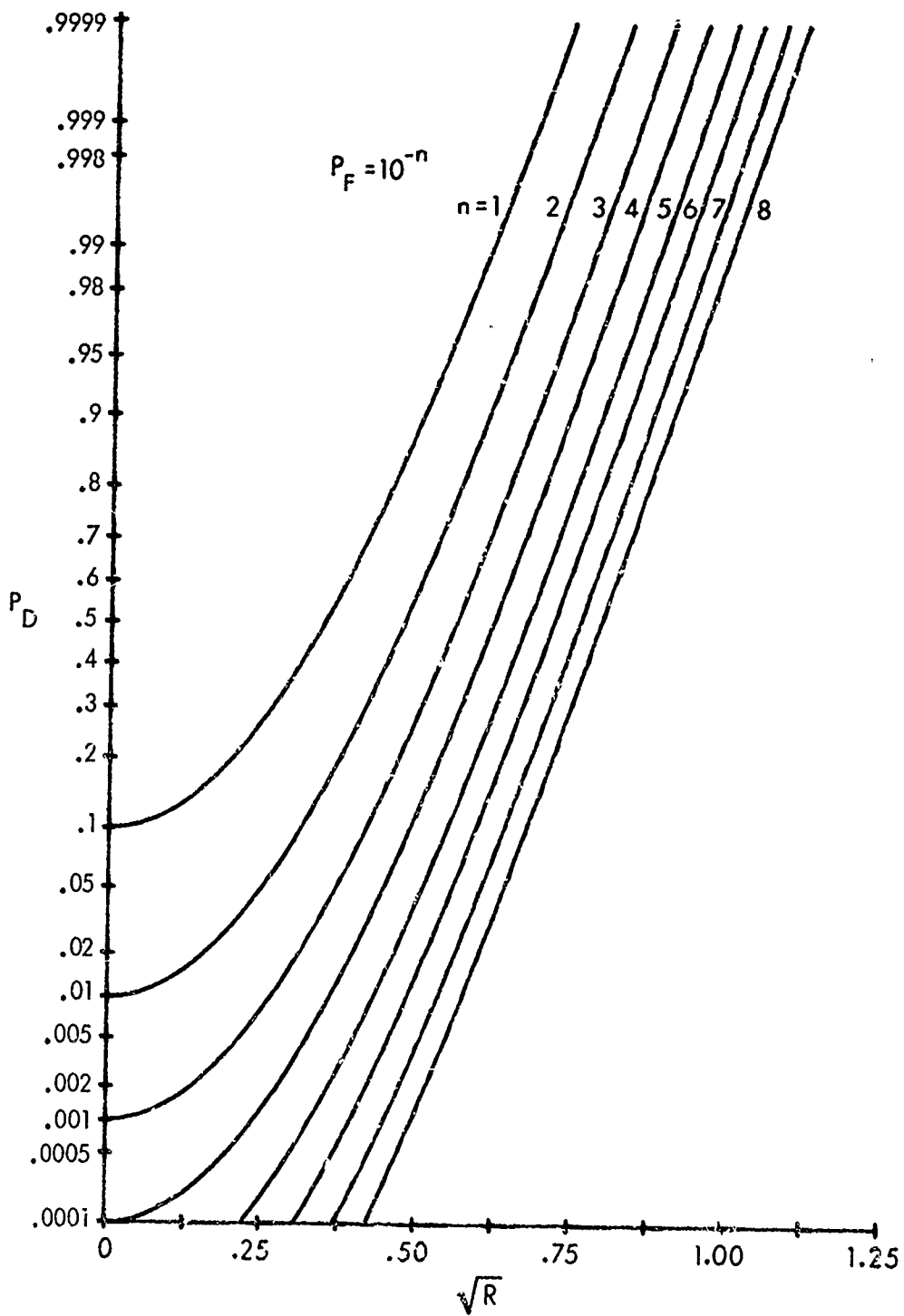


Fig. 22C.  $f = 0$   
 Fig. 22. Detection Probability; NB,  $\hat{\beta} = 128$

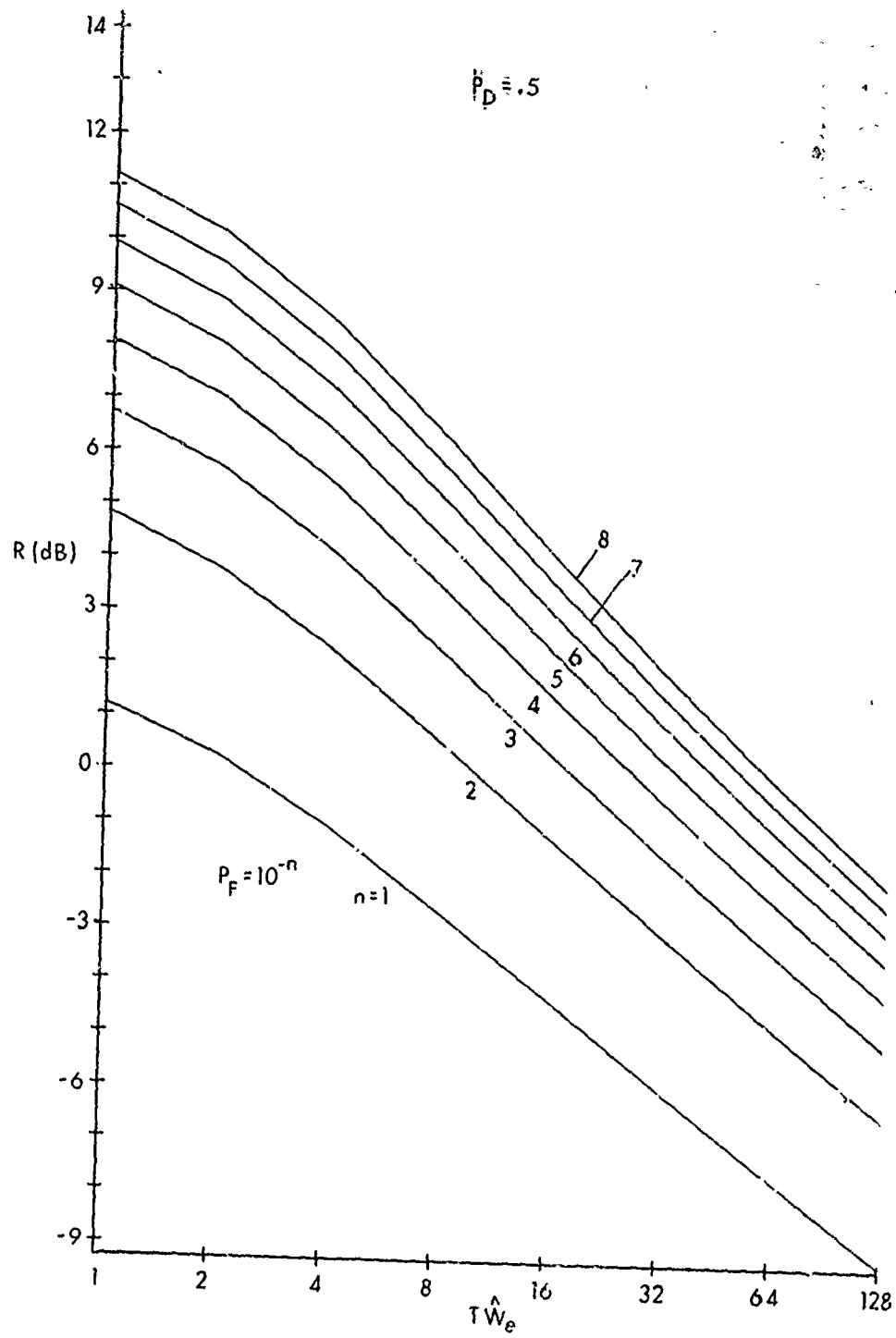


Fig. 23A.  $f = 1$   
Fig. 23. Required Signal-to-Noise Ratio; NB

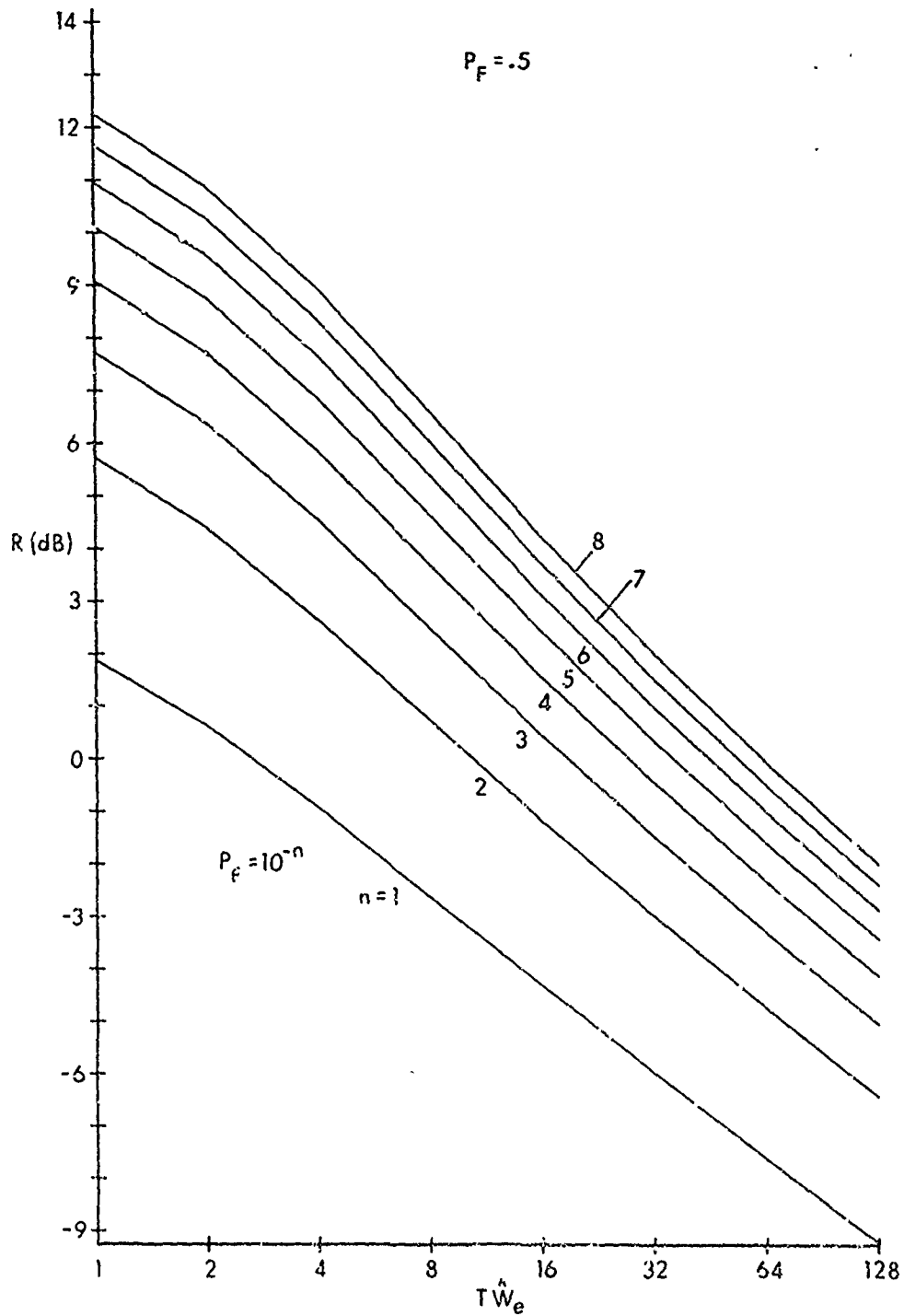


Fig. 23B.  $f = .2$

Fig. 23. Required Signal-to-Noise Ratio; NB

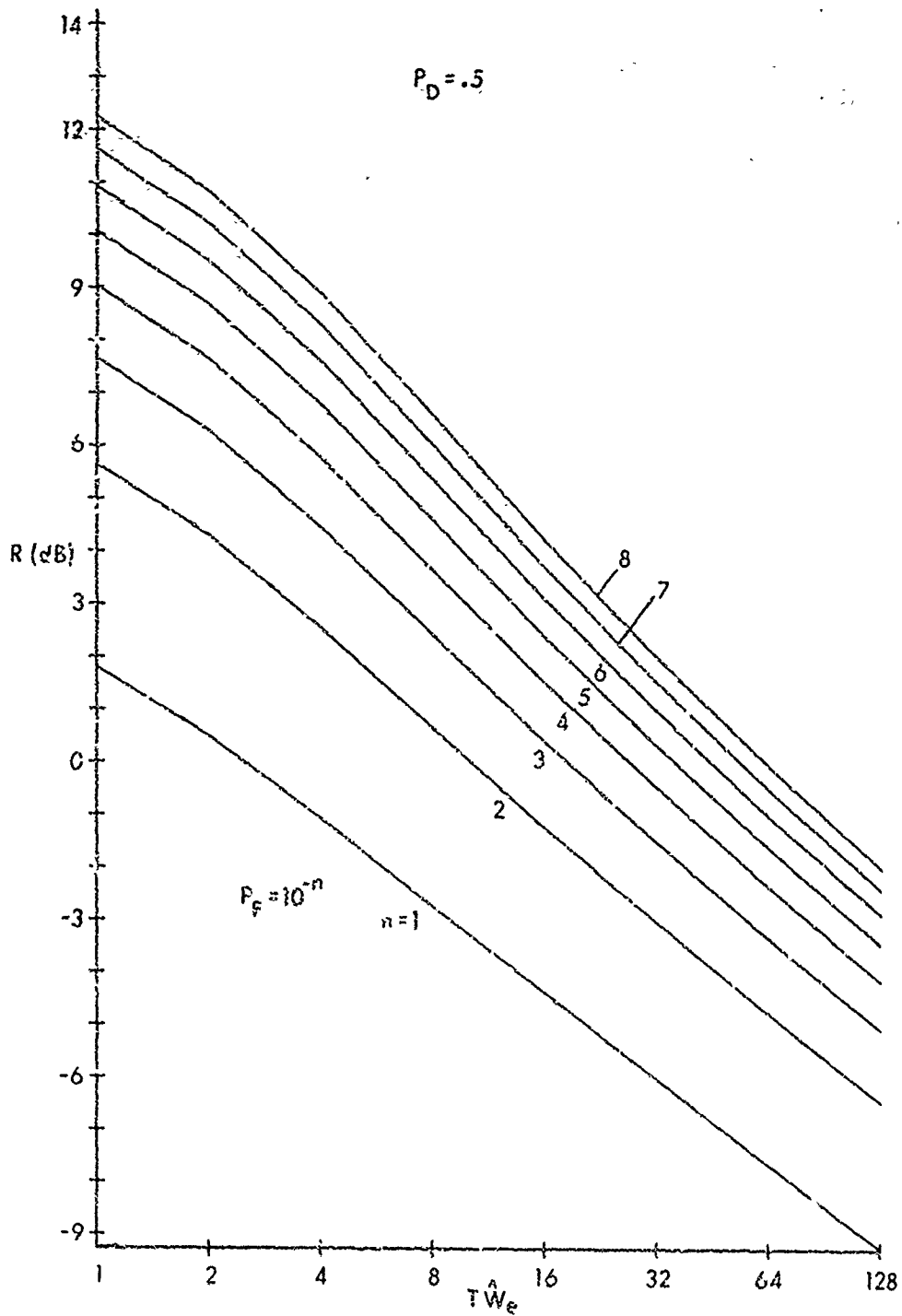


Fig. 23C.  $f = 0$

Fig. 23. Required Signal-to-Noise Ratio; NB

Appendix A  
COMPLEX ENVELOPE RELATIONS

In this appendix, we collect the complex envelope relations that are required in analyzing the narrowband (NB) processor. Consider a stationary zero-mean process  $x(t)$  passed through a time-invariant linear filter, as depicted in Fig. A-1. Here  $U(f)$  is the unit step function:

$$U(f) = \begin{cases} 0, & f < 0 \\ 1, & f > 0 \end{cases} \quad (\text{A-1})$$

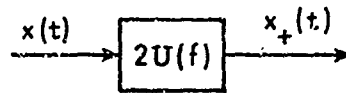


Fig. A-1. Single-Sided Filter

Thus, the output  $x_+(t)$  contains only positive-frequency components. If the spectrum of  $x(t)$  is  $G_x(f)$ , then, from Fig. A-1, the spectrum of  $x_+(t)$  is

$$G_{x_+}(f) = 4U(f)G_x(f) \quad (\text{A-2})$$

Also, since

$$U(f) = 1 + \text{sgn}(f) = 1 + i[-i \text{sgn}(f)] \quad (\text{A-3})$$

we can express

$$x_+(t) = x(t) + ix_H(t) \quad (\text{A-4})$$

where  $x_H(t)$  is the Hilbert transform of  $x(t)$ :

$$x_H(t) = \frac{1}{\pi} \int_{-\infty}^{\infty} dr \frac{x(r)}{t-r} \quad (\text{A-5})$$

Let the "center" frequency of  $G_{x_+}(f)$  be  $f_0$  and let the complex envelope  $\underline{x}(t)$  of  $x(t)$  be defined as

$$\underline{x}(t) = x_+(t) \exp(-i2\pi f_0 t) \quad (\text{A-6})$$

Then the spectrum of the complex envelope is

$$G_{\underline{x}}(f) = G_{x_+}(f+f_0) = 4U(f+f_0) G_x(f+f_0) \quad , \quad (\text{A-7})$$

and the mean magnitude-squared value of the complex envelope is

$$\overline{|\underline{x}(t)|^2} = \int_{-\infty}^{\infty} df G_{\underline{x}}(f) = 4 \int_0^{\infty} df G_x(f) = 2\sigma_x^2 \quad , \quad (\text{A-8})$$

where  $\sigma_x^2$  is the power of process  $x(t)$ .

Let the complex envelope, which is low-frequency (LF), be represented in terms of its real and imaginary components:

$$\underline{x}(t) = x_c(t) + i x_s(t) \quad . \quad (\text{A-9})$$

There follows, using (A-4), (A-6), and (A-9),

$$x(t) = x_c(t) \cos(2\pi f_0 t) - x_s(t) \sin(2\pi f_0 t) \quad . \quad (\text{A-10})$$

Thus,  $x_c(t)$  and  $x_s(t)$  are the in-phase and quadrature components of  $x(t)$ .

Now if the process  $x(t)$  is filtered by a linear filter with transfer function  $H(f)$ , yielding (complex) output  $y(t)$ , it can be shown that

$$\overline{y(t)y(t-\tau)} = \int_{-\infty}^{\infty} df \exp(i2\pi f\tau) G_x(f) H(f) H(-f) \quad . \quad (\text{A-11})$$

Applying this result to Fig. A-1, we obtain

$$\overline{x_+(t)x_+(t-\tau)} = 0 \text{ for all } \tau \quad , \quad (\text{A-12})$$

since  $U(f)$  and  $U(-f)$  are disjoint. Hence, from (A-6),

$$\overline{\underline{x}(t)\underline{x}(t-\tau)} = 0 \text{ for all } \tau \quad . \quad (\text{A-13})$$

Therefore, using (A-9) and (A-13),

$$\begin{aligned} \overline{x_c(t)x_s(t-\tau)} &= \overline{\text{Re}\{\underline{x}(t)\} \text{Im}\{\underline{x}(t-\tau)\}} \\ &= \frac{1}{2} \overline{[\underline{x}(t) + \underline{x}^*(t)] \frac{1}{i2} [\underline{x}(t-\tau) - \underline{x}^*(t-\tau)]} \\ &= \frac{1}{i4} \overline{[-R_{\underline{x}}(\tau) + R_{\underline{x}}^*(\tau)]} = -\frac{1}{2} \text{Im}\{R_{\underline{x}}(\tau)\} \\ &= -\frac{1}{2} \text{Im} \left\{ \int_{-\infty}^{\infty} df \exp(i2\pi f\tau) G_{\underline{x}}(f) \right\} = -\frac{1}{2} \int_{-\infty}^{\infty} df \sin(2\pi f\tau) G_{\underline{x}}(f) \end{aligned} \quad (\text{A-14})$$

where we have defined

$$R_{\underline{x}}(\tau) = \overline{\underline{x}(t) \underline{x}^*(t-\tau)} \quad (\text{A-15})$$

and utilized the fact that  $G_x(f)$  is real (see (A-7)). Now from (A-14), it may be seen that if and only if the LF spectrum  $G_x(f)$  is even about  $f = 0$ , then the processes  $x_c(t)$  and  $x_s(t)$  are uncorrelated for all relative time delays. In terms of the original spectrum  $G_x(f)$ , processes  $x_c(t)$  and  $x_s(t)$  are uncorrelated for all time delays if and only if  $G_x(f)$  is even about  $f_0$  (in  $(0, 2f_0)$ ). In the special case where  $x(t)$  is a Gaussian process (not assumed up to now),  $x_c(t)$  and  $x_s(t)$  are independent processes [Ref. 19, p. 41], since  $x_c(t)$  and  $x_s(t)$  are Gaussian processes (being linear combinations of  $\underline{x}(t)$ ).

Lastly (eliminating the Gaussian assumption again), by a procedure analogous to (A-14),

$$\overline{x_c(t) x_c(t-\tau)} = \overline{x_s(t) x_s(t-\tau)} = \frac{1}{2} \operatorname{Re} \{R_{\underline{x}}(\tau)\} = \frac{1}{2} \int_{-\infty}^{\infty} df \cos(2\pi f\tau) G_{\underline{x}}(f) \quad (\text{A-16})$$

As a special case, the powers are, using (A-8),

$$\overline{x_c^2(t)} = \overline{x_s^2(t)} = \frac{1}{2} \int_{-\infty}^{\infty} df G_{\underline{x}}(f) = \sigma_x^2 \quad (\text{A-17})$$

## Appendix B

DERIVATION OF CHARACTERISTIC FUNCTION  
FOR LOW-FREQUENCY AND NARROWBAND CASES

This appendix consists of two parts: The first part derives the characteristic function (CF) of the decision variable  $l$  for the low-frequency (LF) case, as given by (6)\*; the second part does the same for the narrowband (NB) decision variable  $l$ , as given by (10). \* An example for each case is presented.

## LOW-FREQUENCY CASE

From (6),\*

$$l = \frac{1}{T} \int dt [c(t) + s(t) + n(t)]^2. \quad (\text{B-1})$$

The powers in the zero-mean Gaussian processes  $s(t)$  and  $n(t)$  are  $\sigma_s^2$  and  $\sigma_n^2$ , respectively. Let us now define

$$r(t) = \frac{c(t)}{(\sigma_s^2 + \sigma_n^2)^{1/2}},$$

$$x(t) = \frac{s(t) + n(t)}{(\sigma_s^2 + \sigma_n^2)^{1/2}}. \quad (\text{B-2})$$

Then

$$l = (\sigma_s^2 + \sigma_n^2) p, \quad (\text{B-3})$$

where

$$p \equiv \frac{1}{T} \int dt [r(t) + x(t)]^2. \quad (\text{B-4})$$

Let the correlation of  $x(t)$  be  $R(\tau)$ , which is general here, except that  $R(0) = 1$ , as seen from (B-2);  $s(t)$  and  $n(t)$  are assumed independent of each other. At this point, the deterministic waveform  $c(t)$  is also general.

\* This equation is in the main text of this report.

The CF  $f_{\ell}$  of the random variable  $(RV)\ell$  is related to the CF  $f_p$  of the RV  $P$  according to

$$f_{\ell}(\xi) = \overline{\exp(i\xi\ell)} = \overline{\exp(i\xi(\sigma_s^2 + \sigma_n^2)P)} = f_p((\sigma_s^2 + \sigma_n^2)\xi) \quad , \quad (B-5)$$

using (B-3).

Now we define for the kernel (correlation)  $R$ , the eigenvalues  $\{\lambda_j\}$ , and eigenfunctions  $\{\phi_j\}$ :

$$\lambda_j \int_T du R(t-u) \phi_j(u) = \phi_j(t), \quad t \in T \quad (B-6)$$

Next, we expand  $x(t)$  in the set of eigenfunctions according to

$$x(t) = \sum_j x_j \phi_j(t), \quad t \in T \quad , \quad (B-7)$$

where

$$x_j = \int_T dt x(t) \phi_j(t) \quad , \quad (B-8)$$

since the eigenfunctions are orthonormal [Ref. 1, pp. 98-103]. The RVs  $\{x_j\}$  have the properties

$$\begin{aligned} \bar{x}_j &= 0 \quad , \\ \overline{x_j x_k} &= \iint_T dt du R(t-u) \phi_j(t) \phi_k(u) = \frac{1}{\lambda_j} \delta_{jk} \quad , \end{aligned} \quad (B-9)$$

using the fact that  $x(t)$  has zero-mean and employing (B-8) and (B-6). Since  $x_j$  in (B-8) is a linear operation on the Gaussian process  $x(t)$ , then  $\{x_j\}$  are independent Gaussian variables.

When we employ (B-7) in (B-4), we obtain

$$p = \frac{1}{T} \int_T dt r^2(t) + \frac{2}{T} \sum_j r_j x_j + \frac{1}{T} \sum_j x_j^2 \quad , \quad (B-10)$$

where

$$r_j \equiv \int_T dt r(t) \phi_j(t) \quad . \quad (B-11)$$

Then the CF of RV  $p$  is

$$f_p(\xi) = \overline{\exp(i\xi p)} = \exp\left(i\frac{\xi}{T}\int_T dt r^2(t)\right) \prod_j \left\{ \overline{\exp\left[i\frac{2\xi}{T}r_j x_j + i\frac{\xi}{T}x_j^2\right]} \right\}, \quad (\text{B-12})$$

using (B-10) and the independence of the  $\{x_j\}$ . The  $j$ th average in (B-12) is, letting  $\sigma_j^2 = 1/\lambda_j$  and using (B-9),

$$\begin{aligned} & \int \frac{dx}{\sqrt{2\pi}\sigma_j} \exp\left(-\frac{x^2}{2\sigma_j^2}\right) \exp\left(i\frac{2\xi}{T}r_j x + i\frac{\xi}{T}x^2\right) \\ &= \left(1 - i\frac{2\sigma_j^2\xi}{T}\right)^{-1/2} \exp\left(-\frac{2r_j^2\xi^2/T^2}{\frac{1}{\sigma_j^2} - i2\xi/T}\right), \end{aligned} \quad (\text{B-13})$$

where the square root is principal value. Equation (B-12) can then be expressed as

$$f_p(\xi) = \prod_j \left\{ \left(1 - i\frac{2\xi}{\lambda_j T}\right)^{-1/2} \right\} \exp\left(i\frac{\xi}{T}\int_T dt r^2(t)\right) \exp\left(-\frac{2\xi^2}{T^2} \sum_j \frac{r_j^2}{\lambda_j - i2\xi/T}\right). \quad (\text{B-14})$$

However, employing (B-11), we get

$$\begin{aligned} & \sum_j \frac{r_j^2}{\lambda_j - i2\xi/T} \cdot \iint_T dt du r(t)r(u) \sum_j \frac{\phi_j(t)\phi_j(u)}{\lambda_j - i2\xi/T} \\ &= \iint_T dt du r(t)r(u) \Gamma(t, u; i2\xi/T), \end{aligned} \quad (\text{B-15})$$

where  $\Gamma$  is the resolvent (or reciprocal) kernel of  $R$  [Ref. 20, p. 141, Eq. 64 and p. 134, Eq. 52]. Substituting (B-15) into (B-14) and employing (B-2) yields

$$\begin{aligned} f_p(\xi) &= \prod_j \left\{ \left(1 - i\frac{2\xi}{\lambda_j T}\right)^{-1/2} \right\} \exp\left[i\frac{\xi}{\sigma_s^2 + \sigma_n^2} \frac{1}{T} \int_T dt c^2(t)\right. \\ &\quad \left. - \frac{2\xi^2}{\sigma_s^2 + \sigma_n^2} \frac{1}{T^2} \iint_T dt du c(t)c(u) \Gamma(t, u; i2\xi/T)\right]. \end{aligned} \quad (\text{B-16})$$

Now, if the coherent signal component is absent, that is,  $c(t) = 0$ , this CF must reduce to

$$\left[ D \left( \frac{i 2 \xi}{T} \right) \right]^{-1/2}, \quad (\text{B-17})$$

where  $D$  is the Fredholm determinant [see Ref. 10, p. 18] (notice that the eigenvalues  $\{\lambda_i\}$  here are equal to  $\{1/\lambda_i\}$  in Ref. '10). The square root in (B-17) is not principal value, but must be determined by tracing  $D(i 2 \xi/T)$  from  $\xi = 0$ , where  $D(0) = 1$ , in a continuous fashion. This result follows by inspecting the product of principal value square roots in (B-16). Utilizing (B-17) in (B-16), we obtain the CF of  $p$  as

$$f_p(\xi) = \left[ D(i 2 \xi/T) \right]^{-1/2} \exp \left[ i \frac{\xi}{\sigma_s^2 + \sigma_n^2} \frac{1}{T} \int_T dt c^2(t) - \frac{2 \xi^2}{\sigma_s^2 + \sigma_n^2} \frac{1}{T^2} \iint_T dt du c(t) c(u) \Gamma(t, u; i 2 \xi/T) \right]. \quad (\text{B-18})$$

This CF depends on the Fredholm determinant, on the resolvent kernel of correlation  $R$ , and on the waveform  $c(t)$ . If the Fredholm determinant and the double integral on the resolvent kernel can be expressed in closed form, the CF of  $p$  is available in closed form.

It is convenient to normalize waveform  $c(t)$  as follows: Denote the average power in received waveform  $c(t)$  over the interval  $T$  as

$$P_c = \frac{1}{T} \int_T dt c^2(t), \quad (\text{B-19})$$

and define the normalized waveform

$$c_1(t) = P_c^{-1/2} c(t). \quad (\text{B-20})$$

The average power in  $c_1(t)$  over  $T$  is unity. Also we define two S/Ns:

$$R_c = \frac{P_c}{\sigma_n^2}, \quad R_s = \frac{\sigma_s^2}{\sigma_n^2}. \quad (\text{B-21})$$

These are the ratios of coherent signal power to noise power, and incoherent signal power to noise power, respectively, at the input to the LF processor in Fig. 1. Equation (B-18) can then be expressed as

$$f_p(\xi) = [D(i2\xi/T)]^{-1/2} \exp \left[ i \frac{R_c}{1+R_s} \xi - \frac{2R_c}{1+R_s} \xi^2 \frac{1}{T^2} \iint_T dt du c_1(t) c_1(u) \Gamma(t, u; i2\xi/T) \right]. \quad (\text{B-22})$$

Example: Exponential Correlation; Constant Waveform.

We assume that  $s(t)$  and  $n(t)$  are independent and have the same exponential correlation, as given in (2). \* Then, using (B-2),

$$R(\tau) = \exp(-2W_e |\tau|). \quad (\text{B-23})$$

The coherent waveform is taken to be dc:

$$c_1(t) = 1, \quad t \in T. \quad (\text{B-24})$$

Then, from Ref. 10, Eq. (37),† we have

$$f_p(\xi) \Big|_{c(t)=0} = \exp(\beta) \left[ \frac{1 - i\xi/\beta}{\phi(\xi/\beta)} \sinh(2\beta\phi(\xi/\beta)) + \cosh(2\beta\phi(\xi/\beta)) \right]^{-1/2}, \quad (\text{B-25})$$

where

$$\beta \equiv W_e T, \quad (\text{B-26})$$

$$\phi(u) \equiv (1 - i2u)^{1/2}.$$

The square root for  $\phi$  is principal value; that for  $f_p$  is not, but must be traced continuously from  $\xi = 0$ , where  $f_p(0) = 1$ .

The resolvent kernel is [Ref. 10, p. 21, Eqs. (29) and (30)]

$$\Gamma(t, u; i2\xi/T) = \frac{2\beta}{\omega T \gamma} [\cos(\omega t) \cos(\omega u) - \gamma^2 \sin(\omega t) \sin(\omega u) - \gamma \sin(\omega |t - u|)], \quad t, u, \in T, \quad (\text{B-27})$$

where

$$\omega T = i2\beta\phi(\xi/\beta) \equiv i2\beta\phi \quad (\text{B-28})$$

\* This equation is in the main text of this report.

† The factor 4 in Ref. 10, Eq. (37), should be a 2.

and

$$\begin{aligned}
\gamma &= -i \frac{1 + \cosh(2\beta\phi(\xi/\beta)) + \phi(\xi/\beta) \sinh(2\beta\phi(\xi/\beta))}{\sinh(2\beta\phi(\xi/\beta)) + \phi(\xi/\beta) [1 + \cosh(2\beta\phi(\xi/\beta))]} \\
&= -i \frac{\cosh(\beta\phi) + \phi \sinh(\beta\phi)}{\sinh(\beta\phi) + \phi \cosh(\beta\phi)} \\
&= -i \frac{1 + \phi \tanh(\beta\phi)}{\phi + \tanh(\beta\phi)}.
\end{aligned} \tag{B-29}$$

There follows, after some manipulation,

$$\begin{aligned}
\frac{1}{T^2} \iint_T dt du \Gamma(t, u; i2\xi/T) &= \frac{1}{\beta(1 - i2\xi/\beta)} \\
&\left\{ 1 - \frac{\sinh(2\beta\phi)}{\beta\phi[1 + \cosh(2\beta\phi) + \phi \sinh(2\beta\phi)]} \right\}.
\end{aligned} \tag{B-30}$$

Finally, the CF, (B-22), becomes

$$\begin{aligned}
f_p(\xi) &= \exp(\beta) \left[ \frac{1 - i\xi/\beta}{\phi} \sinh(2\beta\phi) + \cosh(2\beta\phi) \right]^{-1/2} \exp \left[ i \frac{R_c}{1 + R_s} \right] \\
&\frac{\xi}{1 - i2\xi/\beta} \left\{ 1 - i \frac{2\xi}{\beta^2\phi} \frac{\sinh(2\beta\phi)}{1 + \cosh(2\beta\phi) + \phi \sinh(2\beta\phi)} \right\},
\end{aligned} \tag{B-31}$$

where  $\phi$  is given by (B-28) and (B-26) as

$$\phi = (1 - i2\xi/\beta)^{1/2}. \tag{B-32}$$

(As  $\beta \rightarrow 0$ , there follows from (B-31)

$$f_p(\xi) \rightarrow (1 - i2\xi)^{-1/2} \exp \left[ \frac{R_c}{1 + R_s} \frac{i\xi}{1 - i2\xi} \right], \tag{B-33}$$

which may be readily derived as the CF of  $p$  in (B-4) for one sample of  $[r(t) + x(t)]^2$ . The CDF is derived in Appendix C.)

The CDF can be found from (B-31) by employing the methods in Refs. 15 and 16. The square root in (B-31) is not principal value, but must be traced continuously from  $\xi = 0$ , where  $f_p(0) = 1$ .

#### NARROWBAND CASE

From (10), \*

$$\ell = \frac{1}{2T} \int_T dt |\underline{c}(t) + \underline{s}(t) + \underline{n}(t)|^2. \quad (\text{B-34})$$

The powers in zero-mean Gaussian processes  $s(t)$  and  $n(t)$  are  $\sigma_s^2$  and  $\sigma_n^2$ , respectively. We now define

$$\underline{r}(t) = \frac{\underline{c}(t)}{(\sigma_s^2 + \sigma_n^2)^{1/2}}, \quad (\text{B-35})$$

$$\underline{x}(t) = \frac{\underline{s}(t) + \underline{n}(t)}{(\sigma_s^2 + \sigma_n^2)^{1/2}}.$$

As a result,

$$\ell = (\sigma_s^2 + \sigma_n^2) p, \quad (\text{B-36})$$

where

$$p = \frac{1}{2T} \int_T dt |\underline{r}(t) + \underline{x}(t)|^2. \quad (\text{B-37})$$

The correlation of  $\underline{x}(t)$  is  $2\hat{R}(\tau)$ , where  $\hat{R}(\tau)$  is general, except that  $\hat{R}(0) = 1$  (see Appendix A).

The characteristic function (CF) of the random variable (RV)  $\ell$  is

$$f_\ell(\xi) = f_p((\sigma_s^2 + \sigma_n^2) \xi). \quad (\text{B-38})$$

---

\* This equation is in the main text of this report.

In order to evaluate the CF  $f_p$ , we expand  $\underline{r}(t)$  and  $\underline{x}(t)$  in terms of their real and imaginary parts:

$$\begin{aligned}\underline{r}(t) &= r_c(t) + i r_s(t) , \\ \underline{x}(t) &= x_c(t) + i x_s(t) .\end{aligned}\tag{B-39}$$

Then

$$p = \frac{1}{2}(p_c + p_s) ,\tag{B-40}$$

where

$$\begin{aligned}p_c &= \frac{1}{T} \int_T dt [r_c(t) + x_c(t)]^2 , \\ p_s &= \frac{1}{T} \int_T dt [r_s(t) + x_s(t)]^2 .\end{aligned}\tag{B-41}$$

Now if and only if the spectrum  $\hat{G}(f)$  corresponding to  $\hat{R}(\tau)$  is even about  $f = 0$  (that is,  $G_{s,n}(f)$  even about  $f_0$  in  $(0, 2f_0)$ ), then  $x_c(t)$  and  $x_s(t)$  are independent random processes [Ref. 19, p. 41], each with correlation  $\hat{R}(\tau)$ . Then, using (B-40), the low-frequency (LF) results of (B-16), and the symmetry property  $\hat{\Gamma}(t, u; \lambda) = \hat{\Gamma}(u, t; \lambda)$  of the resolvent kernel of  $R$  that is symmetric, we obtain the CF of  $p$  as

$$\begin{aligned}f_p(\xi) &= f_{p_c}\left(\frac{1}{2}\xi\right) f_{p_s}\left(\frac{1}{2}\xi\right) \\ &= \prod_j \left\{ \left(1 - i \frac{\xi}{\hat{\lambda}_j T}\right)^{-1} \right\} \exp \left[ i \frac{\xi}{\sigma_s^2 + \sigma_n^2} \frac{1}{2T} \int_T dt |\underline{c}(t)|^2 \right. \\ &\quad \left. - \frac{\xi^2}{\sigma_s^2 + \sigma_n^2} \frac{1}{2T^2} \iint_T dt du \underline{c}(t) \underline{c}^*(u) \hat{\Gamma}(t, u; i\xi/T) \right] .\end{aligned}\tag{B-42}$$

The average power in  $c(t)$  over  $T$  is, for  $f_0 T \gg 1$ ,

$$P_c = \frac{1}{T} \int_T dt c^2(t) = \frac{1}{2T} \int_T dt |\underline{c}(t)|^2 .\tag{B-43}$$

We now define a normalized waveform,

$$\underline{c}_1(t) = (2P_c)^{-1/2} \underline{c}(t) ,\tag{B-44}$$

for then

$$\frac{1}{T} \int_T dt |\underline{c}_1(t)|^2 = 1. \quad (\text{B-45})$$

The CF in (B-42) can now be expressed as

$$f_p(\xi) = [\hat{D}(i\xi/T)]^{-1} \exp \left[ i \frac{R_c}{1+R_s} \xi \right. \\ \left. - \frac{R_c}{1+R_s} \xi^2 \frac{1}{T^2} \iint_T dt du \underline{c}_1(t) \underline{c}_1^*(u) \hat{\Gamma}(t,u; i\xi/T) \right], \quad (\text{B-46})$$

following the reasoning developed in (B-16), (B-17), and (B-18), and using (B-21). Notice that this CF depends on the complex envelope  $\underline{c}_1(t)$ , and not just on the physical envelope  $|\underline{c}_1(t)|$  of the coherent signal component of the narrowband (NB) deterministic waveform. However, any constant unknown phase in this NB deterministic waveform is irrelevant because it cancels out of the expression  $\underline{c}_1(t) \underline{c}_1^*(u)$ . That is, if complex envelope  $\underline{c}_1(t)$  is expressed as

$$\underline{c}_1(t) = E(t) \exp[i\phi(t) + i\theta], \quad (\text{B-47})$$

where  $E(t)$  is the envelope modulation,  $\phi(t)$  is the phase modulation, and  $\theta$  is an unknown phase independent of time  $t$ , then

$$\underline{c}_1(t) \underline{c}_1^*(u) = E(t) E(u) \exp[i\phi(t) - i\phi(u)] \quad (\text{B-48})$$

is independent of  $\theta$ .

Example: Exponential Correlation; Constant Complex Envelope.

Here we assume the correlation  $\hat{R}(\tau)$  of complex envelope  $\underline{x}(t)$  to be exponential:

$$\hat{R}(\tau) = \exp(-\hat{W}_e |\tau|); \quad \hat{\beta} \equiv \hat{W}_e T. \quad (\text{B-49})$$

The correlation of the corresponding NB waveform is given by a form similar to (7). \* We also take for the complex envelope of the coherent signal component

$$\underline{c}_1(t) = 1, \quad (\text{B-50})$$

\* This equation is in the main text of this report.

which corresponds to a pure sine wave for  $c(t)$ . When an approach analogous to that given above for the LF case is employed, the CF (B-46) becomes\*

$$\begin{aligned}
 f_p(\xi) &= [f_{p_{LP}}(\xi \rightarrow \xi/2, \beta \rightarrow \hat{\beta}/2)]^2 \\
 &= \exp(\hat{\beta}) \left[ \frac{1 - i\xi/\hat{\beta}}{\hat{\phi}} \sinh(\hat{\beta}\hat{\phi}) + \cosh(\hat{\beta}\hat{\phi}) \right]^{-1} \exp \left[ i \frac{R_c}{1 + R_s} \right] \cdot \quad (\text{B-51}) \\
 &\quad \frac{\xi}{1 - i2\xi/\hat{\beta}} \left\{ 1 - i \frac{4\xi}{\hat{\beta}^2\hat{\phi}} \frac{\sinh(\hat{\beta}\hat{\phi})}{1 + \cosh(\hat{\beta}\hat{\phi}) + \hat{\phi} \sinh(\hat{\beta}\hat{\phi})} \right\},
 \end{aligned}$$

where

$$\hat{\phi} \equiv (1 - i2\xi/\hat{\beta})^{1/2}, \quad (\text{B-52})$$

and we have utilized (B-31). (As  $\hat{\beta} \rightarrow 0$ , (B-51) yields

$$f_p(\xi) \rightarrow (1 - i\xi)^{-1} \exp \left[ \frac{R_c}{1 + R_s} \frac{i\xi}{1 - i\xi} \right], \quad (\text{B-53})$$

which may be readily derived as the CF of the RV  $p$  in (B-40) for one sample. The cumulative distribution function (CDF) is derived in Appendix C.)

The CDF can be found from (B-51) by employing the methods in Refs. 15 and 16. There is only one square root involved, that for  $\hat{\phi}$  in (B-52), and it is a principal value.

\*The leading factors in (B-51) agree with Ref. 10, Eq. (44), when we note that his  $\beta$  is  $\hat{\beta} T/2 = \hat{\beta}/2$  here.

## Appendix C

## DETECTION PROBABILITIES FOR ONE SAMPLE

As the observation time  $T$  in (6)\* and (10)\* approaches zero, the decision variables  $l$  take special forms for which the distributions can be evaluated in closed form. Also, the signal and noise spectra are not restricted in any way. Here we utilize some of the notation developed in Appendix B.

## LOW-FREQUENCY PROCESSING

From (6)\* and (B-19), for  $T \rightarrow 0$ ,

$$l = (P_c^{1/2} + s + n)^2 \equiv (P_c^{1/2} + x)^2. \quad (\text{C-1})$$

Then

$$\begin{aligned} \text{Prob}(l > X) &= \text{Prob}(|P_c^{1/2} + x| > X) \\ &= \int_{X^{1/2} - P_c^{1/2}}^{\infty} dx p(x) + \int_{-\infty}^{-X^{1/2} - P_c^{1/2}} dx p(x) \\ &= \Phi\left(\frac{P_c^{1/2} - X^{1/2}}{(\sigma_s^2 + \sigma_n^2)^{1/2}}\right) + \Phi\left(\frac{-P_c^{1/2} - X^{1/2}}{(\sigma_s^2 + \sigma_n^2)^{1/2}}\right) \\ &= \Phi\left(\left(\frac{R_c}{1 + R_s}\right)^{1/2} - \left(\frac{\Lambda_n}{1 + R_s}\right)^{1/2}\right) + \Phi\left(-\left(\frac{R_c}{1 + R_s}\right)^{1/2} - \left(\frac{\Lambda_n}{1 + R_s}\right)^{1/2}\right), \end{aligned} \quad (\text{C-2})$$

since  $x$  is Gaussian with variance  $\sigma_s^2 + \sigma_n^2$ . Here  $\Phi$  is the cumulative distribution function (CDF) for a Gaussian random variable (RV),

$$\Phi(x) \equiv \int_{-\infty}^x dt (2\pi)^{-1/2} \exp(-t^2/2), \quad (\text{C-3})$$

and the normalized threshold  $\Lambda_n$  is defined in (12).\*

We define the fraction  $f$  of the total received signal power that is coherent as

---

\*This equation is in the main text of this report.

$$f = \frac{P_c}{P_c + \sigma_s^2} = \frac{R_c}{R_c + R_s} \equiv \frac{R_c}{R}, \quad (C-4)$$

where  $R$  is the total S/N at the input to Fig. 1. Then (C-2) yields

$$P_D = \Phi\left(\frac{(fR)^{1/2} - \Lambda_n^{1/2}}{(1+R(1-f))^{1/2}}\right) + \Phi\left(\frac{-(fR)^{1/2} - \Lambda_n^{1/2}}{(1+R(1-f))^{1/2}}\right) \quad (C-5)$$

for the detection probability. The false-alarm probability follows by setting  $R = 0$ :

$$P_F = 2\Phi(-\Lambda_n^{1/2}) \quad (C-6)$$

Notice that the signal and noise spectra do not appear in (C-5) or (C-6).

From (C-5) there follows

$$\left. \frac{\partial P_D}{\partial f} \right|_{f=0} = -(2\pi)^{-1/2} \exp\left[-\frac{\Lambda_n}{2(1+R)}\right] \frac{\Lambda_n^{1/2} R}{(1+R)^{3/2}} \quad (C-7)$$

Also,

$$\left. \frac{\partial P_D}{\partial f} \right|_{\substack{f=1 \\ R^{1/2} = \Lambda_n^{1/2} - 1}} = -(2\pi)^{-1/2} \left\{ e^{-1/2 (\Lambda_n^{1/2} - 1)} \left( \frac{1}{2} \Lambda_n^{1/2} - 1 \right) + \exp\left[-\frac{1}{2} (2 \Lambda_n^{1/2} - 1)^2\right] \Lambda_n^{1/2} (\Lambda_n - 1) \right\} \quad (C-8)$$

The meaning and interpretation of these equations are given in Section 3 of the main text.

## NARROWBAND PROCESSING

From (B-37), (B-40), and (B-41), for  $T \rightarrow 0$ ,

$$p = \frac{1}{2} |\underline{r} + \underline{x}|^2 = \frac{1}{2} (r_c + x_c)^2 + \frac{1}{2} (r_s + x_s)^2 \quad (C-9)$$

Then from (B-36) and (C-3),

$$\begin{aligned} \text{Prob}(\ell > X) &= \text{Prob} \left( p > \frac{\Lambda_n}{1+R_s} \right) \\ &= \text{Prob} \left[ (r_c + x_c)^2 + (r_s + x_s)^2 > \frac{2\Lambda_n}{1+R_s} \right] \end{aligned} \quad (C-10)$$

When the variables are changed,  $y_c = r_c + x_c$ ,  $y_s = r_s + x_s$ ,

$$\begin{aligned} \text{Prob}(\ell > X) &= \text{Prob} \left( y_c^2 + y_s^2 > \frac{2\Lambda_n}{1+R_s} \right) \\ &= \iint_R dy_c dy_s \frac{1}{2\pi} \exp \left[ -\frac{(y_c - r_c)^2 + (y_s - r_s)^2}{2} \right] \\ &= \int_0^\infty dt t \int_{-\pi}^\pi d\theta \frac{1}{2\pi} \exp \left[ -\frac{1}{2} \{ t^2 - 2t(r_c \cos \theta + r_s \sin \theta) + r_c^2 + r_s^2 \} \right] \\ &\quad \left( \frac{2\Lambda_n}{1+R_s} \right)^{1/2} \\ &= \int_0^\infty dt t \exp \left[ -\frac{1}{2} t^2 - \frac{1}{2} |\underline{r}|^2 \right] I_0(|\underline{r}| t) \\ &\quad \left( \frac{2\Lambda_n}{1+R_s} \right)^{1/2} \quad (C-11) \\ &= Q \left( |\underline{r}|, \left( \frac{2\Lambda_n}{1+R_s} \right)^{1/2} \right) = Q \left( \left( \frac{2R_c}{1+R_s} \right)^{1/2}, \left( 2 \frac{\Lambda_n}{1+R_s} \right)^{1/2} \right) \end{aligned}$$

where  $R$  is the region outside a circle of radius  $(2\Lambda_n/(1+R_s))^{1/2}$ , and  $Q$  is tabulated in Ref. 21. The probability of detection is

$$P_D = Q \left( \left( \frac{2fR}{1+R(1-f)} \right)^{1/2}, \left( \frac{2\Lambda_n}{1+R(1-f)} \right)^{1/2} \right) \quad (C-12)$$

TR 4233

The probability of false alarm is obtained by setting  $R = 0$ :

$$P_F = \exp(-\Lambda_n) \quad (C-13)$$

Again, the signal and noise spectra do not enter (C-12) and (C-13).

## Appendix D

ASYMPTOTIC BEHAVIOR OF CHARACTERISTIC FUNCTION  
AND ERROR BOUND

The cumulative distribution function (CDF) can be found from the characteristic function (CF) by use of Ref. 16, Eq. (3) :

$$P(X) = \frac{1}{\gamma} - \frac{1}{\pi} \int_0^{\infty} \frac{d\xi}{\xi} \operatorname{Im} \{f(\xi) \exp(-i\xi X)\} . \quad (\text{D-1})$$

(Alternatively, Ref. 16, Eq. (14) or (15), could be used for the problems encountered here.) Since numerical evaluation of this integral must be limited to a finite interval, it is necessary to evaluate the error incurred by terminating the range of the integral. To evaluate this error, the behavior of the CF  $f(\xi)$  for large  $\xi$  must be known.

For the low-frequency (LF) case, the pertinent CF is given in (B-31). It may be shown that for large  $\xi$  the second exponential is upper-bounded by unity, and the leading terms behave as

$$\left(\frac{8}{u}\right)^{1/4} \left[1 - \frac{1+i}{2} u^{-1/2}\right] \exp \left[ \beta \left(1 - u^{1/2} - \frac{1}{4} u^{-1/2}\right) \right] \cdot \quad (\text{D-2})$$

$$\exp \left[ i \left\{ \frac{\pi}{8} + \beta \left( u^{1/2} - \frac{1}{4} u^{-1/2} \right) \right\} \right] \text{ as } \xi \rightarrow \infty ,$$

where  $u = \xi/\beta$ . As an example of the accuracy of this asymptotic form, for  $\beta = 1$  and  $\xi = 250$ , the exact value of the CF is  $1.489962 \cdot 10^{-7} \exp(-i2.692384)$ , whereas the asymptotic expansion in (D-2) gives  $1.490021 \cdot 10^{-7} \exp(-i2.693924)$ . An upper bound on the CF for large  $\xi$  follows from (D-2) as

$$\left(\frac{8}{u}\right)^{1/4} \exp[\beta(1-u^{1/2})] . \quad (\text{D-3})$$

The error in terminating the integral in (D-1) can then be related to the integral

$$\frac{1}{\pi} \int_{u_L}^{\infty} \frac{du}{u} \left(\frac{8}{u}\right)^{1/4} \exp[\beta(1-u^{1/2})] \quad (\text{D-4})$$

$$= \frac{2^{7/4} \exp(\beta)}{\pi} \int_{u_L^{1/2}}^{\infty} dt t^{-3/2} \exp(-\beta t) < \frac{2^{7/4}}{\pi} \frac{\exp[\beta(1-u_L^{1/2})]}{\beta u_L^{3/4}} .$$

TR 4233

Values of  $u_L$  used to keep the error below specified tolerances can be found easily from (D-4). These values are dependent on the exact value of  $\beta$ ; however, they are independent of  $R_c$  and  $R_s$  and are, therefore, conservative.

## Appendix E

## DETECTION PROBABILITY UNDER GAUSSIAN ASSUMPTION

In this appendix, we assume the time-bandwidth product  $\beta$  large enough so that the random variable  $p$  in (B-4) can be assumed Gaussian. In that event, we need only compute the mean and variance of  $p$ . We have

$$\bar{p} = \frac{P_c}{\sigma_s^2 + \sigma_n^2} + 1 = \frac{1+R}{1+R(1-f)} \quad (E-1)$$

using (B-2), (B-19), (B-21), and (19).\* The variance of  $p$  is given by

$$\begin{aligned} \sigma^2(p) &= \frac{1}{T^2} \iint_T dt du [4r(t)r(u)R(t-u) + 2R^2(t-u)] \\ &= \frac{2fR}{1+R(1-f)} \frac{2\beta-1+\exp(-2\beta)}{\beta^2} + \frac{4\beta-1+\exp(-4\beta)}{4\beta^2} \end{aligned} \quad (E-2)$$

using (B-23) and (B-24) for the case of interest here. Then from (B-3), (12),\* and (C-3),

$$\begin{aligned} \text{Prob}(\ell > X) &= \text{Prob}\left(p > \frac{\Lambda_n}{1+R_s}\right) \\ &= \Phi\left(\frac{\bar{p}}{\sigma(p)} - \frac{\Lambda_n}{(1+R(1-f))\sigma(p)}\right) \\ &= \Phi\left(\sqrt{\beta} \frac{1+R - \Lambda_n}{[1+R(1-f)]^{1/2} \left[1+R+3Rf - \frac{1}{4\beta}(1+R+7Rf) + \frac{2Rf}{\beta}\exp(-2\beta) + \frac{1+R-Rf}{4\beta}\exp(-4\beta)\right]^{1/2}}\right) \end{aligned} \quad (E-3)$$

The probability of false alarm is obtained by setting  $R = 0$ :

$$P_F = \Phi\left(\sqrt{\beta} \frac{1 - \Lambda_n}{\left[1 - \frac{1 - \exp(-4\beta)}{4\beta}\right]^{1/2}}\right) \quad (E-4)$$

\* This equation is in the main text of this report.

## LIST OF REFERENCES

1. C. W. Helstrom, Statistical Theory of Signal Detection, Pergamon Press, New York, 1960.
2. S. O. Rice, "Mathematical Analysis of Random Noise" (Parts I and II), Bell System Technical Journal, vol. 23, no. 1, 1944, pp. 283-332, and "Mathematical Analysis of Random Noise" (Part III), Bell System Technical Journal, vol. 24, no. 1, 1945, pp. 46-156.
3. R. C. Emerson, "First Probability Densities for Receivers with Square Law Detectors," Journal of Applied Physics, vol. 24, no. 9, September 1953, pp. 1168-1176.
4. A. J. F. Siegert, "Passage of Stationary Processes through Linear and Non-Linear Devices," Transactions of the IRE, PGIT-3, March 1954, pp. 4-25.
5. M. Kac and A. J. F. Siegert, "On the Theory of Noise in Radio Receivers with Square Law Detectors," Journal of Applied Physics, vol. 18, no. 4, April 1947, pp. 383-397.
6. D. A. Darling and A. J. F. Siegert, "A Systematic Approach to a Class of Problems in the Theory of Noise and Other Random Phenomena — Part I," IRE Transactions on Information Theory, vol. IT-3, no. 1, March 1957, pp. 32-37.
7. A. J. F. Siegert, "A Systematic Approach to a Class of Problems in the Theory of Noise and Other Random Phenomena — Part II, Examples," IRE Transactions on Information Theory, vol. IT-3, no. 1, March 1957, pp. 38-43.
8. D. Slepian, "Fluctuations of Random Noise Power," Bell System Technical Journal, vol. 37, no. 1, January 1958, pp. 163-184.
9. I. Jacobs, "Energy Detection of Gaussian Communication Signals," IEEE 10th National Communications Symposium, October 1964, pp. 440-448.
10. M. I. Schwartz, "Distribution of the Time-Average Power of a Gaussian Process," IEEE Transactions on Information Theory, vol. IT-16, no. 1, January 1970.

11. B. O. Steenson and N. C. Stirling, "The Amplitude Distribution and False Alarm Rate of Filtered Noise," Proceedings of the IEEE, vol. 53, no. 1, January 1965, pp. 42-55.
12. H. E. Robbins, "The Distribution of a Definite Quadratic Form," Annals of Mathematical Statistics, vol. 19, 1948, pp. 226-270.
13. J. Gurland, "Distributions of Definite and Indefinite Quadratic Forms," Annals of Mathematical Statistics, vol. 26, no. 1, March 1955, pp. 122-127.
14. U. Grenander, H. O. Pollak, and D. Slepian, "Distribution of Quadratic Forms in Normal Variates," Journal of the Society for Industrial and Applied Mathematics, vol. 7, December 1959, pp. 374-401.
15. A. H. Nuttall, Numerical Evaluation of Cumulative Probability Distribution Functions Directly from Characteristic Functions, NUSC Report No. 1032, 11 August 1969. Also Proceedings of the IEEE, vol. 57, no. 11, November 1969, pp. 2071-2072.
16. A. H. Nuttall, Alternate Forms and Computational Considerations for Numerical Evaluation of Cumulative Probability Distributions Directly from Characteristic Functions, NUSC Report No. NL-3012, 12 August 1970. Also Proceedings of the IEEE, vol. 58, no. 11, November 1970, pp. 1872-1873.
17. J. S. Bendat and A. G. Piersol, Measurement and Analysis of Random Data, John Wiley and Sons, Inc., New York, 1958, p. 265.
18. A. D. Whalen, Detection of Signals in Noise, Academic Press, New York, 1971.
19. W. B. Davenport and W. L. Root, An Introduction to the Theory of Random Signals and Noise, McGraw-Hill Book Co., Inc., New York, 1958.
20. R. Courant and D. Hilbert, Methods of Mathematical Physics, vol. I, Interscience Publishers, New York, 1953.
21. J. I. Marcum, "Table of Q Functions," Rand Corporation, Santa Monica, California, Research Memorandum No. RM-339, 1 January 1950.